MICROBIOLOGY AND MOLECULAR BIOLOGY REVIEWS, Dec. 2008, p. 590–641 Vol. 72, No. 4
1092-2172/08/$08.00+0 doi:10.1128/MMBR.00016-08

ATP Synthase and the Actions of Inhibitors Utilized To Study Its Roles in Human Health, Disease, and Other Scientific Areas

Sangjin Hong and Peter L. Pedersen*

Department of Biological Chemistry, Johns Hopkins University, School of Medicine, 725 N. Wolfe Street, Baltimore, Maryland 21205-2185

INTRODUCTION

ATP synthase (F_0F_1) is a multisubunit, membrane-associated protein complex that catalyzes the phosphorylation of ADP to ATP at the expense of a proton motive force generated by an electron transport chain in energy-transducing membranes (303, 387). In some organisms, it also works in the reverse direction by hydrolyzing ATP and generating an electrochemical proton gradient across a membrane to support locomotion or nutrient uptake. ATP synthase is present in all living organisms and is located in the membranes of mitochondria, bacteria, and chloroplast thylakoids as well as on the surfaces of various cell types, including endothelial cells (269, 270), keratinocytes (58), and adipocytes (206).

ATP synthase is an exceptionally complicated protein complex. It is divided into two sectors, a soluble globular F_1 catalytic sector and a membrane-bound F_0 proton-translocating sector (Fig. 1) (304, 305). Even the simplest form of ATP synthase, found in nonphotosynthetic eubacteria, contains eight different subunit types, while the chloroplast and photosynthetic bacterial ATP synthase each consists of nine different subunit types (42, 331). The ATP synthase from mitochondria is much more complicated and, excluding regulators, is re-

* Corresponding author. Mailing address: Department of Biological Chemistry, Johns Hopkins University, School of Medicine, 725 N. Wolfe Street, Baltimore, MD 21205-2185. Phone: (410) 955-3827. Fax: (410) 614-1944. E-mail: ppederse@jhmi.edu.

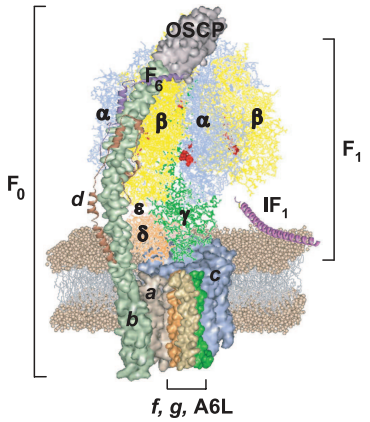

FIG. 1. Current view of the structure of mitochondrial ATP synthase from metazoans. F_1 is composed of α, β, γ, δ, and ε subunits, and F_0 consists of *a*, *b*, *c*, *d*, *e*, *f*, *g*, A6L, and OSCP. IF_1 is a regulatory protein. The coordinates of the subunits used in the structural model are 1E79 for the α, β, γ, δ, and ε subunits; 1ABV for the N-terminal domain of OSCP; 2CLY for F_6, *d*, and the hydrophilic part of the *b* subunit; 1GMJ for IF_1; and 1B9U for the transmembrane part of the *b* subunit. The ac_{10} subcomplex was modeled using the coordinates of the *a* and *c* subunits from 1C17, and the other subunits in the model were constructed manually using Quanta. No positions are assigned to the factor B and the *e* subunit. Here and where indicated in the other figure legends, the coordinates of protein structures were obtained from the PDB.

ported to date to consist of 15 and 17 different subunit types in animals and yeasts (or fungi), respectively (305, 413).

ATP synthase is associated directly or indirectly with various human diseases. One form of Leigh syndrome, a neurodegenerative disease which causes a neuromuscular disorder with a 50% survival rate to 3 years of age, is the consequence of a severe impairment of ATP synthesis. This is due to a mutation in subunit *a* of ATP synthase (99). The neuropathy, ataxia, retinitis pigmentosa syndrome and the familial bilateral striatal necrosis are also caused by the dysfunction of ATP synthase due to mutations within the same subunit (93, 396). In Batten's disease, a lysosomal storage disease also known as neuronal ceroid lipofuscinoses or Kufs' disease, the subunit *c* of ATP synthase has been found as a predominant storage protein (298, 299). In addition, in Alzheimer's disease or presenile dementia, which is a progressive and degenerative disease that attacks the brain, a deficiency of ATP synthase has been observed in mitochondria (357). A low expression of the ATP synthase β subunit and the cytosolic accumulation of the α subunit are detected in Alzheimer's disease, and the intraneuronal cytosolic accumulation of the α subunit is implicated in the neurodegenerative process (73, 208, 367). Moreover, the ATP synthase on the cell surface of endothelial cells has been reported to have an important role in the angiogenesis process required for tumor growth (269–271, 422). Additionally, the ATP synthase F_6 subunit circulating in the blood has been recognized to be involved in the increase of blood pressure (293, 294). Finally, the β subunit of ATP synthase has been identified as a target protein for innate antitumor cytotoxicity mediated by natural killer and interleukin 2-activated killer cells (91).

ATP synthase has also been demonstrated and suggested as a good molecular target for drugs in the treatment of various diseases and the regulation of energy metabolism (16, 38, 72, 193, 202, 367). One of the drugs developed for the treatment of tuberculosis, R207910, was shown to be active against a number of drug-resistant strains of *Mycobacterium tuberculosis* and to eradicate *M. tuberculosis* infection rapidly and effectively (15, 313, 340). The drug has been revealed to block the synthesis of ATP by targeting subunit *c* of ATP synthase. Another drug, Bz-423, which was developed for therapy of the autoimmune disorder systemic lupus erythematosus, kills pathogenic lymphocytes selectively by inducing apoptosis in lymphoid cells (41). Significantly, Bz-423 has been found to inhibit the mitochondrial ATP synthase by binding to the subunit known as oligomycin sensitivity-conferring protein (OSCP) (193). In addition, the inhibition of nonmitochondrial ATP synthase resulted in the inhibition of cytosolic lipid droplet accumulation, suggesting ATP synthase as a molecular target for antiobesity drugs (16). Finally, the inhibition of ATP synthase has been suggested for an antiangiogenic therapeutic strategy to block tumor angiogenesis (17, 59, 269–271, 422). Here, the reaction of ATP synthase inhibitors with the nonmitochondrial ATP synthase of endothelial cells has been shown to inhibit markedly the migration and proliferation of endothelial cells with little effect on intracellular ATP (17).

The aim of this review is to provide insight and encouragement into the development of new ATP synthase-directed agents. We have meticulously categorized most of the natural and synthetic inhibitors of ATP synthase reported to date in accordance with physical/chemical characteristics of the inhibitors and have summarized the current knowledge of the modes of action of these inhibitors. The information provided in this review should prove to be an invaluable resource, not only for obtaining information about the interactions of known effectors, primarily inhibitors of ATP synthase, but for generating new ideas for the development of numerous additional ATP synthase-directed agents that can be used (i) in the treatment of human and animal diseases, (ii) in agriculture as pesticides or herbicides, and (iii) in the developing field of nanotechnology to understand the mechanics of nanomotor function.

PEPTIDE INHIBITORS

α-Helical Basic Peptide Inhibitors

The α-helical basic peptide inhibitors bind to F_1 and inhibit ATPase activity (Table 1). Inhibitors in this group include α-helical structures containing basic residues, which appear to be crucial for their inhibitory activities. The α-helical basic peptide inhibitors include the bacterial/chloroplast ε subunit, melittin, the presequence of yeast cytochrome oxidase subunit IV (WT and its synthetic derivatives), and possibly the inhibitor protein (IF_1) (Fig. 2A).

The bacterial/chloroplast ε subunit, composed of ~120 to 140 amino acid residues, is an endogenous inhibitory subunit in F_1, and inhibits ATPase activities of isolated and membrane-bound bacterial F_1 (BF_1) and chloroplast F_1 (CF_1) (198, 284, 332, 372, 386). The inhibition is reversible and noncompetitive

TABLE 1. α-Helical basic peptide inhibitors

Name	Amino acid sequence (species)[a]	Source	Inhibitory potency (reference)
Bacterial/chloroplast ε subunit	MTLNLCVLTPNRSIWNSEVKEIILST NSGQIGVLPNHAPTATAVDIGILR IRLNDQWLTLALMGGFARIGNNE ITILVNDAERGSDIDPQEAQQTLE IAEANLRKAEGKRQKIEANLALR RARTRVEASNTISS (spinach)	Natural regulatory peptide	1–3 ε mol/mol[c] CF_1(-ε)[b] (spinach Ca^{2+}-ATPase) (332); ~0.73 μg/μg[c] (spinach CF_1-Ca^{2+}-ATPase) (284); ~15 nM[c] (EF_1-ATPase) (372); 100 nM[c] (EF_1-ATPase, rotation rate of 60-nm beads) (282); 10 nM[d] (EF_1-ATPase) (386); 2.1 nM[e] (*Thermosynecoccus ascicula* F_1, αβγ complex) (212); 94% inhibition at 10 ε mol/mol CF_1(-ε) (spinach Ca^{2+}-ATPase) (289)
IF_1	MAVTALAARTWLGVWGVRTMQA RGFGSDQSENVDRGAGSIREAGG AFGKREQAEEERYFRAQSREQL AALKKHHEEEIVHHKKEIERLQK EIERHKQKIKMLKHDD (human)	Natural regulatory peptide	0.25 μM[c] (bovine heart MF_1-ATPase) (143); 1.2 μM[c] at 21°C and 0.84 μM at 37°C (bovine heart MF_1-ATPase) (446); 300 μg/mg protein[c] (*T. pyriformis* SMP-ATPase) (404); 34 μg/mg protein[c] (*C. asciculate* SMP-ATPase) (439); 0.24 μM[d] (rat liver MF_1-ATPase) (229)
Melittin	GIGAVLKVLTTGLPALISWIKRKRQ Q-NH_2	*Apis mellifera* (honey bee)	5 μM[c] (bovine heart MF_1-ATPase) (52); 12 μM[c] (bovine heart MF_1-ATPase) (143)
WT[f]	MLSLRQSIRFFKPATRTLCSSRYL L-NH_2	Subunit IV of yeast cytochrome *c* oxidase	16 μM[c] (bovine heart MF_1-ATPase) (52)
Δ11,12	MLSLRQSIRFPATRTLCSSRYLL-NH_2	Synthetic	29 μM[c] (bovine heart MF_1-ATPase) (52)
Syn-A2	MLSRLSLRLLSRLSLRLLSRYLL-NH_2	Synthetic	42 nM[c] (bovine heart MF_1-ATPase) (52); 290 nM[c] (bovine heart MF_1-ATPase) (143); 1.7 μM[c] (*Bacillus* PS3 F_1-ATPase) (143)
Syn-C	MLSSLLRLRSLSLLRLRLSRYLL-NH_2	Synthetic	58 nM[c] (bovine heart MF_1-ATPase) (52); 160 nM (bovine heart MF_1-ATPase) (143); 1.6 μM[c] (*Bacillus* PS3 F_1-ATPase) (143)

[a] Where a species is indicated, sequences vary with species.
[b] CF_1 without ε subunit.
[c] I_{50}.
[d] K_i.
[e] K_d.
[f] Leader sequence of subunit IV of yeast cytochrome *c* oxidase.

with substrates (372, 386). It has no inhibitory effect on ATP synthesis and is required in the chloroplast ATP synthase for ATP synthesis in the light (289, 389, 402). The inhibition of F_1-ATPase by the ε subunit is controlled by the electrochemical gradient and ADP/ATP balance (389), and the C-terminal α-helical domain is responsible for its inhibitory activity (168, 212, 289). At high proton motive forces and low ATP concentrations, the C-terminal α-helical domain of the ε subunit performs large conformational changes from the hairpin conformation to a "lifted-up" extended conformation, shifting its position ~70 Å to interact with the $\alpha_3\beta_3$ hexagon ring (389, 402). In the "lifted-up" extended conformation, the C-terminal helix lies close to the β-DELSEED motif of the β subunit, and the direct electrostatic interaction between the β-DELSEED motif and the basic residues in the C-terminal domain of the ε subunit leads to the inhibition of ATP hydrolysis (168).

IF_1 is a natural regulatory peptide of 56 to 87 residues found in mitochondria (Fig. 2A). It binds to F_1 with a 1:1 stoichiometric ratio and inhibits the ATP hydrolysis of mitochondrial ATP synthase without affecting ATP synthesis. The inhibition is reversible and noncompetitive, and the binding of IF_1 to F_1 requires the presence of ATP (178, 228, 229, 409). IF_1 is more potent against the whole membrane-bound ATP synthase (F_0F_1-ATPase) complex than isolated F_1 (144, 409, 411). IF_1 inhibits the ATPase activity of mitochondrial ATP synthase and has no ATPase inhibitory effect against BF_1 (143). The yeast IF_1 can cross-react with animal F_1, whereas the potato IF_1 shows no inhibitory effect against animal F_1 (60, 319). IF_1 proteins from animals are considerably (18 to 31 residues) longer than those from plants and fungi (176). In a study of truncated bovine IF_1 for inhibitory activity, the minimal inhibitory sequence was shown to localize within residues 14 to 47 (411). The adjoining residues 10 to 13 and 48 to 56 are considered to play a stabilizing role. In the crystal structure of F_1 with IF_1, the N-terminal domain of IF_1 is bound at the interface between α_{DP} and β_{DP} subunits and also has contacts with β_{TP}386, α_E355, and the γ subunit (61). It has been suggested that the inhibitory mode of action of IF_1 could be similar to that of the bacterial ε subunit (260, 402). IF_1 is considered to play its inhibitory role by impeding the closure of the α_{DP}-β_{DP} catalytic interface to prevent the hydrolysis of bound ATP (61, 141). Cross-linking and intrinsic phosphorescence decay studies implicate IF_1 as being functionally associated with the mitochondrial ε subunit (260, 373). Both proteins are in close proximity in the crystal structure of the F_1-IF_1 complex (141).

Melittin, which is a 26-residue peptide known as the princi-

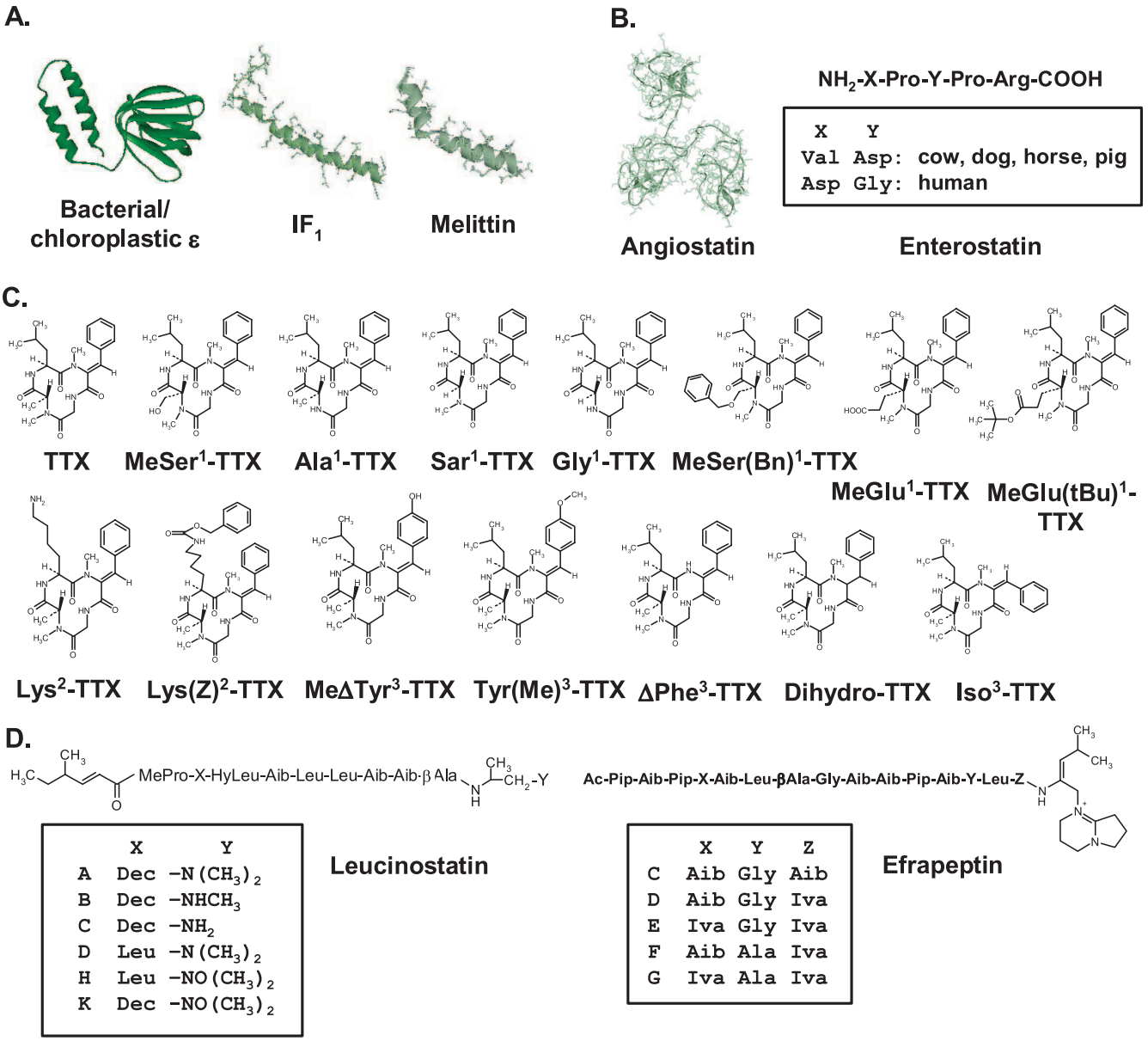

FIG. 2. Structures of peptide inhibitors. (A) α-Helical basic peptide inhibitors. The coordinates of the inhibitors are 1BSN for the bacterial/chloroplast ε subunit, 1GMJ for IF_1, and 2MLT for melittin. (B) Angiostatin and enterostatin. The coordinate for the structure is 1KI0. (C) Tentoxin and tentoxin analogs. (D) Leucinostatins and efrapeptins.

pal active component of bee venom and which has a powerful anti-inflammatory effect, inhibits the ATPase activity of F_1 (52, 143). The 25-residue presequence of yeast cytochrome oxidase subunit IV (WT) and its synthetic derivatives, Syn-A2, Syn-C, and Δ11,12, also inhibit ATP hydrolysis by F_1 (52, 143). Melittin, WT, Syn-A2, and Syn-C (and possibly Δ11,12) form basic and amphiphilic α-helical structures (191, 337, 338, 393). Melittin, Syn-A2, and Syn-C have been suggested to bind to F_1 at the same site as IF_1 (143), and WT and Δ11,12, which are derivatives of Syn-A2 and Syn-C, are considered to also play similar inhibitory roles. Syn-A2 and Syn-C are very effective inhibitors among amphiphilic peptide inhibitors, showing 50% inhibitory (I_{50}) values of about 40 to 50 nM for inhibition of bovine F_1-ATPase activity (52). Syn-A2 inhibits the ATPase activity of bovine F_1 noncompetitively in a parabolic manner, whereas Syn-C exhibits mixed inhibition and melittin shows noncompetitive hyperbolic inhibition (52).

Angiostatin and Enterostatin

Angiostatin is a 57-kDa N-terminal fragment of a larger protein, plasmin, which is also a fragment of plasminogen. Angiostatin has a triangular structure with three to five contiguous kringle domains, and it acts as a natural angiogenesis inhibitor (Fig. 2B) (1). It binds to the α and β subunits of ATP synthase and inhibits its ATP hydrolysis (269, 270). In an experiment with bovine F_1 and human angiostatin, the angiosta-

TABLE 2. Tentoxin and tentoxin analogs

Name or abbreviation	Sequence	Molecular formula	Inhibitory potency (reference)
Tentoxin	Cyclo-(L-*N*-methyl-Ala^1-L-Leu^2-*N*-methyl-Δ^ZPhe^3-Gly^4)	$C_{22}H_{30}N_4O_4$	~0.6 mol/mol[a] (spinach CF_1-ATPase) (179); 50 nM[a] (spinach CF_1(-ε)-ATPase) (69); 0.4–0.6 μM[a] (lettuce chloroplasts, photophosphorylation) (380); 10 nM[b] (spinach CF_1(-ε)-ATPase) (350); 30–60 μM[b] (60°C, TF_1-ATPase) (351); 8–10 nM[c] (spinach CF_1(-ε)-ATPase) (350, 351)
MeSer^1-TTX	Cyclo-(L-*N*-methyl-Ser^1-L-Leu^2-*N*-methyl-Δ^ZPhe^3-Gly^4)	$C_{22}H_{30}N_4O_5$	50 nM[a] (spinach CF_1(-ε)-ATPase) (69); 0.5 μM[a] with 2 min incubation and 0.1 μM[a] with 30 min incubation in the dark (spinach thylakoids, ATP synthesis) (316); 15 nM[c] (spinach CF_1(-ε)-ATPase) (351)
Ala^1-TTX	Cyclo-(L-Ala^1-L-Leu^2-*N*-methyl-Δ^ZPhe^3-Gly^4)	$C_{21}H_{28}N_4O_4$	34 nM[c] (spinach CF_1(-ε)-ATPase) (351)
Sar^1-TTX	Cyclo-(L-*N*-methyl-Gly^1-L-Leu^2-*N*-methyl-Δ^ZPhe^3-Gly^4)	$C_{21}H_{28}N_4O_4$	45 nM[c] (spinach CF_1(-ε)-ATPase) (351)
Gly^1-TTX	Cyclo-(L-Gly^1-L-Leu^2-*N*-methyl-Δ^ZPhe^3-Gly^4)	$C_{20}H_{26}N_4O_4$	34 nM[c] (spinach CF_1(-ε)-ATPase) (351)
MeSer(Bn)^1-TTX	Cyclo-(L-*N*-methyl-Ser(Bn)^1-L-Leu^2-*N*-methyl-Δ^ZPhe^3-Gly^4)	$C_{29}H_{36}N_4O_5$	0.5 μM[a] (spinach CF_1(-ε)-ATPase) (69); 0.5 μM[c] (spinach CF_1(-ε)-ATPase) (351)
MeGlu^1-TTX	Cyclo-(L-*N*-methyl-Glu^1-L-Leu^2-*N*-methyl-Δ^ZPhe^3-Gly^4)	$C_{24}H_{32}N_4O_6$	5 μM[a] (spinach CF_1(-ε)-ATPase) (69)
MeGlu(tBu)^1-TTX	Cyclo-(L-*N*-methyl-Glu(tBu)^1-L-Leu^2-*N*-methyl-Δ^ZPhe^3-Gly^4)	$C_{28}H_{41}N_4O_6$	2 μM[a] (spinach CF_1(-ε)-ATPase) (69); 1.5 μM[c] (spinach CF_1(-ε)-ATPase) (351)
Lys^2-TTX	Cyclo-(L-*N*-methyl-Ala^1-L-Lys^2-*N*-methyl-Δ^ZPhe^3-Gly^4)	$C_{22}H_{31}N_5O_4$	3 μM[a] (spinach CF_1(-ε)-ATPase); 2 μM[c] (spinach CF_1(-ε)-ATPase) (351)
Lys(Z)^2-TTX	Cyclo-(L-*N*-methyl-Ala^1-L-Lys(Z)^2-*N*-methyl-Δ^ZPhe^3-Gly^4)	$C_{30}H_{37}N_5O_6$	1 μM[a] (spinach CF_1(-ε)-ATPase) (69); 0.75 μM[c] (spinach CF_1(-ε)-ATPase) (351)
MeΔTyr^3-TTX	Cyclo-(L-*N*-methyl-Ala^1-L-Leu^2-*N*-methyl-Δ^ZTyr^3-Gly^4)	$C_{22}H_{30}N_4O_5$	0.05 μM[a] (spinach CF_1(-ε)-ATPase) (69); 12 nM[c] (spinach CF_1(-ε)-ATPase) (351)
Tyr(Me)^3-TTX	Cyclo-(L-*N*-methyl-Ala^1-L-Leu^2-*N*-methyl-Δ^ZTyr(Me)^3-Gly^4)	$C_{23}H_{32}N_4O_5$	0.05 μM[a] (spinach CF_1(-ε)-ATPase) (69); 10 nM[c] (spinach CF_1(-ε)-ATPase) (351)
ΔPhe^3-TTX	Cyclo-(L-*N*-methyl-Ala^1-L-Leu^2-Δ^ZPhe^3-Gly^4)	$C_{21}H_{28}N_4O_4$	0.8 μM[c] (spinach CF_1(-ε)-ATPase) (351)
Dihydro-TTX	Cyclo-(L-*N*-methyl-Ala^1-L-Leu^2-*N*-methyl-Phe^3-Gly^4)	$C_{22}H_{32}N_4O_4$	0.5 μM[c] (spinach CF_1(-ε)-ATPase) (351)
Iso^3-TTX	Cyclo-(L-*N*-methyl-Ala^1-L-Leu^2-*N*-methyl-Δ^EPhe^3-Gly^4)	$C_{22}H_{30}N_4O_4$	8.7 μM[c] (spinach CF_1(-ε)-ATPase) (351)

[a] I_{50}.
[b] K_i.
[c] K_d.

tin bound strongly to F_1 and completely inhibited ATPase activity (269). Angiostatin was also found to inhibit ATP generation by the nonmitochondrial ATP synthase located on endothelial cells that comprise the human umbilical vein, with 1 μM angiostatin inhibiting about 81% of the ATP synthesis activity (270). However, no ATP synthesis by plasma membrane ATP synthase was reported in human vascular endothelial cells (325), and the inhibition of ATP synthesis of nonmitochondrial ATP synthase by ATP synthase-specific inhibitors is still controversial.

Enterostatin is a pentapeptide released from procolipase during dietary fat digestion (Fig. 2B). Enterostatin binds to the ATP synthase β subunit and inhibits ATP synthesis (38, 39, 301). Binding of enterostatin to the mitochondrial ATP synthase in insulinoma cells leads to an ~31% decrease of ATP production accompanied by an increase in thermogenesis and oxygen consumption (38). The binding of enterostatin to F_1 is inhibited by β-casomorphin, a peptide derived from the digestion of β-casein in milk (38, 39, 301).

Tentoxin and Its Derivatives

The properties and inhibitory potencies of tentoxin and its analogs are summarized in Table 2. Tentoxin is a natural cyclic tetrapeptide produced by phytopathogenic fungi, *Alternaria* species (19, 257, 342). In aqueous solution, tentoxin exists as four interconverting conformations in different proportions (51, 37, 8, and 4%) resulting from a "conformational peptide flip" (318). At low concentrations, tentoxin acts as an uncompetitive inhibitor of the ATPase activity of CF_1 derived from certain sensitive plant species but not of homologous CF_1s from chloroplasts of some other plant species. Also, tentoxin does not inhibit the ATPase activity of F_1s derived from bacteria or mitochondria (19, 378, 380). Tentoxin also inhibits ATP synthesis in chloroplasts from the sensitive species. In contrast to the above, tentoxin at high concentrations strongly stimulates ATPase activity of CF_1 (379) and partially reactivates the proton transport-coupled activity of the membrane-bound CF_0F_1 (369). Based on labeling studies, tentoxin-sus-

TABLE 3. Leucinostatins and efrapeptins

Name	Molecular formula	Source	Synonyms	Inhibitory potency (reference)
Leucinostatin	A, $C_{62}H_{111}N_{11}O_{13}$; B, $C_{61}H_{109}N_{11}O_{13}$; C, $C_{60}H_{107}N_{11}O_{13}$; D, $C_{56}H_{101}N_{11}O_{11}$; H, $C_{57}H_{103}N_{11}O_{12}$; K, $C_{62}H_{111}N_{11}O_{14}$	A, *P. lilacinus, P. marquandii*, and *P. abruptus*; B, *P. lilacinus* and *P. marquandii*; C, *P. lilacinus*; D, *P. lilacinus* and *P. marquandii*; H and K, *P. marquandii*	A, A20668, paecilotoxin A, CC-1014; B, paecilotoxin B; C, paecilotoxin C; D, paecilotoxin D; H, paecilotoxin H; K, paecilotoxin K	11 μg/mg protein[a] (*Crithidia asciculate* SMP-ATPase) (439); 2 μg inhibitor/ml[a] (spinach chloroplast, photophosphorylation) (242); 0.1–0.4 μg/mg protein (rat liver mitochondria, ATPase) (328)
Efrapeptin	C, $C_{80}H_{137}N_{18}O_{16}^{+}$; D, $C_{81}H_{139}N_{18}O_{16}^{+}$; E, $C_{82}H_{141}N_{18}O_{16}^{+}$; F, $C_{82}H_{141}N_{18}O_{16}^{+}$; G, $C_{83}H_{143}N_{18}O_{16}^{+}$	*Tolypocladium* species	Efrastatin, A23871	0.56 mol/mol F_1[a] (bovine heart MF_1-ATPase) (83); 70 ng/ml[a] (*C. asciculate* MF_1-ATPase) (173); 0.3 μM[a] (human umbilical vein endothelial cell, nonmitochondrial ATP synthase, ATP synthesis) (17); 0.5 μg/ml[a] (*R. rubrum* chromatophores, photophosphorylation) (241); 0.05–0.5 μg of inhibitor/mg protein[a] (*T. pyriformis* SMP-ATPase) (404); 21.5 μM[b] (EF_1-ATPase) (436); 10 nM[c] (bovine heart MF_1-ATPase) (83); complete inhibition at 2.4 mol inhibitor/mol enzyme (bovine heart SMP-ATPase and ATP synthesis) (83)

[a] I_{50}.
[b] K_i.
[c] K_d.

ceptible CF_1 is considered to contain a high-affinity inhibitory binding site and one or two low-affinity stimulatory binding sites (69, 265, 317, 350). The binding of tentoxin to a low-affinity binding site releases the inhibitory effect caused by binding of tentoxin to the high-affinity binding site and reactivates the enzyme. The binding of a tentoxin molecule to the third site with very low affinity results in overactivation (265). In the crystal structure of the CF_1-tentoxin complex, a tentoxin molecule is bound at the high-affinity binding site located in a cleft at an αβ subunit interface. Here, it blocks the contact between αArg-297 and βAsp-83 (153, 155), restrains the movements of these residues, and also restrains conformational changes at the catalytic interface. This may arrest the catalytic αβ interface in the closed conformation and thereby hinder its transformation into the open conformation (153, 155).

MeSer[1]-TTX, Ala[1]-TTX, Sar[1]-TTX, Gly[1]-TTX, MeSer(Bn)[1]-TTX, MeGlu[1]-TTX, MeGlu(tBu)[1]-TTX, Lys[2]-TTX, Lys(Z)[2]-TTX, MeΔTyr[3]-TTX, MeΔTyr(Me)[3]-TTX, ΔPhe[3]-TTX, dihydro-TTX, and Iso[3]-TTX are synthetic analogs of tentoxin in which an amino acid residue is mutated at the residue number indicated (316, 351) (Fig. 2C). MeSer[1]-TTX appears to inhibit isolated CF_1 and the membrane-bound enzyme (CF_0CF_1) in thylakoids and proteoliposomes the same way and with the same efficiency as tentoxin. However, MeSer[1]-TTX exhibits much weaker reactivation of CF_1 than tentoxin at high concentrations (69). On the other hand, MeΔTyr(Me)[3]-TTX shows similar activities as tentoxin in both inhibitory and stimulatory potencies (69). MeSer(Bn)[1]-TTX, MeGlu[1]-TTX, Glu(tBu)[1]-TTX, Lys[2]-TTX, and MeSer[1]-TTX analogs exhibit inhibitory activities with lower affinities but show no stimulatory effects (69).

Leucinostatins and Efrapeptins

The leucinostatins (A to D, H, and K) are nonapeptide antibiotics produced by *Paecilomyces* (Fig. 2D and Table 3). Leucinostatin A is produced by *Paecilomyces lilacinus*, *P. marquandii*, and *P. abruptus* (434), leucinostatin B by *P. lilacinus*, and *P. marquandii* (266), leucinostatin C by *P. lilacinus* (259), leucinostatin D by *P. lilacinus* and *P. marquandii* (259, 339), and leucinostatin H and K by *P. marquandii* (259, 339). Leucinostatins adopt an α-helical conformation, and contains three Aib residues and some uncommon amino acid residues (71). Different types of leucinostatin differ in the kinds of amino acid at position 2 (Dec or Leu) and in the substitution pattern at the terminal nitrogen atom [$-N(CH_3)_2$, $-NHCH_3$, $-NH_2$, or $-NO(CH_3)_2$]. Leucinostatins bind to the F_0 part of ATP synthases (127, 404, 439) and inhibit oxidative phosphorylation in mitochondria and photophosphorylation in chloroplasts (224, 242, 328). Leucinostatins have no inhibitory activity on isolated F_1-ATPase (127, 439).

Efrapeptins are a group of lipophilic peptide antibiotics (efrapeptins C to G) produced by *Tolypocladium* species (Fig. 2D and Table 3). Efrapeptin inhibits both ATP hydrolysis and ATP synthesis reactions of the ATP synthase from mitochondria, chloroplasts, and photosynthetic bacteria by binding at the F_1 catalytic domain (2, 164, 173, 224, 232, 241, 242). Efrapeptin inhibits the ATP synthase from some, but not all, nonphotosynthetic bacteria, including thermophilic *Bacillus* strain PS3 (343, 436). The mode of inhibition by efrapeptin during ATP synthesis is competitive with ADP and phosphate (83). Efrapeptin also binds to the nonmitochondrial ATP synthase of endothelial cells and inhibits extracellular

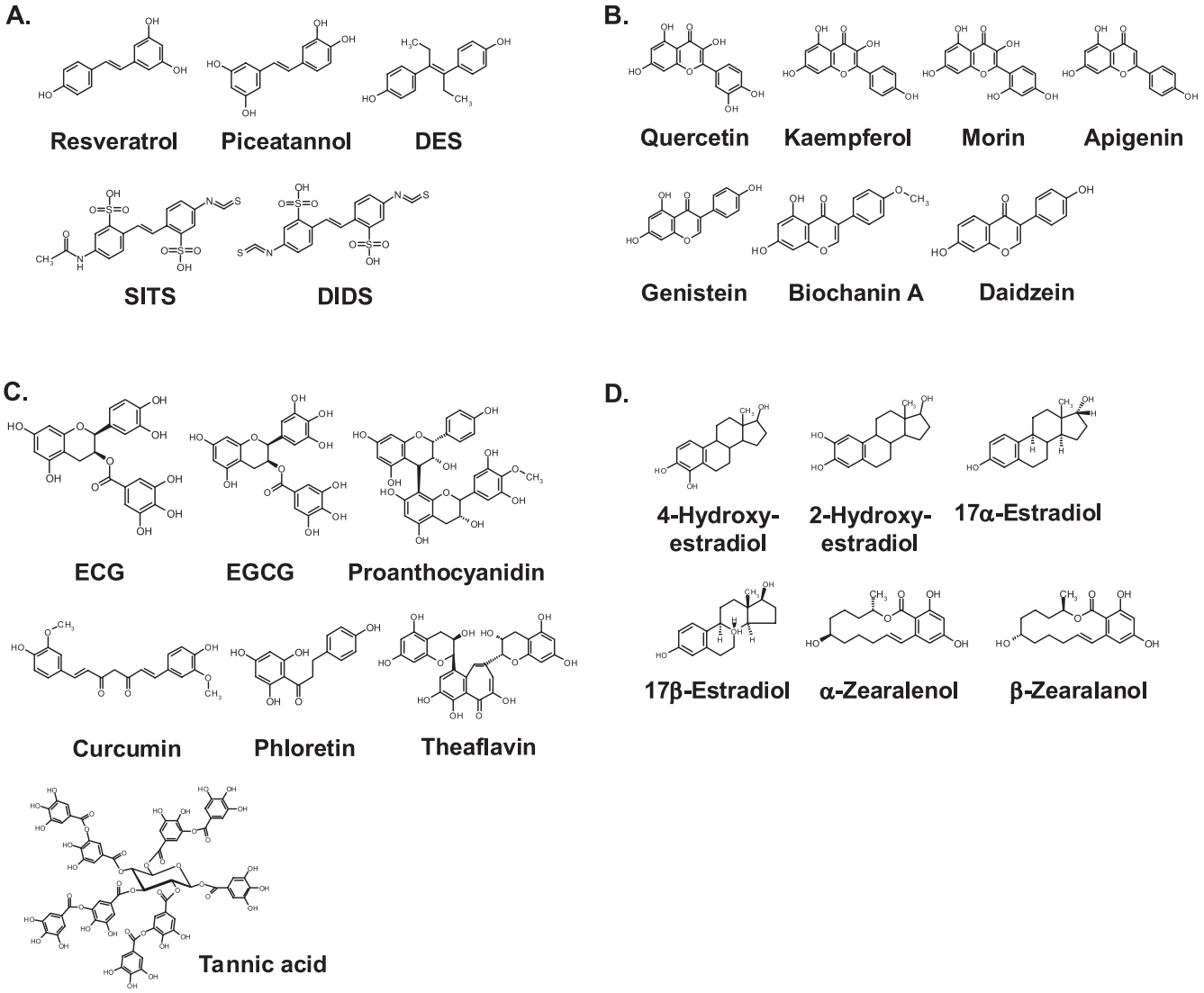

FIG. 3. Structures of polyphenolic phytochemicals, estrogens, and structurally related compounds. (A) Stilbenes. SITS, 4-Acetamido-4′-isothiocyanostilbene 2,2′-disulfonate; DIDS, 4,4′-diisothiocyanatostilbene-2,2′-disulfonic acid. (B) Flavones and isoflavones. (C) Other polyphenolic phytochemicals. ECG, epicatechin gallate; EGCG, epigallocatechin gallate. (D) Steroidal estradiols and estrogen metabolites.

ATP synthesis (17). In the crystal structure of the F_1-ATPase–efrapeptin complex, a single efrapeptin molecule is bound in the large central cavity of F_1 lined with β_E, α_E, α_{TP}, and the α-helical structure of the γ subunit. The binding of efrapeptin is stabilized predominantly by hydrophobic interactions between efrapeptin and the residues in the cavity and also by two potential intermolecular hydrogen bonds (2). Efrapeptin is believed to inhibit the ATP synthase by preventing the β_E subunit from converting into a nucleotide binding conformation.

POLYPHENOLIC PHYTOCHEMICALS, ESTROGENS, AND STRUCTURALLY RELATED COMPOUNDS

Phytochemicals are naturally occurring bioactive nonnutrient compounds derived from plants. They possess chemopreventive or chemotherapeutic effects associated with reduced risk of various diseases, including cancer, and they bind to multiple molecular targets in the body (30, 286, 395). Phytochemicals are categorized into various groups, and among these are the polyphenolic phytochemicals. Some of the polyphenolic phytochemicals, many of which are phytoestrogens, bind to the ATP synthase and inhibit its ATPase activity. (Fig. 3) (143, 448, 449). The effects of polyphenolic phytochemicals on the ATPase activity of ATP synthase are additive, and the phenolic structures that comprise the polyphenolic phytochemicals play an important role in their inhibitory potencies (448). Two or more phenolic structures appear to be required, and the position of hydroxy groups seems to affect significantly the inhibitory effectiveness of polyphenolic phytochemicals on the ATP synthase (448).

Some endogenous and synthetic estrogens also target ATP synthase. Endogenous steroidal estradiols and estrogen metabolites and synthetic nonsteroidal stilbene estrogens bind to mitochondrial ATP synthase and inhibit its ATPase activity (450, 451).

TABLE 4. Stilbenes

Name or abbreviation	Molecular formula	Source	Other names	Inhibitory potency, I_{50} (reference)
Resveratrol	$C_{14}H_{12}O_3$	Grapes and red wine	3,4′,5-Stilbenetriol; 3,4′,5-trihydroxystilbene	27.7 μM (rat brain SMP, ATP synthesis) (448); 14 μM (rat liver MF_1-ATPase) (449); 19 μM (rat brain M F_0F_1-ATPase) (448); 6.4 μM (bovine heart MF_1-ATPase) (143); 2 μM (human umbilical vein endothelial cell, nonmitochondrial ATP synthase, ATP synthesis) (17)
Piceatannol	$C_{14}H_{12}O_4$	Seeds of *Euphorbia lagascae*	3,5,3′,4′-Tetrahydroxystilbene; 3-hydroxyresveratol	8–9 μM (rat brain MF_0F_1 ATPase) (448, 449); 4 μM (rat liver MF_1-ATPase) (449); 6.1 μM (bovine heart MF_1-ATPase) (143); 1.5 μM (human umbilical vein endothelial cell, nonmitochondrial ATP synthase, ATP synthesis) (143); ~70% inhibition at 10 μM (bovine heart MF_1-ATPase) (325)
DES	$C_{18}H_{20}O_2$	Synthetic	Diethylstilbestrol; (*E*)-4,4′-(1,2-diethyl-1,2-ethenediyl)bisphenol; 4,4′-dihydroxydiethylstilbene; (*E*)-3,4-bis(4-hydroxyphenyl)-3-ascic; Acnestrol; Antigestil; Comestrol; Cyren; Desma; Dibestrol; Distilbene; Estrobene; Pabestrol; Stilbetin; Vagestrol	10 μM (rat liver MF_0F_1-ATPase) (252); 10–25 μM (rat brain MF_0F_1-ATPase) (451)
SITS	$C_{17}H_{14}N_2O_7S_3$	Synthetic	4-Acetamido-4′-isothiocyanostilbene 2,2′-disulfonate	~1.3 μM (*V. parahaemolyticus* F_0F_1-ATPase) (290); 95% inhibition at 25 μM (*V. parahaemolyticus* F_1-ATPase) (344)
DIDS	$C_{16}H_{10}N_2O_6S_4$	Synthetic	4, 4′-D-Isothiocyanatostilbene-2,2′-disulfonic acid; diisothiocyanatostilbene-2,2-disulfonic acid	20.9 μM (rat liver MF_1ATPase) (40)

Stilbenes

Stilbenes consist of two phenolic rings linked by a spacer containing a double bond (Fig. 3A). Stilbene phytoalexins, resveratrol, and piceatannol are natural phytochemicals found in grapevine organs such as berries, leaves, canes, and roots. They inhibit the ATPase activity of mitochondrial ATP synthase by targeting the F_1 catalytic headpiece (Table 4) (325, 448, 449). The mode of inhibition by resveratrol is mixed (448). In contrast to the above, resveratrol and piceatannol show no inhibition of ATPase activity of F_1 from thermophilic *Bacillus* strain PS3 (TF_1) (143). Resveratrol and piceatannol bind to a hydrophobic pocket between the hydrophobic tip in the C-terminal region of the γ subunit and the hydrophobic inside of an annulus provided by the β_{TP} subunit (142). The binding of these inhibitors, stabilized by hydrophobic interactions and hydrogen bonds, is believed to block the rotation of the γ subunit, inhibiting both the hydrolysis and synthesis of ATP. Resveratrol and piceatannol are bound to a single binding site in F_1, and there are no equivalent sites between the γ subunit and either the β_{DP} or β_E subunit.

Diethylstilbestrol (DES) is a synthetic nonsteroidal estrogen. DES targets F_0 and inhibits both ATPase and ATP-dependent proton translocation activities of both membrane-bound and isolated F_0F_1 from mitochondria (252, 451). DES inhibits membrane-bound F_0F_1 with half-maximal and maximal inhibitory effects at about 10 and 60 μM, respectively (252). For the isolated F_0F_1, the concentration for 50% inhibition is 10 μM, and maximal inhibition of ATPase activity is about 90%. In contrast, DES has little effect on the ATPase activity of the F_1 moiety, exhibiting only ~20% inhibition at 60 μM. The binding site of DES is considered to be structurally distinct from other types of F_0 inhibitors, as DES provides no protection against the inhibition of the F_0F_1 complex by *N*,*N*′-dicyclohexylcarbodiimide (DCCD), which is protected by oligomycin, venturicidin, and tricyclohexyltin. The combination of DES and DCCD produces a synergic inhibitory effect at low concentrations (<20 μM).

4-Acetamido-4′-isothiocyanostilbene 2,2′-disulfonate and 4,4′-di-isothiocyanatostilbene-2,2′-disulfonic acid are structurally very analogous and have been known as anion exchanger inhibitors. They also bind to ATP synthase and inhibit its catalytic activity. 4-Acetamido-4′-isothiocyanostilbene 2,2′-disulfonate strongly inhibits the ATPase activity of both F_1 and F_0F_1 from *Vibrio parahaemolyticus* (290, 344). 4,4′-Di-isothiocyanatostilbene-2,2′-disulfonic acid also inhibits both the hydrolysis and synthesis of ATP in submitochondrial particles (SMP) and also ATP hydrolysis of isolated F_1 from rat liver mitochondria (40).

Flavones and Isoflavones

Flavones and isoflavones are flavonoid-related polyphenolic compounds. Flavones and isoflavones differ in the position of a phenyl group on the 4H-1-benzopyr-4-one skeleton. Flavones are produced in various plants, whereas isoflavones are produced almost exclusively by beans. The flavones, quercetin,

TABLE 5. Flavones and isoflavones

Name	Molecular formula	Source	Other names	Inhibitory potency (reference)
Quercetin	$C_{15}H_{10}O_7$	Various plants	3,3′,4′,5,7-Pentahydroxyflavone; natural yellow 10; meletin; flavin meletin; quercetol; Xanthaurine	5 kmol/mol[a] (232), 85 μM[a] (343) (bovine heart MF_1-ATPase); 180 μM[a] (bovine heart SMP-ATPase) (343); 50 μM[a] (rat brain F_0F_1-ATPase) (448); 3 μM[a] (rat liver F_1-ATPase) (449); 2 kmol/mol[a] (spinach CF_1-ATPase) (232); 2.6 μg/mg protein[a] (*C. asciculate* SMP-ATPase) (439); 0.2 mM[b] (pig heart MF_1-ATPase) (100); 27 μM[c] (bovine heart MF_1-ATPase) (232); 46% inhibition at 5 μM (*C. thermoaceticum* membrane-bound F_0F_1-ATPase) (190)
Kaempferol	$C_{15}H_{10}O_6$	Delphinium, witch-hazel, grapefruit, and other plant sources	Kempferol; campherol; indigo yellow; nimbecetin; pelargidenolon; populnetin; rhamnolutein; 3,4′,5,7-tetrahydroxyflavone; trifolitin	55 μM[a] (rat brain MF_0F_1-ATPase) (448)
Morin	$C_{15}H_{10}O_7$	Various plants	2′,3,4′,5,7-Pentahydroxyflavone; 2′,4′,5,7-tetrahydroxyflavan-3-ol; 3,5,7,2′,4′-pentahydroxyflavonol; al-morin; aurantica; calico yellow; osage orange	60 μM[a] (rat brain MF_0F_1-ATPase) (448)
Apigenin	$C_{15}H_{10}O_5$	Parsley, artichoke, basil, celery and other plants	4′,5,7-Trihydroxyflavaone; 2-(*p*-hydroxyphenyl)-5,7-dihydroxychromone; apigenol; chamomile; spigenin	105 μM[a] (rat brain MF_0F_1-ATPase (448)
Genistein	$C_{15}H_{10}O_5$	Soybean	4′,5,7-Trihydroxyisoflavone; genisteol; genisterin; prunetol; sophoricol; differenol A	55 μM[a] (rat brain MF_0F_1-ATPase) (448); 10% inhibition at 50 μM (rat liver F_1-ATPase) (449)
Biochanin A	$C_{16}H_{12}O_5$	Soybean	Biochanin; 4′-methylgenistein; 5,7-dihydroxy-4′-methoxyisoflavone; CCRIS 5449; 5,7-dihydroxy-4′-methoxyisoflavone	65 μM[a] (rat brain MF_0F_1-ATPase) (448)
Daidzein	$C_{15}H_{10}O_4$	Soybean	4′,7-Dihydroxyisoflavone; daidzeol; 7-hydroxy-3-(4-hydroxyphenyl)-4-benzopyrone	127 μM[a] (rat brain MF_0F_1-ATPase) (448)

[a] I_{50}.
[b] K_i.
[c] K_d.

kaempferol, morin, and apigenin inhibit ATP hydrolysis (Fig. 3B). Specifically, quercetin inhibits the ATPase activities of mitochondrial F_1 (MF_1) and F_0F_1 (223, 448, 449) and also these activities in spinach chloroplasts (96), *Escherichia coli* (130), and *Clostridium thermoaceticum* (190). However, quercetin inhibits neither the ATPase activity of TF_1 (343), a thermophilic bacterial ATP synthase, nor the ATP synthetic activity of mitochondrial ATP synthase (F_0F_1) (223). In contrast, quercetin has a stimulatory effect on photophosphorylation (218). Kaempferol and morin have inhibitory potencies similar to that of quercetin on the ATPase activity of mitochondrial F_0F_1, while apigenin, in which the 3-hydroxyl group in the chromone moiety is absent, shows about half the inhibitory potency (Table 5) (448).

Genistein, biochanin A, and daidzein are isoflavone phytoalexins found in soybeans. Genistein inhibits noncompetitively both the ATP hydrolysis and ATP synthesis activities of mitochondrial ATP synthase, most likely by targeting F_0 (448, 449). Biochanin A inhibits the ATPase activity of mitochondrial F_0F_1 with an inhibitory potency similar to that of genistein. Compared to genistein and biochanin, daidzein contains only one hydroxyl group in the 4-chromone moiety and shows about half the inhibitory potency (448).

Other Polyphenolic Phytochemicals

Catechins are flavonoid compounds called flavan 3-ols. They are abundant in green tea, which includes four main catechins, epicatechin, epicatechin gallate, epigallocatechin, and epigallocatechin gallate. Among the catechins, epicatechin gallate and epigallocatechin gallate are inhibitors of the ATP hydrolysis activity of ATP synthase (Fig. 3C) (448). Epigallocatechin gallate, in which one more hydroxyl group is attached in the catechol moiety of epicatechin gallate, shows about three times higher potency than epicatechin gallate in the inhibition of ATPase activity of mitochondrial F_0F_1.

Grape seed proanthocyanidin extract, curcumin, an active ingredient of the Indian curry spice, and phloretin from apples inhibit the ATPase activity of mitochondrial F_0F_1. Theaflavin, a phytochemical from tea, and tannic acid, anionic polymers from the bark of trees, also exhibit inhibitory effects on the ATPase activity of mitochondrial F_0F_1 (Table 6) (448).

Steroidal Estradiols and Estrogen Metabolites

Endogenous steroidal estradiols and estrogen metabolites have inhibitory effects on mitochondrial ATP synthase (Fig. 3D

TABLE 6. Other polyphenolic phytochemicals

Name or abbreviation	Molecular formula	Source	Other names	Inhibitory potency, I_{50} (reference)
ECG	$C_{22}H_{18}O_{10}$	Green tea	(−)Epicatechin gallate; epicatechin-3-gallate; epicatechin-3-galloyl ester	45 μM (rat brain MF_0F_1-ATPase) (448)
EGCG	$C_{22}H_{18}O_{11}$	Green tea	(−)-Epigallocatechin gallate; (−)-epigallocatechin gallate; (−)-epigallocatechin-3-*O*-gallate; CCRIS 3729; tea catechin	17 μM (rat brain MF_0F_1-ATPase) (448)
GSPE	$C_{31}H_{28}O_{12}$	Grape seed	Grape seed proanthocyanidin extract; polyhydroxyflavan-3-ol	30 μg of inhibitor/ml (rat brain F_0F_1-ATPase) (448)
Curcumin	$C_{21}H_{20}O_6$	*Curcuma longa*	Natural yellow 3; 1,7-bis(4-ascicul-3-methoxyphenyl)-1,6-heptadiene-3,5-dione	40 μM (rat brain MF_0F_1 ATPase) (448)
Phloretin	$C_{15}H_{14}O_5$	Mainly from apples	Phloretol; 2′,4′,6′-trihydroxy-3-(*p*-hydroxyphenyl)propiophenone; dihydronaringenin; β-(*p*-hydroxyphenyl)-2,4,6-trihydroxypropiophenone	40% inhibition at 70 μM (rat brain MF_0F_1-ATPase) (448)
Theaflavin	$C_{29}H_{24}O_{12}$	Tea	1,8-Bis((2*R*,3*R*)-3,5,7-trihydroxy-2*H*-1-benzopyran-2-yl)-3,4,6-trihydroxy-5*H*-benzocyclohepten-5-one	20 μg of inhibitor/ml (rat brain F_0F_1-ATPase) (448)
Tannic acid	A mixture of related compounds (mainly glucose esters of gallic acid)	Bark of trees	Gallotannic acid; gallotannin; glycerite; tannin	5 μg of inhibitor/ml (rat brain F_0F_1-ATPase) (448)

and Table 7) (451). Two catecholestrogens, 4-hydroxyestradiol and 2-hydroxyestradiol, inhibit the ATPase activity of the mitochondrial ATP synthase, and the 4-hydroxyestradiol is about twofold more effective than the 2-hydroxyestradiol. 17β-Estradiol and 17α-estradiol inhibit the ATPase activity of solubilized brain mitochondrial fractions by 7 and 25% at 14 and 42 μM, respectively. Two micoestrogens, α-zearalenol and β-zearalenol, also inhibit mitochondrial F_0F_1-ATPase activity. The I_{50} value of α-zearalenol is about 50 μM, and the inhibitory potency of α-zearalenol is about three- to fourfold stronger than

TABLE 7. Steroidal estradiols and estrogen metabolites

Name	Molecular formula	Source	Other names	Inhibitory potency, I_{50} (reference)
4-Hydroxyestradiol	$C_{18}H_{24}O_3$	Natural estrogen	4-Hydroxyestradiol-17β; 4-hydroxy-17-β−estradiol; estra-1,3,5(10)-triene-3,4,17-β-triol	55 μM (rat brain MF_0F_1-ATPase) (451)
2-Hydroxyestradiol	$C_{18}H_{24}O_3$	Natural estrogen	(17β)-Estra-1,3,5(10)-triene-2,3,17-triol; estra-1,3,5(10)-triene-2,3,17-β-triol	110 μM (rat brain MF_0F_1-ATPase) (451)
17-α-Estradiol	$C_{18}H_{24}O_2$	Natural estrogen	1,3,5-Estratriene-3,17-α-diol; 3,17-dihydroxyestratriene; 3,17-α-dihydroxyoestra-1,3,5(10)-triene; epiestradial; epiestradiol; estra-1,3,5(10)-triene-3,17α-diol; oestra-1,3,5(10)-triene-3,17α-diol; estradiol-17-α; α-estradiol	25% inhibition at 42 μM (rat brain MF_0F_1-ATPase) (451)
17-β-Estradiol	$C_{18}H_{24}O_2$	Natural estrogen	1,3,5-Estratriene-3,17-β-diol; 17-β-estra-1,3,5(10)-triene-3,17-diol; 17-β-OH-estradiol; 17-β-OH-estradiol; 17-β-oestra-1,3,5(10)-triene-3,17-diol; 17β-oestra-1,3,5(10)-triene-3,17-diol; 3,17-epidihydroxyestratriene; 3,17-epidihydroxyoestratriene; 3,17-β-dihydroxy-1,3,5(10)-oestratriene; 3,17-β-estradiol; 3,17-β−estradiol; Aerodiol; Aquadiol	7% inhibition at 14 μM (rat brain MF_0F_1-ATPase) (451)
α-Zearalenol	$C_{18}H_{24}O_5$	Natural mycoestrogen	(4*S*,8*R*,12*E*)-8,16,18-Trihydroxy-4-methyl-3-oxabicyclo[12.4.0]octadeca-12,15,17,19-tetraen-2-one; trans-zearalenol	50 μM (rat brain MF_0F_1-ATPase) (451)
β-Zearalanol	$C_{18}H_{24}O_5$	Natural mycoestrogen	(8*S*,12*E*)-8,16,18-Trihydroxy-4-methyl-3-oxabicyclo[12.4.0]octadeca-12,15,17,19-tetraen-2-one	150–200 μM (rat brain MF_0F_1-ATPase) (451)

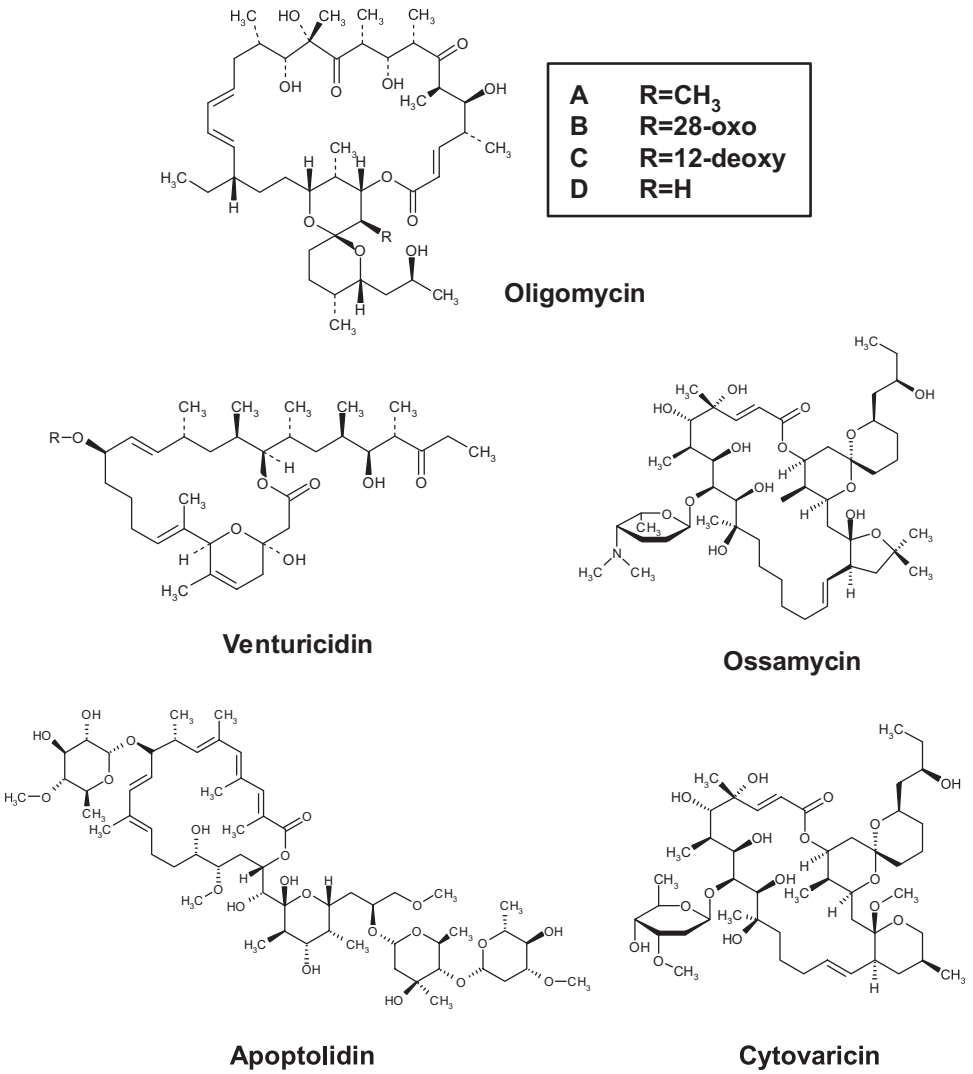

FIG. 4. Structures of polyketide inhibitors.

that of β-zearalenol. The mechanism of inhibition by the steroidal estradiols and estrogen metabolites is not defined clearly, but the ATP synthase OSCP subunit has been identified as an estradiol binding protein, and it has been suggested that the inhibition is mediated by the binding of estrogens to OSCP (450).

POLYKETIDE INHIBITORS

Polyketides are polymers of two-carbon ketide units synthesized by polyketide synthases. Macrolides belong to the polyketide class and contain a macrolide ring, a large lactone ring to which one or more deoxy sugars, usually cladinose and desosamine, are attached (Fig. 4). Some natural macrolides, apoptolidin, cytovaricin, oligomycin, ossamycin, and venturicidin are elaborated by *Nocardiopsis* spp. and various strains of *Streptomyces* and are known as potent inhibitors of ATP synthase (Table 8) (205, 207, 225, 330, 358, 359). The binding sites of the macrolide inhibitors are located within the F_0 part of the complex.

Oligomycins are a closely related group of 26-membered macrolides with both lactone moieties and double bonds. Oligomycins are produced in various strains of *Streptomyces*. They include six different types, A, B, C, D, E, and F, based on the R groups attached to the macrolide ring and sugar. Oligomycin D is also named rutamycin. Other specific oligomycins include peliomycin and botrycidin; the latter is known also as venturicidin X. Oligomycin inhibits ATP synthases from mitochondria and the chromatophores of photosynthetic bacteria (85, 150, 151, 253, 311, 347, 360). However, it has no or only a weak effect on photophosphorylation activity in chloroplasts and on membrane-bound ATPase activity of nonphotosynthetic bacteria (22, 36, 118, 285, 311, 376). Mutagenesis studies that cause resistance to oligomycin in yeast implicate a target site residing at the interface of subunits *a* and *c*, with an involvement of both Gly23 and Glu59 of the N- and C-terminal transmembrane helices of subunit *c*, respectively (97, 192, 280). Yeast Glu59 of subunit *c* is equivalent to *E. coli* Asp61, located in the middle of the membrane, and is believed to be involved in proton translocation that drives ATP synthesis.

TABLE 8. Polyketide inhibitors

Name	Molecular formula	Source	Other names	Inhibitory potency (reference)
Oligomycin	A, $C_{45}H_{74}O_{11}$; B, $C_{45}H_{72}O_{12}$; C, $C_{45}H_{74}O_{10}$; D, $C_{44}H_{72}O_{11}$; E, $C_{45}H_{72}O_{13}$; F, $C_{46}H_{76}O_{11}$	A, B, and C, *Streptomyces diastratochroogenes*; D, *Streptomyces griseus, Streptomyces aureofaciens, Streptomyces rutgersensis*	D, Rutamycin, 26-demethyl-oligomycin A, A272	152 μg inhibitor/mg protein[a] (*E. coli* membrane vesicle, pH gradient formation) (311); 7.1 μg inhibitor/mg protein[a] (*C. asciculate* SMP-ATPase) (439); 2.0–3.0 μg inhibitor/mg protein[a] (*S. cerevisiae* SMP-ATPase) (150, 151); A, 0.3 μM[a] (human NCI-60 cell lines, F_0F_1-ATPase) (348); 15 ng inhibitor/mg protein[b] (*N. crassa* SMP-ATPase) (112); 0.21 μM[b] (bovine heart MF_0F_1-ATPase) (85); 95% inhibition at 0.4 μg inhibitor/mg protein (bovine heart SMP-ATPase) (140); D, 75% inhibition at 0.5 μg/ml (rat liver SMP-ATPase) (423)
Peliomycin	$C_{46}H_{76}O_{14}$	Various strains of *Streptomyces*		4.5 μg inhibitor/mg protein[a] (*S. cerevisiae* SMP-ATPase) (150)
Venturicidin	A, $C_{41}H_{57}NO_{11}$; B, $C_{40}H_{64}NO_{10}$; X, $C_{34}H_{54}O_7$	*Streptomyces aureofaciens*, *Streptomyces griseolus, Streptomyces halstedii, Streptomyces xanthophaeus, Streptomyces hygroscopicus*	X, botrycidin	9 μg inhibitor/mg protein[a] (*E. coli* pH gradient formation by membrane vesicle) (311); 11 μg inhibitor/mg protein[a] (*E. coli* membrane-bound ATPase) (311); 0.13 μg inhibitor/mg protein[a] (150); 0.06–0.18[a] (A and B) and 11.0[a] (X) μg inhibitor/mg protein (*S. cerevisiae* SMP-ATPase) (151); 5–11 μg inhibitor/mg protein[a] (*T. pyriformis*) (404); 3.0 μg/mg protein[a] (*C. asciculate* SMP-ATPase) (439); 0.5 μM[a] (spinach thylakoids, photophosphorylation) (447); 0.5 μM[a] (spinach thylakoids, ATPase) (447)[a]
Ossamycin	$C_{50}H_{87}NO_{14}$	*S. hygroscopicus* subsp. *ossamyceticus*		1.3 μg of inhibitor/mg protein[a] (*S. cerevisiae* SMP-ATPase) (150); 46 μg of inhibitor/mg protein[a] (*E. coli* pH gradient formation by membrane vesicle) (311); 8 μM[a] (human NCI-60 cell lines, F_0F_1-ATPase) (348)
Apoptolidin	$C_{58}H_{96}O_{21}$	*Nocardiopsis* sp.		4–5 μM[b] (*S. cerevisiae* membrane-bound F_0F_1-ATPase) (349); 18 μM[a] (human NCI-60 cell lines, F_0F_1-ATPase) (348)
Cytovaricin	$C_{48}H_{82}O_{15}$	*Streptomyces* sp. strain H-230	H-230	1 μM[a] (human NCI-60 cell lines, F_0F_1-ATPase) (348); 0.4 μM[b] (*S. cerevisiae* membrane-bound F_0F_1-ATPase) (349)

[a] I_{50}.
[b] K_i.

Peliomycin, produced from various strains of *Streptomyces* (323, 358), is cytotoxic to mammalian cells, with limited antimicrobial and antifungal activities. The inhibitory properties of peliomycin on ATP synthesis by oxidative phosphorylation in mitochondria mimic those of rutamycin (423).

Venturicidin consists of three different types, A, B, and X, where venturicidin X is an aglycone of venturicidin A or B (401). It binds to subunit *c* of the ATP synthase and inhibits both proton translocation and membrane-bound ATPase activities from bacteria, chloroplasts, and mitochondria (62, 251, 311, 423, 447). The region conferring venturicidin resistance or hypersensitivity in ATP synthase is located in the middle of the membrane, and most of this region overlaps with that for oligomycin resistance (123, 131, 280).

Ossamycin is a 24-membered macrolide produced in *Streptomyces hygroscopicus* subsp. *ossamyceticus* (209, 359). Ossamycin inhibits both the ATPase and oxidative phosphorylation activities of mitochondrial ATP synthase (150, 423). It has no direct effect on *E. coli* F_1 (EF_1) or F_0, but it does inhibit ATP-driven proton transport by uncoupling ATP

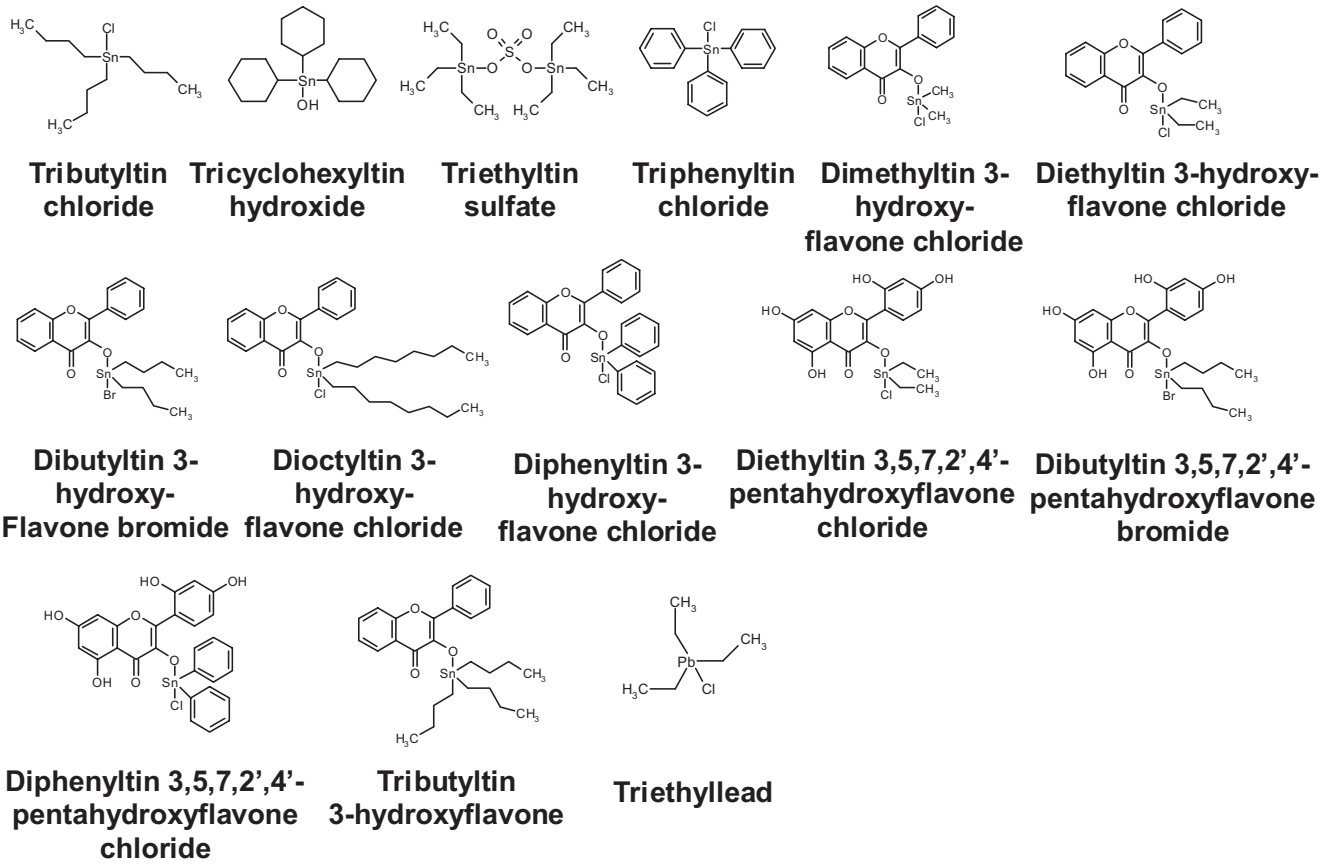

FIG. 5. Structures of organotin compounds and structural relatives.

hydrolysis from proton transport (311). The binding site of ossamycin in mitochondrial ATP synthase lies close to the boundaries of regions that cause oligomycin and venturicidin resistance in subunit *c*. This site contains residues Leu53 to Leu57 (yeast sequence) in the C-terminal transmembrane helix (131).

Apoptolidin and cytovaricin are 20- and 26-membered macrolides found in *Nocardiopsis* spp. and *Streptomyces* sp. strain H-230, respectively. Both apoptolidin and cytovaricin inhibit membrane-bound mitochondrial ATP synthase. The precise binding sites of apoptolidin and cytovaricin are not yet defined. However, they are believed to be located at regions where oligomycin and ossamycin bind, as the chemical backbones of these inhibitors are structurally similar to those of oligomycin and ossamycin (349).

ORGANOTIN COMPOUNDS AND STRUCTURAL RELATIVES

Organotin compounds are organic compounds that contain tin. They are classified as R_4Sn, R_3SnX, R_2SnX_2, and $RSnX_3$. Among these, R_3SnX organotin compounds have been used as biocides and pesticides and are known to inhibit ATP synthase (Fig. 5) (148–150, 190, 252, 403–405, 418, 437). Some R_4Sn organotin compounds, such as tributyltin 3-hydroxyflavone, also inhibit ATP synthase (405). The organotin compounds inhibit both ATP hydrolysis and ATP synthesis catalyzed by the membrane-bound and isolated F_0F_1 complex. However, they have no effect on the ATPase activity of isolated F_1 (Table 9). Organotin compounds react noncovalently with the ATP synthase, and the inhibitory effect of the compounds is reversed by mono- and dithiols such as dithiothreitol and mercaptoethanol (437). The sites of action of organotin compounds are located in the ion channel within subunit *a*. Here, they are believed to inhibit ATP synthase by competing with Na^+ or H^+ for the same binding site (418). Diorganotin-3-hydroxyflavone complexes such as dibutyltin 3-hydroxyflavone bromide and diphenyltin 3-hydroxyflavone chloride show a marked fluorescence enhancement on binding to mitochondrial ATP synthase (405).

POLYENIC α-PYRONE DERIVATIVES

α-Pyrone (or 2-pyrone) is a six-membered cyclic unsaturated ester. Its derivatives are widely distributed in nature, and some α-pyrone-containing mycotoxins, such as aurovertin, citreoviridin, and asteltoxin, inhibit ATP synthase by targeting F_1 (Fig. 6).

Aurovertin is an antibiotic from *Calcarisporium arbuscula*. Five different types of aurovertins (A to E) have been reported (Table 10). Aurovertin inhibits the ATPase activity of F_1 from mitochondria and mesophilic bacteria (108, 189), whereas it has no inhibitory effect on thermophilic TF_1 (196, 343). It binds to the ATP synthase β subunit and inhibits its ATPase activity

TABLE 9. Organotin compounds and structural relatives

Name	Molecular formula	Other names	Inhibitory potency (reference)
Tributyltin chloride	$C_{12}H_{27}ClSn$	TBT-Cl; tributylchlorostannane; chlorotributyltin; tri-*n*-butyltin chloride; monochlorotributyltin; tri-*n*-butylchlorotin; tributylstannyl chloride	200 nM[b] (*E. coli* and *I. tartaricus* F_0F_1-ATPase) (418); 47% inhibition at 1 μM and 87% inhibition at 5 μM (*C. thermoaceticum* membrane-bound F_0F_1-ATPase) (190); 80% inhibition at 1 μM (TF_0F_1-ATPase) (403)
Tricyclohexyltin hydroxide	$C_{18}H_{34}OSn$	Cyhexatin; tricyclohexylhydroxytin; hydroxytricyclohexylstannane; tricyclohexylhydroxystannane; tricyclohexylstannanol; Plictran; tricyclohexylstannium hydroxide	92.9% inhibition at 37 μM (rat liver MF_0F_1-ATPase) (252)
Triethyltin sulfate	$C_{12}H_{30}O_4SSn_2$	Triethylstannium hydrogen sulfate; bis(triethyltin) sulfate; triethylhydroxytin sulfate	0.13 μg of inhibitor/mg protein[a] (*S. cerevisiae* SMP-ATPase) (150, 151); 3–7 μg of inhibitor/mg protein[a] (*T. pyriformis* SMP-ATPase) (404); 1.2 μg/mg protein[a] (*C. asciculate* SMP-ATPase) (439)
Triphenyltin chloride	$C_{18}H_{15}ClSn$	Chlorotriphenylstannane; chlorotriphenyltin; triphenylchlorotin	<10 μM[a] (bovine heart SMP-ATPase) (437)
Dimethyltin 3-hydroxyflavone chloride	$C_{17}H_{15}ClO_3Sn$		12–13 nmol inhibitor/mg protein[a] (rat liver SMP-ATPase) (405)
Diethyltin 3-hydroxyflavone chloride	$C_{19}H_{19}ClO_3Sn$		1.5 nmol inhibitor/mg protein[a] (rat liver SMP-ATPase) (405)
Dibutyltin 3-hydroxyflavone bromide	$C_{23}H_{27}BrO_3Sn$		0.7–0.9 nmol inhibitor/mg protein[a] (rat liver SMP-ATPase) (405)
Dioctyltin 3-hydroxyflavone chloride	$C_{31}H_{43}ClO_3Sn$		12–13 nmol inhibitor/mg protein[a] (rat liver SMP-ATPase) (405)
Diphenyltin 3-hydroxyflavone chloride	$C_{27}H_{19}ClO_3Sn$		1.5 nmol inhibitor/mg protein[a] (rat liver SMP-ATPase) (405)
Diethyltin 3,5,7,2′,4′-pentahydroxy flavone chloride	$C_{19}H_{19}ClO_7Sn$		5–6 nmol inhibitor/mg protein[a] (rat liver SMP-ATPase) (405)
Dibutyltin 3,5,7,2′,4′-pentahydroxy flavone bromide	$C_{23}H_{27}BrO_7Sn$		0.6–0.8 nmol inhibitor/mg protein[a] (rat liver SMP-ATPase) (405)
Diphenyltin 3,5,7,2′,4′-pentahydroxy flavone chloride	$C_{27}H_{19}ClO_7Sn$		3.5–4 nmol inhibitor/mg protein[a] (rat liver SMP-ATPase) (405)
Tributyltin 3-hydroxyflavone	$C_{27}H_{36}O_3Sn$		1.5–2 nmol inhibitor/mg protein[a] (rat liver SMP-ATPase) (405)
Triethyllead	$C_6H_{15}ClPb$	Triethylplumbane	16–17 μM[a] (rat liver SMP-ATPase) (275)

[a] I_{50}.
[b] K_i.

uncompetitively (108, 189). There are two or three binding sites for aurovertin in F_1 in the presence of ADP: one high-affinity site (K_d [dissociation constant] of 0.2 to 1 μM) and the others (one or two) of lower affinity (K_d of 3 to 6 μM) (188, 416). In contrast, two high-affinity sites are observed in the presence of ATP (188). In the crystal structure of one F_1-aurovertin complex (410), two aurovertin B molecules are bound at two equivalent sites within the β_{TP} and β_E subunits. These sites are located in a cleft between the nucleotide binding and C-terminal domains of the subunits and do not overlap with the nucleotide binding sites. In β_{TP}, the pyrone ring of aurovertin interacts with α-Glu399 of α_{TP}. However, in β_E the pyrone ring has no equivalent interaction with α_E, as the aurovertin bound in β_E is too far from α_E. The interactions between aurovertin and amino acids are mainly hydrophobic. In β_{DP}, the interface between α_{DP} and β_{DP} is tightly packed, making the aurovertin binding pocket inaccessible (410). In the binding of aurovertin to F_1, β-Arg398 (*E. coli* sequence) appears to play an important role, as mutations in this residue confer aurovertin resistance (230, 231, 424). In bacteria that are naturally resistant to aurovertin, the β-Arg398 residue is replaced with other amino acid residues (172, 343). Aurovertin is believed to inhibit F_1 by preventing catalytic interface closure involved in the cyclic interconversion of catalytic sites (410, 430). In addition, aurovertin increases the affinity of F_1 for phosphate (307). Aurovertin fluoresces weakly at 470 nm, and this is enhanced by 50- to 60-fold when aurovertin binds to F_1 (74, 136, 232). The fluorescence increase is considered to be due to the limited mobility of aurovertin at its binding site and has been used to monitor inhibition of F_1-ATPase activity (74, 136).

Aurovertin B has been tested for the treatment of breast cancer cells as an anticancer agent and has shown strong inhibition of the proliferation of breast cancer cell lines, whereas it showed little influence on normal cells (180). Aurovertin B

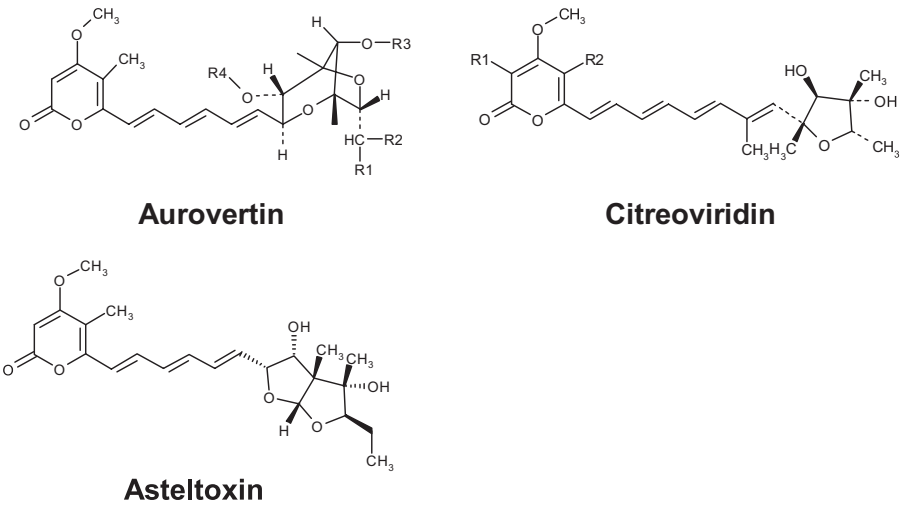

FIG. 6. Structures of polyenic α-pyrone derivatives.

induced apoptosis of cancer cells and arrested their cell cycles in G_0/G_1 phase.

Citreoviridin, produced by some molds of the genera *Penicillium* and *Aspergillus*, inhibits the ATPase activities of F_1 from bacteria and mitochondria by binding to the ATP synthase β subunit (136, 353) (Table 10). However, ATP synthases from some species are resistant (404, 439). In sensitive species, citreoviridin acts as an uncompetitive inhibitor of ATP hydrolysis by soluble and membrane-bound ATP synthase and as a noncompetitive inhibitor of ATP synthesis by the membrane-bound ATP synthase enzyme (354). The binding of citreoviridin to F_1 or its isolated β subunit is noncompetitive with respect to aurovertin (136). Although the binding site of citreoviridin within the β subunit is not clarified, it has been suggested that citreoviridin and aurovertin interact at separate sites (136). Citreoviridin fluoresces weakly at 530 nm when irradiated at 380 nm. However, unlike aurovertin, enhancement is not observed when bound to F_1 (233). Light converts

TABLE 10. Polyenic α-pyrone derivatives

Name	Molecular formula	Source	Inhibitory potency (reference)
Aurovertin	A, $C_{27}H_{34}O_9$; B, $C_{25}H_{32}O_8$; C, $C_{24}H_{30}O_8$; D, $C_{25}H_{32}O_9$; E, $C_{23}H_{30}O_7$	*C. arbuscula*	9.2 μmol/mg protein[a] and 25 μM[c] (aurovertin A, bovine heart MF_1-ATPase) (232); 2 μM[a] (aurovertin B, EF_1-ATPase) (353); 17–30 nmol/mg protein[a] and 0.1 μM[c] (aurovertin B, bovine heart MF_1-ATPase) (232); 2 nmol/mg protein[a] and 0.6 μM[c] (aurovertin C, bovine heart SMP) (232); 0.9 μM[a] (aurovertin D, EF_1-ATPase) (353); 1 μM[a] (aurovertin D, EF_1-ATPase) (436); 9–20 nmol/mg protein[a] and 60 nM[c] (aurovertin D, bovine heart MF_1-ATPase) (232); 1.6 μmol/mg protein[a] and 22 μM[c] (aurovertin E, bovine heart SMP) (232); 80 nM[a] (rat liver MF1-ATPase) (108); 66% inhibition at 10 μM (bovine heart MF_1-ATPase) (325)
Citreoviridin	A, $C_{23}H_{30}O_6$; B, unknown; C, $C_{23}H_{30}O_6$; D, $C_{24}H_{32}O_6$	A, *Penicillium citreoviride*, *Penicillium toxicarium*, *Penicillium ochrosalmoneum*, *Aspergillus terreus*; B, *A. terreus*; C, *A. terreus*; D, *A. terreus*	60 μM[a] (EF_1-ATPase) (353); 1.11 μmol/mg protein[a] (bovine heart MF_1-ATPase) (232); 2 μM[b] (*S. cerevisiae* MF_1-ATPase) (136); 4.23 μM[b] (354) (bovine heart MF_1-ATPase); 2.82 μM[b] (354), 6.1 μM[b] (354) (bovine heart SMP-ATPase); 3.1 μM[c] (232), 4.1 μM[c] (354) (bovine heart MF_1-ATPase); 60 μM[c] (EF_1-ATPase) (353)
Asteltoxin	$C_{23}H_{30}O_7$	*A. stellatus* Curzi, *E. variecolor*	10 μM[a] (EF_1-ATPase) (352); ~450 nM[a] (state 3 respiration of rat liver mitochondria) (200); 8 μM[c] (EF_1-ATPase) (352)

[a] I_{50}.
[b] K_i.
[c] K_d.

citreoviridin to its stereoisomer, isocitreoviridin, which has no effect on either ATP hydrolysis or ATP synthesis catalyzed by ATP synthase (354).

Asteltoxin is made in *Aspergillus stellatus* Curzi and *Emericella variecolor*. It contains a unique 2,8-dioxabicyclooctane ring and inhibits both BF_1 and MF_1 with a stoichiometry of 1:1 in the presence of ADP (Table 10) (200, 352). As asteltoxin fails to inhibit aurovertin-resistant mutants, it is believed to bind to the same site as aurovertin (352). Asteltoxin binding to F_1 shows an enhancement of fluorescence (emission maximum, 470 nm; excitation maximum, 385 nm). The ADP-stimulatory effect and the Mg^{2+}-quenching effect on the fluorescence enhancement of asteltoxin binding are similar to those observed for aurovertin. However, the stimulatory effect on phosphate binding to F_1 observed with aurovertin is not observed with asteltoxin (352).

CATIONIC INHIBITORS

Amphiphilic Cationic Dyes

Amphiphilic cationic dyes containing a basic amine group and a lipophilic portion (Fig. 7A) inhibit the ATPase activities of both F_1 and F_0F_1. Most exhibit a stronger inhibitory effect on the ATPase activity of F_0F_1 than on that of F_1 (Table 11).

Rhodamines are a group of fluorone dyes made by fusing an amino derivative of phenol with phthalic anhydride, and they include rhodamine B, rhodamine 123, and rhodamine 6G. Rhodamine B and rhodamine 123 inhibit the ATPase activity of MF_1 from bovine heart in a parabolic, noncompetitive manner, whereas inhibition by rhodamine 6G is mixed (433). In contrast, rhodamine 6G acts as an uncompetitive inhibitor of MF_1 and as a noncompetitive inhibitor for isolated and membrane-bound ATP synthase F_0F_1 from yeast (433). Rhodamine B and rhodamine 123 are considered to bind F_1 at more than one binding sites, while rhodamine 6G at high concentrations is believed to bind at least two binding sites (52). The precise location of rhodamine 6G binding sites in the three-dimensional structure of F_1 has yet to be identified (143).

Rosaniline, malachite green, and brilliant green are closely related in structure. Rosaniline and malachite green inhibit MF_1 in a parabolic mixed fashion, indicating at least two binding sites at high concentrations (52).

Quinacrine inhibits reversibly the ATPase activities of EF_1 and bovine MF_1 with a similar inhibitory potency (220, 268). This agent inhibits the ATP hydrolysis activity of F_1 competitively when Mg^{2+} is at a constant concentration and ATP at a variable concentrations (220, 268). Quinacrine mustard is a quinacrine derivative in which a diethyl group attached to the tertiary amino group is replaced by a bischloroethyl groups. The quinacrine mustard binds to F_1 and alkylates β subunits. The inhibition of the ATPase activity of F_1 by quinacrine mustard is irreversible (220) and is due, at least in part, to modification of one or more of the carboxylic acid side chains in the β subunit DELSEED region and possibly also to modification of unspecified amino acid side chains between residues β302 and 356 in the bovine sequence (53). The rate of inactivation of MF_1 and TF_1 by quinacrine mustard is inhibited by ATP, whereas the rate of inactivation of EF_1 is stimulated by ATP (54).

Acridine orange and coriphosphine are acridine derivatives that inhibit the ATPase activity of MF_1 in a mixed fashion (52). Pyronin Y, a xanthene derivative, inhibits the ATPase activities of F_0F_1 from mitochondria and *E. coli* (52, 268). Here, the inhibitory effect on the mitochondrial ATPase is more potent for F_0F_1 (>100-fold) than for F_1 (52).

Dequalinium is a quinoline derivative that inhibits the ATPase activities of F_1 from both mitochondria and bacteria (52, 268, 296, 329, 452). Dequalinium inhibits chloroplast Ca^{2+}-ATPase, whereas it stimulates chloroplast Mg^{2+}-ATPase (329). The inhibition of ATPase activity by dequalinium is reversible, hyperbolic, and noncompetitive for MF_1 and TF_1 in the dark (52, 268, 296, 329, 452). A long lag is observed in the inhibition of TF_1 by dequalinium that is not observed for the inhibition of MF_1 (296). Dequalinium, upon illumination at 350 nm, inactivates F_1-ATPase with pseudo-first-order kinetics (296, 329, 452, 454). This is accompanied by derivatization of βPhe420 in TF_1 (296), βMet183 in CF_1 (329), and αPhe403, αPhe406, and a side chain within residues 440 to 459 of the β subunit in bovine heart MF_1 (454).

Safranin O inhibits the ATPase activities of membrane-bound F_0F_1 from both bovine heart mitochondria and *E. coli* (52, 268). Safranin O also inhibits soluble MF_1 with weaker inhibitory potency (52). Nile blue A inhibits the ATPase activity of membrane-bound F_0F_1 from mitochondria, whereas it has no inhibitory effect on isolated F_1 (52). Ethidium bromide inhibits noncompetitively ATP hydrolysis by both MF_1 and F_0F_1 from *Saccharomyces cerevisiae* (82, 433), with similar inhibitory potencies (66, 82).

TALAs and Related Compounds

Tertiary amine local anesthetics (TALAs) are composed of an aromatic portion, an intermediate chain, and a terminal amine group (Fig. 7B) (370). The intermediate chain contains either an ester (tetracaine and procaine) or an amide (dibucaine and lidocaine) group. In procainamide, the ester group in procaine is replaced with an amide. Chlorpromazine and trifluoroperazine are cationic phenothiazine derivatives. The TALAs are known to inhibit primarily sodium influx through sodium-specific ion channels in the neuronal cell membrane. However, they can also bind to ATP synthases from mitochondria and some bacteria and can inhibit ATP hydrolysis activity (Table 12) (76, 406).

TALAs inhibit both membrane-bound and soluble MF_1. Inhibition of MF_1 is reversible, and the concentration ranges for inhibition are near those for blocking nerve conduction (76). The hydrophobicity of TALAs seems to determine their relative affinities for F_1, as the inhibitory potencies are directly correlated with the octanol/water partition coefficient (76). Among the TALAs, procainamide shows activation of the ATPase activity of F_1 at low concentrations prior to its inhibition of F_1 at high concentrations. This is not observed with other TALAs (76). The mechanism of the inhibitory action of TALAs on MF_1 is still controversial, with one view implicating the induction of the structural dissociation of the multisubunit structure of F_1 (76) and a second view the interaction with the catalytic sites of F_1 (221).

In contrast to the case for the mitochondrial ATP synthase, the TALAs inhibit bacterial ATP synthases selectively. For

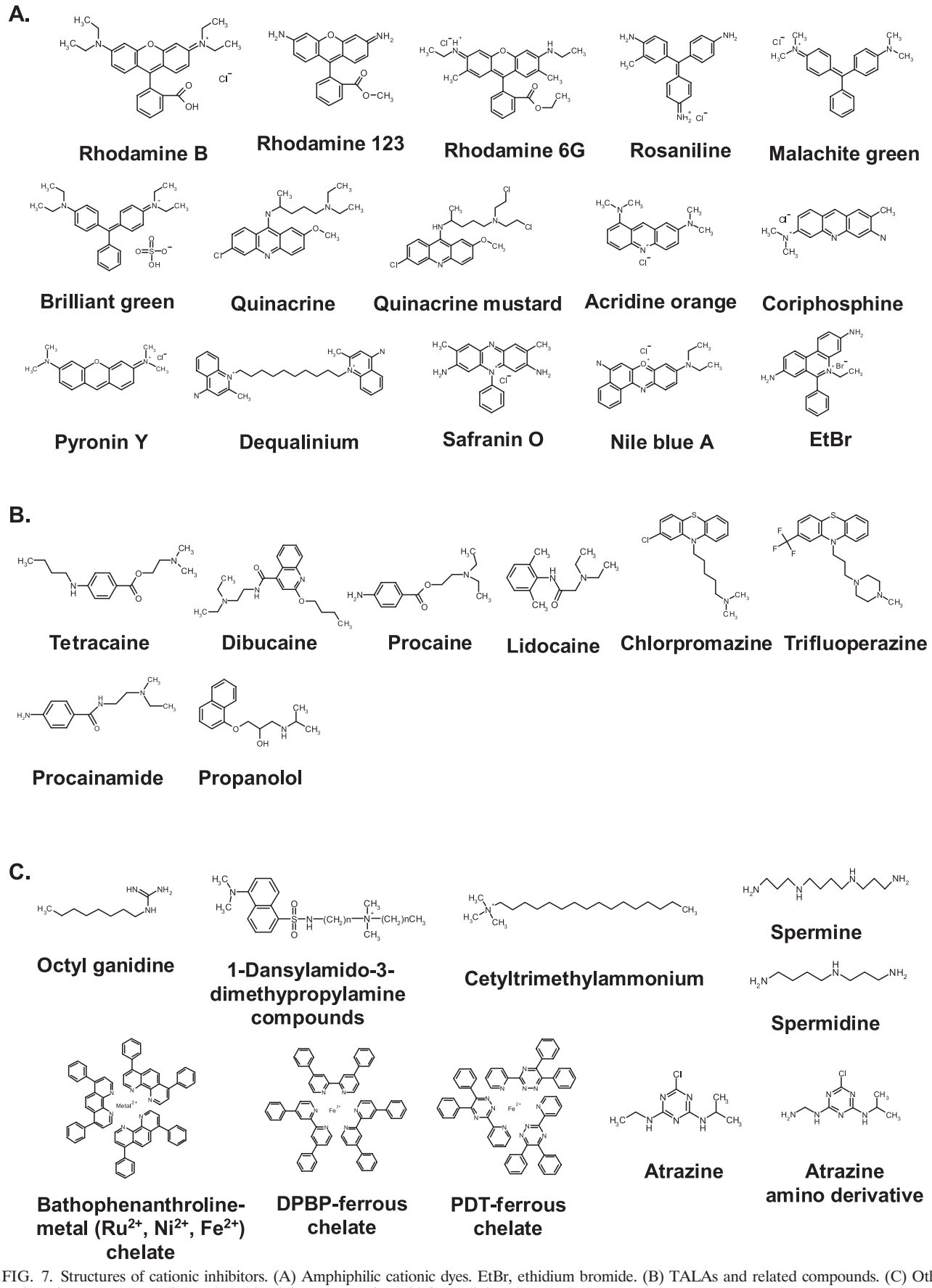

FIG. 7. Structures of cationic inhibitors. (A) Amphiphilic cationic dyes. EtBr, ethidium bromide. (B) TALAs and related compounds. (C) Other organic cations. DPBP, 4,4-diphenyl-2,2-bipyridine; PDT, 3-(2-pyridyl)-5,6-diphenyl-1,2,4-triazine.

TABLE 11. Amphiphilic cationic dyes

Name or abbreviation	Molecular formula	Other names	Inhibitory potency (reference)
Rhodamine B	$C_{28}H_{31}ClN_2O_3$	*N*-(9-(2-Carboxyphenyl)-6-(diethylamino)-3*H*-xanthen-3-ylidene)-*N*-ethylethanaminium chloride; rheonine B; rhodamine O; rhodamine S	475 μM[a] (bovine heart MF_1-ATPase) (52); 125 μM[a] (bovine heart MF_0F_1-ATPase) (52)
Rhodamine 123	$C_{21}H_{17}ClN_2O_3$	3,6-Diamino-9-(2-(methoxycarbonyl)phenyl)xanthylium chloride; RH 123	270 μM[a] (bovine heart MF_1-ATPase) (52); 141 μM[a] (bovine heart MF_0F_1-ATPase) (52); 580 μM[a] (EF_0F_1-ATPase) (268); 177 μM[b] (rat liver MF_1-ATPase) (113)
Rhodamine 6G	$C_{28}H_{31}ClN_2O_3$	Basic rhodamine yellow; rhodamine J	10 μM[a] (bovine heart MF_1-ATPase) (52); 27 μM[a] (bovine heart MF_1-ATPase) (143); 2 μM[a] (bovine heart MF_0F_1-ATPase) (52); 34 μM[a] (EF_0F_1-ATPase) (268); 2.4 μM[b] (*S. cerevisiae* MF_1-ATPase) (433); 1.95 μM[b] (*S. cerevisiae* MF_0F_1-ATPase) (433); 1.91 μM[b] (*S. cerevisiae* SMP-ATPase) (433)
Rosaniline	$C_{20}H_{20}ClN_3$	Magenta base; 4-((4-aminophenyl)(4-imino-2,5-cyclohexadien-1-ylidene)methyl)-2-methylbenzenamine	15 μM[a] (bovine heart MF_1-ATPase) (52); 16 μM[a] (bovine heart MF_0F_1-ATPase) (52)
Malachite green	$C_{23}H_{25}N_2Cl$	Aniline green; benzal green; Victoria green; (4-(4-dimethylaminobenzhydriylidene)cyclohexa-2,5-dienylidene)dimethylammonium chloride	14 μM[a] (bovine heart MF_1-ATPase) (52); 7 μM[a] (bovine heart MF_0F_1-ATPase) (52)
Brilliant green	$C_{27}H_{33}N_2.HO_4S$	Basic green 1; (4-(4-(diethylamino) benzhydrylene)cyclohexa-2,5-dien-1-ylidene)diethylammonium hydrogen sulfate	27 μM[a] (EF_0F_1-ATPase) (268)
Quinacrine	$C_{23}H_{30}ClN_3O$	2-Methoxy-6-chloro-9-diethylaminopentylaminoacridine; 3-chloro-7-methoxy-9-(1-methyl-4-diethylaminobutylamino)acridine; mepacrine	580 μM[a] (EF_0F_1-ATPase) (268); 580 μM[a] (bovine heart MF_1-ATPase) (220); 440 μM[b] (bovine heart MF_1-ATPase) (220)
Quinacrine mustard	$C_{23}H_{28}Cl_3N_3O$	Quinacrine mustard dihydrochloride; 2-methoxy-6-chloro-9-(3-(ethyl-2-chloroethyl)aminopropylamino)acridine dihydrochloride; 9-[4-(bis(2-chloroethyl)amino)-1-methylbutylamino]-6-chloro-2-methoxyacridine dihydrochloride	5.3 μM[a] (EF_0F_1-ATPase) (268); 27 μM[c] (bovine heart MF_1-ATPase) (53)
Acridine orange	$C_{17}H_{19}N_3Cl$	3,6-Acridinediamine, *N,N,N′,N′*-tetramethyl-, monohydrochloride; 3,6-bis(dimethylamino)acridine hydrochloride; rhoduline orange	180 μM[a] (bovine heart MF_1-ATPase) (52); 1 μM[a] (bovine heart MF_0F_1-ATPase) (52); 68 μM[a] (EF_0F_1-ATPase) (268)
Coriphosphine	$C_{16}H_{17}N_3.HCl$	Coriphosphine O; coriphosphine OX; 3-amino-6-(dimethylamino)-2-methylacridine monohydrochloride	480 μM[a] (bovine heart MF_1-ATPase) (52); 16 μM[a] (bovine heart MF_0F_1-ATPase) (52)
Pyronin Y	$C_{17}H_{19}ClN_2O$	Pyronine; pyronin G	1.65 mM[a] (bovine heart MF_1-ATPase) (52); 10 μM[a] (bovine heart MF_0F_1-ATPase) (52); 70 μM[a] (EF_0F_1-ATPase) (268)
Dequalinium	$C_{30}H_{40}N_4$	1,1′-(1,10-Decanediyl)bis(4-amino-2-methylquinolinium	8 μM[a] (52), 12 μM[a] (452), 46 μM[a] (143) (bovine heart MF_1-ATPase); 24 μM[a] (EF_0F_1-ATPase) (268); 50 μM[a] (TF_1-ATPase, photoinactivation) (296);19 mM (*Bacillus* PS3 ATPase, αβγ complex) (143); 4 μM[b] (spinach CF_1, Ca^{2+}-ATPase) (329); 12.5 μM[c] (TF_1-ATPase) (296); 12.5 μM[c] (bovine heart MF_1-ATPase) (452)
Safranin O	$C_{20}H_{19}ClN_4$	Basic red 2; 3,7-diamino-2,8-dimethyl-5-phenylphenazinium chloride; safranine T	1.14 mM[a] (bovine heart MF_1-ATPase) (52); 175 μM[a] (bovine heart MF_0F_1-ATPase) (52); 330 μM[a] (EF_0F_1-ATPase) (268)
Nile blue A	$C_{20}H_{20}N_3OCl$	Nile blue; Nile blue AX; 5-amino-9-(diethylamino)benzo(a)phenoxazine-7-ium chloride	>2,000 μM[a] (bovine heart MF_1-ATPase) (52); 16 μM[a] (bovine heart MF_0F_1) (52)
EtBr	$C_{21}H_{20}BrN_3$	Ethidium bromide; homidium bromide; AI3–62997; 2,7-diamino-10-ethyl-9-phenylphenanthridinium bromide	220 μM[a] (*S. cerevisiae* MF_1-ATPase) (82); 250 μM[a] (*Trypanosoma cruzi* F_0F_1-ATPase) (66); 279 μM[b] (*S. cerevisiae* MF_1-ATPase) (433); 256 μM[b] (*S. cerevisiae* MF_0F_1-ATPase) (433); 263.6[b] μM (*S. cerevisiae* SMP-ATPase) (433)

[a] I_{50}.
[b] K_i.
[c] K_d.

TABLE 12. Tertiary amine local anesthetics and related compounds

Name	Molecular formula	Other names	Inhibitory potency, I_{50} (reference)
Tetracaine	$C_{15}H_{24}N_2O_2$	Dicaine; 2-(dimethylamino)ethyl *p*-(butylamino)benzoate; dimethylaminoethyl *p*-butyl-aminobenzoate; *p*-butylaminobenzoyl-2-dimethylaminoethanol	0.7–0.83 mM (76), 1.1 mM (406), 1.95 mM (343) (bovine heart MF_1-ATPase); 1.4 mM (76), 1.79 mM (343) (bovine heart SMP-ATPase)
Dibucaine	$C_{20}H_{29}N_3O_2$	2-Butoxy-*N*-(2-(diethylamino)ethyl) cinchoninamide; 2-butoxy-*N*-(2-DEAE) quinoline-4-carboxamide; cincainum; cinchocaine; Dermacaine; dibucainum; Nupercaine; Percamine; Sovcaine; α-butyloxycinchonic acid-γ-diethylethylenediamine	0.19–0.5 mM (bovine heart MF_1-ATPase) (76); 0.26 mM (bovine heart SMP-ATPase) (76); 29% inhibition at 1 mM (*M. phlei* F_1-ATPase) (4); 55.7% inhibition at 1 mM (*M. phlei* membrane-bound ATPase) (4)
Procaine	$C_{13}H_{20}N_2O_2$	2-DEAE-4-aminobenzoate; DEAE *p*-aminobenzoate; *p*-aminobenzoyldiethylaminoethanol; procain; Spinocaine	1.8 mM (343), 15–17 mM (76) (bovine heart MF_1-ATPase); 8.4 mM (343), 9.5 mM (76) (bovine heart SMP-ATPase)
Lidocaine	$C_{14}H_{22}N_2O$	2-(Diethylamino)-*N*-(2,6-imethylphenyl) acetamide; cappicaine; Duncaine; Esracaine; Isicaine; Lidocaine; Maricaine; xycaine; Xylocaine	12–16 mM (76), 18.2 mM (343) (bovine heart MF_1-ATPase); 10 mM (76), 22 mM (343) (bovine heart SMP-ATPase)
Chlorpromazine	$C_{17}H_{19}N_2SCl$	2-Chloro-10-(3-(dimethylamino)propyl) phenothiazine; Aminazin; Aminazine; Chlor-Promanyl; Chlorderazin; Chlorpromados; Contomin; Elmarin; Esmind; Fenactil; Largactil; Megaphen; Novomazina; Proma; Phenactyl; Promactil; Propaphenin; Prozil; Psychozine; Sanopron; Thorazine; Torazina; Wintermin	50 μM(54), 60 μM (343), 50–150 μM (221) (bovine heart MF_1-ATPase); 26 μM (76), 450 μM (343) (bovine heart SMP-ATPase); 150 μM (EF_1-ATPase) (54); 30.8–56.0 μM (bovine heart MF_0F_1-ATPase) (87); 6.5–12 μM (bovine heart MF_0F_1, photoinactivation) (87)
Trifluoperazine	$C_{21}H_{24}F_3N_3S$	10-(3-(4-Methyl-1-piperazinyl)propyl)-2-(trifluoromethyl)phenothiazine; trifluoromethylperazine	17.2–30.5 μM (bovine heart MF_0F_1-ATPase) (87); 3.0–5.5 μM (bovine heart MF_0F_1, photoinactivation) (87)
Procainamide	$C_{13}H_{21}N_3O$	4-Amino-*N*-(2-(diethylamino)ethyl)benzamide	17–35 mM (76), 33 mM (343) (bovine heart MF_1-ATPase); 31 mM (bovine heart SMP-ATPase) (76)
Propranolol	$C_{16}H_{21}NO_2$	1-((1-Methylethyl)amino)-3-(1-naphthalenyloxy)-2-propanol	210 μM (343), 0.87–1.4 mM (76) (bovine heart MF_1-ATPase); 310 μM at 37°C and 880 μM at 60°C (TF_1-ATPase) (343); 660 μM (343), 840 μM (76) (bovine heart SMP-ATPase)

example, they exhibit no inhibition of F_1 from the thermophilic bacterium PS3 under the conditions tested (343). However, tetracaine and dibucaine do inhibit the ATPase activity of the membrane-bound ATP synthase from the bacterium *Mycobacterium phlei* (4), whereas procaine and lidocaine show no inhibitory effects. In addition, tetracaine and dibucaine show no or partial inhibition of the ATPase activity of soluble F_1, in contrast to full inhibition of the ATPase activity of the membrane-bound ATP synthase. Upon inhibition (uncompetitive) of the membrane-bound ATP synthase from *M. phlei* by tetracaine and dibucaine, proton conductivity is markedly inhibited. Tetracaine and DCCD are not mutually exclusive in binding to the ATP synthase from *M. phlei*, and they appear to bind to separate binding sites within the proton-translocating "F_0" region (4).

Chlorpromazine and trifluoroperazine interact with various subunit types of F_1 and F_0. Both bind to membrane-bound subunits more readily than to soluble subunits, with trifluoroperazine binding to hydrophobic subunits more extensively than chlorpromazine (88). The binding sites of chlorpromazine and trifluoroperazine are not identical and mutually nonexclusive (87, 88). Upon photoactivation with UV light, the phenothiazine moiety of chlorpromazine and trifluoroperazine forms covalent bonds with the ATP synthase, leading to its irreversible inhibition. In other studies, chlorpromazine has been shown to protect MF_1 and EF_1 against both cold-induced dissociation and inactivation by DCCD (54). This agent is believed to cause inhibition by interacting with the catalytic site at position βGlu188 (bovine sequence). However, in other studies, chlorpromazine has been shown to stimulate the ATPase activity of TF_1 both at 37°C and at low concentrations (below 0.6 mM) at 23°C. It shows no inhibition up to 1.2 mM at 37°C or 60°C (54).

Propranolol is a nonselective beta blocker for the treatment of hypertension. It is not a TALA and has no ester or amide group in the intermediate chain. However, it is structurally

TABLE 13. Other organic cations

Name or abbreviation	Molecular formula	Other names	Inhibitory potency (reference)
Octyl guanidine	$C_9H_{21}N_3$		300 μM[a] (bovine heart SMP- and MF_1-ATPase) (92); 330 μM[a] (rat liver SMP-ATPase) (300)
1-Dansyl amido-3-dimethypropylamine compounds	$C_{20}H_{32}N_3O_2S$ ($n = 2$) $C_{23}H_{38}N_3O_2S$ ($n = 5$) $C_{27}H_{46}N_3O_2S$ ($n = 9$) $C_{33}H_{58}N_3O_2S$ ($n = 15$)		1.4 mM[a] ($n = 2$), 0.4 mM[a] ($n = 5$), 7.9 μM[a] and 4.4 μM[b] ($n = 9$), and 3.4 μM[a] ($n = 15$) (bovine heart SMP-ATPase) (116)
Cetyltrimethylammonium	$C_{19}H_{42}N$	Cetrimonium; cetrimonum; cetyltrimethylammonium; hexadecyltrimethylammonium; trimethylhexadecylammonium	80 μM[b] (bovine heart MF_1-ATPase) (31)
Spermine	$C_7H_{19}N_3$	4-Azaoctamethylenediamine	Inhibitory effect at 1–2 mM range (185); ~55% inhibition at 2 mM with 2 mM Mg^{2+} (rat liver MF_1-ATPase) (185)
Spermidine	$C_{10}H_{26}N_4$	1,4-Bis(aminopropyl) butanediamine; diaminopropyltetramethylenediamine	Inhibitory effect at 2.5–5 mM range (rat liver MF_1-ATPase) (185)
Bathophenan throline-metal (Ru^{2+}, Ni^{2+}, Fe^{2+}) chelate	$C_{24}H_{16}N_2$, $3C_{24}H_{16}N_2 \cdot Ru$, $3C_{24}H_{16}N_2 \cdot Ni$, $3C_{24}H_{16}N_2 \cdot Fe$	1,10-Bathophenanthroline; 4,7-diphenyl-1,10-phenanthroline; bathophenanthroline ruthenium(II); Ru-Tdpa; tris(4,7-diphenyl-1,10-phenanthroline)ruthenium (II); 4,7-diphenyl-1,10-phenanthroline-ferrous chelate; BPh_3Fe^{2+}	For BPh, almost complete inhibition at 5 μM (bovine heart MF1) (315); for $BPh_3 \cdot Fe^{2+}$, 30 nmol/mg protein[b] (*N. crassa* SMP-ATPase) (112); 100% inhibition at 0.67 μM (bovine heart MF_1-ATPase) (63)
DPBP-ferrous chelate	$3C_{22}H_{16}N_2 \cdot Fe$	4,4-Diphenyl-2,2-bipyridine	85% inhibition at 0.67 μM and 99% inhibition at 3.33 μM (bovine heart MF_1-ATPase) (63)
PDT-ferrous chelate	$3C_{20}H_{14}N_4 \cdot Fe$	3-(2-Pyridyl)-5,6-diphenyl-1,2,4-triazine	73% inhibition at 0.67 μM and 95% inhibition at 3.33 μM (bovine heart MF_1-ATPase) (63)
Atrazine	$C_8H_{14}ClN_5$	6-Chloro-*N*-ethyl-*N′*-(propan-2-yl)-1,3,5-triazine-2,4-diamine	
Atrazine amino derivative	$C_7H_{13}ClN_6$	*N*-(Aminomethyl)-6-chloro-*N′*-(propan-2-yl)-1,3,5-triazine-2,4-diamine	

[a] I_{50}.
[b] K_i.

analogous to TALAs. The main action of propanolol is to block the action of epinephrine on both β1- and β2-adrenergic receptors, but it also targets ATP synthase. Propranolol inhibits the mitochondrial ATPase activities of both membrane-bound ATP synthase and isolated F_1 (76, 343). It also inhibits TF_1 at both 37°C and 60°C with nearly the same effective concentrations as that for inhibition of membrane-bound mitochondrial ATP synthase (76, 343).

Other Organic Cations

Alkylguanidines (Fig. 7C) that possess an alkyl chain of more than six carbons inhibit the ATPase activities of both membrane-bound and isolated MF_1 (92, 300). The inhibition by octylguanidine, an alkylguanidine, is fully reversible, and the octylguanidine prevents cold-induced dissociation of F_1 (92).

1-Dansylamido-3-dimethypropylamine compounds are dansylated organic cationic inhibitors (Fig. 7C). They inhibit both ATP hydrolysis and ATP synthesis at similar concentrations (116). The 1-dansylamido-3-dimethypropylamine compounds inhibit the ATPase activities of both isolated and membrane-bound F_1 and exhibit more potent inhibitory effect on the membrane-bound F_1 than the isolated enzyme. The 1-dansylamido-3-dimethypropylamine compounds with longer alkyl groups (decyl and hexadecyl) have stronger inhibitory activity than those with short groups (propyl and hexyl) (Table 13). The binding site(s) of these compounds is not clarified but is considered to be located on the β subunit (116).

Cetyltrimethylammonium inhibits the ATPase activities of soluble and membrane-bound F_1 in a noncompetitive manner (31). The inhibition is reversible and can be reversed by dilution. The inhibition of membrane-bound F_1 shows a more complex pattern than that of isolated F_1 with a sigmoidal dependence on the concentration of cetyltrimethylammonium. Also, cetyltrimethylammonium potentiates inhibition of membrane-bound ATP synthase by oligomycin, and vice versa. It lowers the K_i of the ATP synthase for oligomycin by about 1 order of magnitude. The inhibitory effect by cetyltrimethylammonium is believed to be due to an interaction of negatively charged residues buried in a hydrophobic environment of F_1.

Spermine and spermidine are polyamines distributed widely in nature. Both activate the ATPase activity of membrane-bound ATP synthase at low physiological concentrations (312, 374) and inhibit it at high concentrations (185). Spermine and spermidine also inhibit the ATPase activity of isolated F_1. Inhibition by spermine (1 to 2 mM range) is much greater than that by spermidine (2.5 to 5 mM range) and is uncompetitive with variable concentrations of ATP in the presence of Mg^{2+} but competitive when both ATP and Mg^{2+} concentrations are variable. Spermine and spermidine bind to ATP, an event that

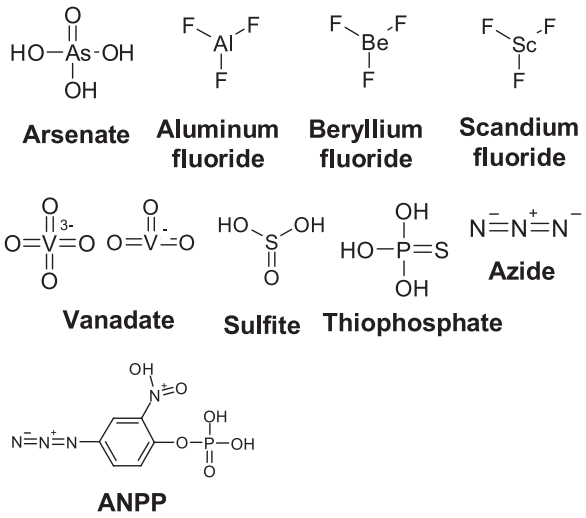

FIG. 8. Structures of phosphate analogs.

is inhibited by Mg^{2+}. In fact, the inhibition of the ATPase activities of membrane-bound and isolated F_1 by polyamines is considered to be due to their direct binding to ATP. In contrast to their ATPase-inhibitory actions, spermine and spermidine stimulate catalysis in SMP of both succinate-dependent ATP synthesis and P_i-ATP exchange (185).

Octahedral bathophenanthroline (BPh_3)-metal chelates inhibit MF_1 in an uncoupler-reversible fashion (63–65, 315). They bind to the ATP synthase β subunit and form a complex with a stoichiometic ratio of 3 mol BPh_3-Me^{2+}/mol F_1. Full inhibition is observed with 0.67 μM of BPh_3-Fe^{2+} for MF_1 from bovine heart (63). BPh_3-Fe^{2+} competes with aurovertin for binding to the β subunit. The inhibition is relieved by addition of uncouplers of oxidative phosphorylation via a process that involves direct interaction of the uncouplers with the inhibitory chelates. In fact, inhibitor-uncoupler adducts are believed to be formed (63). BPh_3-Ni^{2+} and BPh_3-Ru^{2+} are equally efficient inhibitors in the uncoupler-reversible inhibition of MF_1 (63, 65). Moreover, BPh_3-Fe^{2+} protects F_1 from cold-induced dissociation and light-induced inactivation by Rose bengal in an uncoupler-reversible manner (64). The related chelates 4,4-diphenyl-2,2-bipyridine and 3-(2-pyridyl)-5,6-diphenyl-1,2,4-triazine with Fe^{2+} also inhibit MF_1, but with weaker inhibitory potencies than BPh_3-metal chelates (63).

Atrazine is a globally used triazine herbicide that inhibits photosynthetic electron transport by binding the plastoquinone binding protein in photosystem II (382). Atrazine also targets ATP synthase from sperm and mitochondria, inhibiting the ATP synthesis activity of ATP synthase (170). The amino derivative of atrazine in which a terminal methyl group is replaced with an amino group is more potent in inhibition of ATP synthesis.

SUBSTRATES AND SUBSTRATE ANALOGS

Phosphate Analogs

Arsenate mimics the γ-phosphate of ATP. It inhibits ATP synthesis at the active site of ATP synthase by competing with phosphate (Fig. 8 and Table 14) (81, 264, 307). Arsenate blocks the $P_i \leftrightarrow H_2O$ exchange and also the ATP$\leftrightarrow P_i$ exchange catalyzed by the ATP synthase (201) and is a more effective inhibitor when the concentration of phosphate is low (307). Thus, at 40 μM phosphate, 4.6 mM arsenate inhibits phosphate binding to bovine heart MF_1 by 84%.

The phosphate analogs aluminum fluoride and beryllium fluoride also bind to the catalytic sites of ATP synthase by mimicking the γ-phosphate of ATP (48, 107, 195, 243, 256). The inhibition by these fluorides of aluminum and beryllium involves ADP, Mg^{2+}, and the fluoride ion (F^-). In fact, no inhibition occurs without fluoride. Inhibition also occurs when IDP, GDP, or CDP replaces ADP (187, 243). Aluminum fluoride and beryllium fluoride inhibit F_1 to the same extent via a "quasi-irreversible" process (243). The inhibitory species recognized by F_1 are AlF_3 and AlF_4^- for aluminum fluoride (48, 256) and BeF^+, BeF_2, and BeF_3^- for beryllium fluoride (187, 195). In crystals of F_1 grown with ADP and one of the inhibitors (AlF_4^- or BeF_3^-), two catalytic sites are occupied, one in the β_{TP} subunit and the other in the β_{DP} subunit (195, 256). Only one catalytic site, β_{DP}, is occupied with aluminum fluoride (AlF_3) in the crystal grown in the presence of ADP, adenylyl imidodiphosphate (AMP-PNP), and the inhibitor. No bound aluminum fluoride or beryllium fluoride is found in the α and β_E subunits. Three basic residues located in the vicinity of the γ-phosphate site, βLys162, βArg189, and αArg373, are involved in coordination of the inhibitors and are considered to provide charge stabilization (256).

Scandium fluoride (ScF_x) binds to F_1 of ATP synthase and inhibits its ATPase activity (279). ScF_x forms a tight-binding inhibitory ternary complex with MgADP at the catalytic sites, and the MgADP · ScF_x complex acts as a transition state analog. The inhibition by ScF_x is Mg^{2+} dependent, and ADP is also required for strong inhibition. The inhibition is reversible, and the ATPase activity is slowly regained in a single exponential reactivation process.

Two vanadate species, VO_4^{3-} and VO_3^-, inhibit F_1-ATPase (77, 210, 211, 344). Orthovanadate (VO_4^{3-}) binds to the catalytic sites and forms a transition-like state MgADP · V_i-F_1 complex in the presence of ADP and Mg^{2+}. The inhibition of rat liver MF_1 by orthovanadate is reversible, with a restoration of original activity to a level close to 90% (210, 211), whereas EF_1 is resistant to orthovanadate (6). In the presence of UV and O_2, the cleavage of the β subunit from rat liver MF_1 occurs at position Ala158 in the P-loop (210, 211). In the crystal structure of F_1 with vanadate from the same source, one vanadate ion is found in each catalytic site of the β subunit (77). The vanadate in this transition-like state is located in a charged pocket surrounded by βLys162, βGlu188, βArg189, and βArg260 and is complexed with ADP and Mg^{2+}. Moreover, the vanadate is positioned closer to P-loop βAla158 than is phosphate in the F_1-ADP,P_i ground state structure. It has been proposed that the positioning of βAla158 closer to the γ-phosphate of ATP in the transition state may help facilitate the dehydration of ADP and P_i (to give water) and therefore facilitate ATP synthesis (77).

Magnesium fluoride inhibits F_1 by acting also as an apparent transition state analog in combination with MgADP (5). Like vanadate, it mimics the γ-phosphate of ATP in the transition state. The inhibition is slow and reversible and requires ADP.

Sulfite is known as an effective activator of F_1-ATPase. How-

TABLE 14. Phosphate analogs

Name or abbreviation	Molecular formula	Inhibitory potency (reference)
Arsenate	AsO_4	84% inhibition at 4.6 mM at low conc of phosphate (40 μM) (bovine heart MF_1-ATPase) (307)
Aluminum fluoride	AlF_3 and AlF_4^-	10 μM[a] of $AlCl_3$ in the presence of 5 mM NaF and 100 μM ADP (bovine heart MF_1-ATPase) (243)
Beryllium fluoride	BeF^+, BeF_2, and BeF_3^-	10 μM[a] of $BeCl_2$ in the presence of 5 mM NaF and 100 μM ADP (bovine heart MF_1-ATPase) (243); 20 μM[a] of $BeCl_2$ in the presence of 2.5 mM NaF with 80 μM ADP with 50 mM Cl^- (45 min incubation), 20 mM SO_4^{2-} (14 min incubation), or 20 mM SO_3^- (2 min incubation) (bovine heart MF_1-ATPase) (187)
Scandium fluoride	ScF_x	60 μM[a] and 95% inhibition at 0.3 mM in the presence of 2.5 mM MgSO4, 1 mM ADP, and 10 mM NaF (279)
Vanadate	VO_4^{3-} and VO_3^-	VO_4^{3-}, 50% inhibition in ~45 min and ~80% inhibition in ~2 h at 200 μM in the presence of 200 μM each of $MgCl_2$ and ADP (rat liver MF_1-ATPase) (210); VO_3^-, 30% inhibition at 300 μM (*V. parahaemolyticus* F_1-ATPase) (344)
Magnesium fluoride	MgF_x	50% inhibition at 1mM NaADP, 1 mM NaF, and 11–12 mM $MgCl_2$ with 5–12 h preincubation (EF_1-ATPase) (5)
Sulfite	SO_3^{2-}	3.5 mM[a] and maximal 70% at 10 mM (*P. denitrificans* F_0F_1, ATP synthesis) (295)
Thiophosphate	SPO_3^{3-}	K_m, 1.5 μM in the presence of 1 mM from 4.5 μM in the absence (pea SMP-ATP synthesis) (254)
Azide	N_3^-	~10^{-5} M[b] (bovine heart MF_1-ATPase) (412); ~25 μM[b] (EF_1-ATPase) (287); 71% inhibition at 1 mM (*V. parahaemolyticus* F_1-ATPase) (344); >90% inhibition at 0.5 mM (EF_1-ATPase) (287); 55% inhibition at 500 μM (*C. thermoaceticum* F_1-ATPase) (190)
ANPP	$C_6H_4N_4O_6P$	25 μM[a] (spinach CF_1-ATPase, photoinactivation) (321); 60 μM[b] in the dark (bovine heart MF_1-ATPase) (227)

[a] I_{50}.
[b] K_i.

ever, it can also play a role as an inhibitor of the reversal of ATP synthase as a mixed-type inhibitor in the presence of ADP and phosphate (Fig. 8 and Table 14). The sulfite diminishes the rate of ATP synthesis of *Paracoccus denitrificans* with an I_{50} of 3.5 mM (295). The mechanism of sulfite inhibition is uncertain, but it has been suggested that the action of inhibitory ADP is involved in the binding of nucleotides to noncatalytic sites (249), and the binding of sulfite to the noncatalytic sites increases the K_i for inhibitory ADP (295, 327).

Thiophosphate is a group of compounds in which a phosphorus atom is bonded to one or more sulfur and zero or more oxygen atoms, and it is found in a number of insecticides. A thiophosphate, SPO_3^{3-}, has been shown to inhibit ATP synthesis in mitochondria (254, 363). It inhibits the $P_i \leftrightarrow$ ATP exchange in SMP from bovine heart mitochondria competitively and also inhibits ATP synthesis noncompetitively with respect to ADP without a change in K_m for ADP (363). In contrast, in pea SMP, thiophosphate decreases the K_m of the enzyme for ADP (254).

Azide inhibits the ATPase activity of F_1 from mitochondria, bacteria, and chloroplasts (25, 46, 126, 274, 278, 287, 391, 412). Azide has no inhibitory effect on ATP synthesis (25). The inhibition by azide is noncompetitive (287, 391) and occurs only in the presence of ADP and ATP (274). The binding of inhibitory azide requires prior binding of both ADP and Mg^{2+} (160, 278). Azide binds to the catalytic site in β_{DP} of F_1 and resides adjacent to the β-phosphate of ADP, mimicking the nonbridging oxygen atom of the γ-phosphate (46). The binding of azide in the β_{DP} catalytic site is very tight, and the azide is closely associated via hydrogen bonds with βLys162 in the P-loop and αArg373 (46). The inhibition is dependent on ATP concentration (274) and is reversed by addition of phosphate, possibly by competing for the azide binding site (262, 274).

Azido-2-nitrophenyl phosphate (ANPP) is a photoaffinity phosphate analog in which the 4-azido-2-nitrophenyl group is attached to phosphate (Fig. 8 and Table 14). ANPP inhibits F_1 as a competitive inhibitor in the dark by specifically targeting γ-phosphate binding sites within the nucleotide binding pockets on the β subunit of isolated F_1 or on both α and β subunits of membrane-bound F_0F_1 (154, 227). However, upon photoirradiation with visible light, ANPP inactivates the enzyme by binding covalently to these subunits. This occurs most frequently on βTyr 311, together with βIle304 and βGln308 in MF_1, and on the analogous βTyr 328, together with βVal329 and βPro330 in CF_1 (133, 258). Phosphate added before photoirradiation protects the photoinactivation by ANPP. The stoichiometry for full photoinactivation of F_1 is approximately 1 mol of ANPP/mol of CF_1 (321).

Divalent Metal Ions

Divalent metal ions are usually activators of F_1, but in their free form, they can also function as inhibitors at high concentrations (47, 98, 174, 278, 291, 365). Free Mg^{2+} acts as a linear competitive inhibitor (98, 365). The inhibition of CF_1 by free Mg^{2+} requires the presence of a tightly bound ADP at the

TABLE 15. Divalent metal ions

Name	Inhibitory potency (reference)
Inhibitory free Mg^{2+}	2.8 mM[a] (*P. blakesleeanus* MF_1-ATPase) (98); 3 mM[a] (ox heart MF_1-ATPase) (365); 20 μM[a] (lettuce CF_1-ATPase) (174); 7 μM[a] (*R. rubrum* F_1-ATPase) (291); 10–15 μM[b] and 4 μM[b] (spinach CF_1-ATPase) (278)
Inhibitory free Mn^{2+}	5 μM[a] (lettuce CF_1-ATPase) (174)
Inhibitory free Ca^{2+}	5–7 μM[a] (lettuce CF_1-ATPase) (174)

[a] K_i.
[b] K_d.

catalytic site (160, 278). The K_i values are variable, and CF_1 and BF_1 are about 2 orders of magnitude more sensitive to the inhibition by free Mg^{2+} than is MF_1. Free Mn^{2+} and Ca^{2+} ions also inhibit F_1-ATPase in a competitive manner and are more effective than free Mg^{2+} in inhibition of CF_1 (Table 15) (174).

Purine Nucleotides and Nucleotide Analogs

Excess free ATP is also an inhibitor of ATP synthase (Tables 16 and 17 and Fig. 9A) (98, 291, 365). Inhibition of ATPase activity of F_1 by free ATP can be competitive (in the photosynthetic bacterium *Rhodospirillum rubrum* [291], biphasic (in *Phycomyces blakesleeanus* [98], or second order/parabolic (in ox heart mitochondria (365).

ADP is a substrate for F_1, but preincubation of F_1 with ADP and Mg^{2+} induces hysteretic inhibition (32, 102, 261). The inhibition arises when medium Mg^{2+} combines with F_1 to which ADP is bound to only a single catalytic site in the absence of bound P_i. The onset of the inhibition is rather slow (seconds to minutes). The Mg^{2+}ADP-induced inhibition can be slowly and partially reversed by addition of ATP in the absence of Mg^{2+} (272), and the recovery of ATPase activity requires the binding of ATP at a noncatalytic site. The recovery is promoted by anions such as bicarbonate and sulfite (272, 412). The inhibition can arise from the medium ADP, but ADP produced at the catalytic site by ATP hydrolysis can also start Mg^{2+}ADP-induced inhibition. F_1 from chloroplasts is more readily inhibited than F_1 from mitochondria, whereas EF_1 is not susceptible to Mg^{2+}ADP-induced inhibition under conditions where Mg^{2+} is not in huge excess (6, 106). The Mg^{2+}ADP-induced inhibition of F_1 also occurs in the intact ATP synthase with no or low proton motive force. However, sufficient proton motive force can drive the ATP synthase to remove the inhibitory Mg^{2+}ADP without altering net ATP synthesis (47).

GTP and formycin 5′-triphosphate (FTP) bind to empty noncatalytic sites on CF_1 in the presence of Mg^{2+} and inhibit its ATPase activity (159). Binding of GTP or FTP to two sites causes more inhibition than binding to one site, and the GTP has stronger inhibitory potency than FTP. With GTP or FTP bound at two noncatalytic sites, the GTP inhibits the ATPase activity about 90%, and the FTP about 80%. After a 15-min incubation period, about 50% maximal inhibition is achieved with 5 to 10 μM GTP or FTP for spinach CF_1-ATPase.

2′,3′-*O*-(2,4,6-trinitrophenyl) ATP (TNP-ATP) and TNP-ADP are ribose-modified chromophoric and fluorescent analogs of ATP and ADP in which a trinitrophenyl group is attached to the 2′ and 3′ hydroxyls of ribose (Fig. 9A). These compounds have been used widely for various assays of ATP binding to proteins. Both compounds are potent inhibitors of F_1 with high affinity, and the TNP-ATP is hydrolyzable by F_1 from mitochondria, chloroplasts, and bacteria (157, 219, 273, 368, 429). The inhibition of ATP hydrolysis by TNP-ATP or TNP-ADP has been reported to be competitive (157) or biphasic (277). These nucleotide analogs bind to both catalytic and noncatalytic sites of F_1. Their binding is noncooperative at the three noncatalytic sites and cooperative at the three catalytic sites (429).

2-Azido-TNP-ATP, a 2-azido derivative of TNP-ATP, inhibits F_1 catalyzed ATP hydrolysis biphasically (Fig. 9B and Table 18) (276). Bicarbonate decreases the degree of inhibition by 2-azido-TNP-ATP. The K_m and V_{max} for 2-azido-TNP-ATP hydrolysis are similar to those for TNP-ATP hydrolysis. Upon UV illumination of the F_1-ATPase complex with the bound 2-azido-TNP-ATP, it is incorporated into the complex covalently and inactivates the F_1-ATPase irreversibly.

Linear-benzoadenosine diphosphate (lin-benzo-ADP) is a fluorescent adenine-modified ADP analog in which the adenine ring is laterally extended by the insertion of a benzene ring between the pyrimidine and imidazole ring (Fig. 9A) (199, 428). Lin-benzo-ADP binds to all six nucleotide binding sites. The affinities for lin-benzo-ADP to three α subunits and one β subunit of MF_1 from bovine heart are low (K_d = 1 to 2 μM), whereas the affinities for the other two β subunits are very high (K_d <10 nM) (428). Inhibition by lin-benzo-ADP is competitive and has complex kinetics of inhibition. Lin-benzo-ADP is fluorescent, and its fluorescence spectrum is extensively quenched by adding F_1. As expected, this fluorescence quenching is reversed by adding ADP (199).

5′,5′-Diadenosine oligophosphates (AP_xA) are compounds which have a chain of phosphoryl groups linking two adenosine moieties. The AP_xA that have a long chain of phosphoryl groups (AP_4A, AP_5A, and AP_6A) has been shown to inhibit the ATP hydrolysis activity of MF_1, whereas compounds that have a shorter chain (AP_2A and AP_3A) showed stimulatory effects (417). The inhibition by AP_4A, AP_5A, and AP_6A required the presence of at least one vacant noncatalytic site, and the maximal level of inhibition was 80%. AP_4A was the most potent, and its stoichiometry for maximal inhibition was near 1 mol/mol of F_1. In contrast, a contradictory result has also been reported in the inhibition of the same enzyme by AP_5A, and no inhibition was observed up to 100 μM (325).

AMP-PNP is a nonhydrolyzable ATP analog in which the terminal bridge oxygen of the triphosphate moiety is replaced by an NH group (444). AMP-PNP has been used widely in kinetic studies of F_1 and has been found to be a potent competitive inhibitor in ATPase assays of either the soluble or membrane-bound enzyme from bovine heart (37, 147, 306, 361) However, AMP-PNP is reported to be noncompetitive in ATPase assays with membrane-bound rat liver F_1 (361). The K_i values reported are variable (14 nM to 0.5 μM) (37, 84, 255, 306, 361). AMP-PNP has no effect on the ATP synthesis activity of ATP synthase, although it is a potent inhibitor of F_1-catalyzed ATP hydrolysis (302, 306). It binds to both catalytic and noncatalytic sites, and when it is bound to the latter

TABLE 16. Properties of purine nucleotides and nucleotide analogs

Name or abbreviation	Molecular formula	Source	Other names
Excess free ATP	$C_{10}H_{16}N_5O_{13}P_3$	Natural	Adenosine triphosphate; adenosine 5′-triphosphate
ADP	$C_{10}H_{15}N_5O_{10}P_2$	Natural	Adenosine diphosphate; adenosine 5′-diphosphate
GTP	$C_{10}H_{16}N_5O_{14}P_3$	Natural	Guanosine triphosphate; guanosine 5′-triphosphate
FTP	$C_{10}H_{16}N_5O_{13}P_3$	Synthetic	Formycin triphosphate; formycin 5′-triphosphate; formycin A 5′-triphosphate
TNP-ATP	$C_{16}H_{17}N_8O_{19}P_3$	Synthetic; fluorescent	2′,3′-*O*-(2,4,6-Trinitrophenyl) adenosine 5′-triphosphate
TNP-ADP	$C_{16}H_{15}N_8O_{16}P_2$	Synthetic; fluorescent	2′,3′-*O*-(2,4,6-Trinitrophenyl) adenosine 5′-triphosphate
TNP-Ado	$C_{16}H_{13}N_8O_{10}$	Synthetic; fluorescent	(2′,3′)-*O*-(2,4,6-Trinitrocyclohexadienylidine) adenosine
Lin-benzo-ADP	$C_{14}H_{17}N_5O_{10}P_2$	Synthetic; fluorescent	Linear-benzoadenosine diphosphate
AP_4A	$C_{20}H_{28}N_{10}O_{19}P_4$	Natural extracellular mediator	Diadenosine tetraphosphate; 5′,5′′′-diadenosine tetraphosphate
AP_5A	$C_{20}H_{14}N_{10}O_{22}P_5$	Natural extracellular mediator	Diadenosine pentaphosphate
AP_6A	$C_{20}H_{30}N_{10}O_{25}P_6$	Natural extracellular mediator	Diadenosine hexaphosphate; diadenosine 5′,5′′′′-P1,P6-hexaphosphate
AMP-PNP	$C_{10}H_{17}N_6O_{12}P_3$	Synthetic	Adenylyl imidodiphosphate; p[NH]ppA; γ-imino-ATP
GMP-PNP	$C_{10}H_{17}N_6O_{13}P_3$	Synthetic	5′-Guanylyl imidodiphosphate; p[NH]ppG
IMP-PNP	$C_{10}H_{16}N_5O_{13}P_3$	Synthetic	Inosine-5′-[(β,γ)-imido]triphosphate
$AMP(CH_2)P$	$C_{11}H_{17}N_5O_9P_2$	Synthetic	Adenosine 5′-methylenediphosphate; adenosine-5′-(α,β-methylene)-diphosphate; α,β-methylene ADP
RhATP	$C_{10}H_{23}N_5O_{16}P_3Rh$ (tridentate RhATP)	Synthetic	Bidentate RhATP, bidentate tetraaquarhodium-adenosine 5′-triphosphate [$Rh(H_2O)_4ATP$]; tridentate RhATP, tridentate triaquarhodium-adenosine 5′-triphosphate [$Rh(H_2O)_3ATP$]
CrATP or $Cr(NH_3)_4ATP$	$C_{10}H_{26}CrN_5O_{17}P_3$ (bidentate CrATP)	Synthetic	Monodentate CrATP, monodentate pentaaquachromium-adenosine 5′-triphosphate [$Cr(H_2O)_5ATP$]; monodentate $Cr(NH_3)_4ATP$, Monodentate tetraaminemonoaquachromium-adenosine 5′-triphosphate [$Cr(NH_3)_4(H_2O)ATP$]; bidentate CrATP, bidentate tetraaquachromium-adenosine 5′-triphosphate [$Cr(H_2O)_4ATP$]; bidentate $Cr(NH_3)_4ATP$, bidentate tetraaminechromium-adenosine 5′-triphosphate; bidentate $Cr(NH_3)_2ATP$, bidentate biaminebiaquachromium-adenosine 5′-triphosphate [$Cr(NH_3)_2(H_2O)_2ATP$]
$Co(NH_3)_4ATP$	$C_{10}H_{34}CoN_9O_{13}P_3$	Synthetic	Bidentate tetraaminecobalt-adenosine 5′-triphosphate; bidentate cobalt(III)tetraamine-adenosine 5′-triphosphate
3′-*O*-Acetyl-ATP	$C_{16}H_{17}N_8O_{19}P_3$	Synthetic	Acetyl adenosine triphosphate
3′-*O*-Acetyl-ADP	$C_{16}H_{16}N_8O_{16}P_2$	Synthetic	Acetyl adenosine diphosphate
3′-*O*-Caproyl-ADP	$C_{16}H_{25}N_5O_{11}P_2$	Synthetic	Caproyl adenosine diphosphate
3′-*O*-Enanthyl-ADP	$C_{17}H_{27}N_5O_{11}P_2$	Synthetic	Enanthyl adenosine diphosphate
3′-*O*-Caprylyl-ADP	$C_{18}H_{29}N_5O_{11}P_2$	Synthetic	Caprylyl adenosine diphosphate
F-ADP/DMAN-ADP	$C_{23}H_{23}N_6O_{11}P_2$	Synthetic; fluorescent	3′-*O*-[1-(5-Dimethylamino)-naphthoyl]adenosine diphosphate; 3′-*O*-(5-dimethylaminonaphthoyl-1)-adenosine diphosphate
F-ATP	$C_{23}H_{25}N_6O_{14}P_3$	Synthetic; fluorescent	3′-*O*-[1-(5-Dimethylamino)-naphthoyl]adenosine triphosphate; 3′-*O*-(5-dimethylaminonaphthoyl-1)-adenosine triphosphate
3′-*O*-(1-Naphthoyl)-ADP/N-ADP	$C_{21}H_{21}N_5O_{11}P_2$	Synthetic; fluorescent	3′-*O*-(Naphthoyl-1)adenosine diphosphate; 3-NP-ADP
3′-*O*-(1-Naphthoyl)-ATP	$C_{21}H_{22}N_5O_{14}P_3$	Synthetic; fluorescent	3′-*O*-(Naphthoyl-1)adenosine triphosphate
3′-*O*-(2-Naphthoyl)-ADP	$C_{21}H_{22}N_5O_{14}P_3$	Synthetic	3′-*O*-(2-Naphthoyl)-adenosine 5′-diphosphate
BzATP	$C_{24}H_{24}N_5O_{15}P_3$	Synthetic; photoreactive	3′-*O*-(4-Benzoyl) benzoyl ATP; 3′-*O*-(4-benzoyl)benzoyladenosine 5′-triphosphate
BzADP	$C_{24}H_{23}N_5O_{12}P_2$	Synthetic; photoreactive	3′-*O*-(4-Benzoyl) benzoyl ADP; 3′-*O*-(4-benzoyl)benzoyladenosine 5′-diphosphate
t-Butylacetyl-ADP	$C_{16}H_{25}N_5O_{11}P_2$	Synthetic	*tert*-Butylacetyl-adenosine 5′-diphosphate

Continued on following page

TABLE 16—*Continued*

Name or abbreviation	Molecular formula	Source	Other names
3′-*O*-Phenylacetyl-ADP	$C_{18}H_{21}N_5O_{11}P_2$	Synthetic	3′-*O*-Phenylacetyl-adenosine 5′-diphosphate
3′-*O*-Phenylbutyryl-ADP	$C_{20}H_{25}N_5O_{11}P_2$	Synthetic	3′-*O*-Phenylbutyryl-adenosine 5′-diphosphate
3′-*O*-Benzoyl-ADP	$C_{17}H_{19}N_5O_{11}P_2$	Synthetic	3′-*O*-Benzoyl-ADP
3′-*O*-[*N*-(2-Nitrophenyl)-γ-aminobutyryl]-ADP	$C_{20}H_{25}N_7O_{13}P_2$	Synthetic	3′-*O*-[*N*-2-Nitrophenyl-γ-aminobutyryl]-adenosine 5′-diphosphate
3′-*O*-[*N*-(4-Nitrophenyl)-γ−aminobutyryl]-ADP	$C_{20}H_{25}N_7O_{13}P_2$	Synthetic	3′-*O*-[*N*-(4-Nitrophenyl)-γ-aminobutyryl]-adenosine 5′-diphosphate
3′-*O*-(1-Naphthylacetyl)-ADP	$C_{22}H_{23}N_5O_{11}P_2$	Synthetic	3′-*O*-(1-Naphthylacetyl)-adenosine 5′-diphosphate
3′-*O*-(2-Naphthyl acetyl)-ADP	$C_{22}H_{23}N_5O_{11}P_2$	Synthetic	3′-*O*-(2-Naphthylacetyl)-adenosine 5′-diphosphate
3′-*O*-(1-Anthranoyl)-ADP	$C_{25}H_{23}N_5O_{11}P_2$	Synthetic	3′-*O*-(1-Anthranoyl)-adenosine 5′-diphosphate
3′-*O*-(9-Anthranoyl)-ADP	$C_{25}H_{23}N_5O_{11}P_2$	Synthetic	3′-*O*-(9-Anthranoyl)-adenosine 5′-diphosphate
FSBI	$C_{17}H_{15}FN_4O_8S$	Synthetic	5′-*p*-Fluorosulfonylbenzoylinosine; 5′-4-Fsbi
FSBA	$C_{17}H_{16}FN_5O_7S$	Synthetic	5′-*p*-Fluorosulfonylbenzoyladenosine; 5′-(4-(fluorosulfonyl)benzoyl)adenosine; 5-Fsba
FSBεA	$C_{19}H_{16}FN_5O_7S$	Synthetic	5′-*p*-Fluorosulfonylbenzoylethenoadenosine; 5′-(4-fluorosulfonylbenzoyl)-1,*N*(6)-ethenoadenosine; FSB epsilon A; Fsbn-ethenoadenosine
AP_2-PL	$C_{18}H_{22}N_6O_{12}P_2$	Synthetic	Adenosine diphosphopyridoxal; PLP-AMP; ADP-pyridoxal; pyridoxal 5′-diphospho-5′-adenosine; 5′-adenosine-5′-diphosphopyridoxal
AP_3-PL	$C_{18}H_{23}N_6O_{15}P_3$	Synthetic	Adenosine triphosphopyridoxal; adenosine 5′-(tetrahydrogen triphosphate), mono((4-formyl-5-hydroxy-6-methyl-3-pyridinyl)methyl) ester
AP_4-PL	$C_{18}H_{24}N_6O_{18}P_4$	Synthetic	Adenosine tetraphosphopyridoxal; adenosine tetraphosphate pyridoxal
oATP	$C_{10}H_{14}N_5O_{13}P_3$	Synthetic	2′,3′-Dialdehyde of ATP; dial-ATP
oADP	$C_{10}H_{13}N_5O_{10}P_2$	Synthetic	2′,3′-Dialdehyde of ADP
oAMP	$C_{10}H_{12}N_5O_7P$	Synthetic	2′,3′-Dialdehyde of AMP
Cibacron blue	$C_{29}H_{17}N_7O_{11}S_3Cl$	Synthetic; protein synthesis inhibitor	
BzAF	$C_{34}H_{21}NO_7$	Synthetic; photoreactive	4-Benzoyl(benzoyl)-1-amidofluorescein

sites, it induces hysteretic inhibition to the same extent as ADP (34, 37).

Guanylyl imidodiphosphate (GMP-PNP) and inosine-5′-[(β,γ)-imido]triphosphate (IMP-PNP) are analogs of GTP and ITP, respectively, in which the bridge oxygen atom between the β and γ phosphorus atoms is replaced by an NH group. The inhibition by GMP-PNP versus GTP and ITP is competitive (361), whereas inhibition versus ATP is competitive (37) or mixed (361). Unlike AMP-PNP, GMP-PNP shows no induction of hysteretic inhibition (34). IMP-PNP inhibits ITP hydrolysis potently, whereas it inhibits ATP hydrolysis only at low concentrations of ATP below 100 μM (362). At high concentrations of ATP, IMP-PNP stimulates the rate of ATP hydrolysis. In contrast, the stimulation of ATP hydrolysis by IMP-PNP is not seen in the presence of bicarbonate, and IMP-PNP inhibits ATP hydrolysis competitively.

Adenosine 5′-methylenediphosphate is an analog of ADP in which the bridge oxygen atom between the α and β phosphorus atoms is replaced by a CH_2 group. Adenosine 5′-methylenediphosphate inhibits ATP synthesis competitively with respect to ADP (254, 363) and inhibits $P_i \leftrightarrow$ ATP exchange uncompetitively (363).

Exchange-inert metal-nucleotide complexes are stable, inert octahedral complexes of Cr(III), Co(III), or Rh(III) with ATP and ADP (383). The exchange-inert metal-nucleotide complexes inhibit ATP synthase by binding to F_1 (44, 158, 383, 384, 432). Chromium complexes of ATP and ADP, i.e., α,β-CrADP, β,γ-CrATP, and α,β,γ-CrATP, are competitive inhibitors of MF_1 with respect to MgATP (383, 432). β,γ-CrATP and α,β,γ-CrATP inhibit F_1 by binding at the catalytic site and α,β-CrATP by binding at a regulatory site (432). The binding sites show no significant selectivity for the steric arrangement of the chromium complexes. β,γ-CrATP and α,β,γ-CrATP bind to the catalytic site with the same affinity, although they have different steric arrangements of the chromium (β,γ-CrATP with monocyclic coordination at the metal ion and α,β,γ-CrATP with bicyclic coordination). Two diastereomers of α,β-CrADP (Λ and Δ isomers) also exert similar inhibitory effects (432). Monodentate $Cr(NH_3)_4$ATP, bidentate/tridentate RhATP, bidentate $Cr(NH_3)_4$ATP, and bidentate $Co(NH_3)_4$ATP are mixed noncompetitive inhibitors of F_1 (44, 158, 383, 384). All the amine and aqua exchange-inert metal-nucleotide complexes are mutually exclusive during ATP hydrolysis and appear to bind the same site(s) (383).

3′-acetyl ATP and 3′-acetyl ADP are monoacetylated adenine nucleotides in which an acetyl group is attached to the 3′ hydroxyl group of ribose. 3′-Acetyl ATP and 3′-acetyl ADP inhibit the ATPase activity of MF_1 in a competitive fashion with ATP and ADP, respectively (355, 394). They bind to catalytic sites, but no reactions occur; i.e., the 3′-acetyl ADP is not phosphorylated, and the 3′-acetyl ATP is not hydrolyzed (355).

3′-*O*-[1-(5-dimethylamino)-naphthoyl]ADP (F-ADP or DMAN-ADP) and 3′-*O*-(1-naphthoyl)ADP (N-ADP) are fluorescent analogs of ADP in which 5-dimethyl amino-naphthoyl and naphthoyl groups are attached to the 3′ hydroxyls of ribose, respectively (356, 397, 427). Both inhibitors are potent competitive inhibitors of both ATP hydrolysis and ATP syn-

TABLE 17. Inhibitory potencies of purine nucleotides and nucleotide analogs

Name or abbreviation	Inhibitory potency (reference)
Excess free ATP	1 Mg^{2+}/8–10 ATP[a] (*R. rubrum* F_1-ATPase) (291); 1 mM[b] (*R. rubrum* F_1-ATPase) (291); 5% inhibition at 12 mM (*P. blakesleeanus* F_1-ATPase) (98)
ADP	15–17 μM[b] (bovine heart MF_1-ATPase) (272, 362); 8.6–9 μM[b] (rat liver SMP-ATPase) (263, 272)
GTP	5–10 μM[a] for 15 min (spinach CF_1-ATPase) (159)
FTP	5–10 μM[a] for 15 min (spinach CF_1-ATPase) (159)
TNP-ATP	100 nM[a] (bovine heart MF_1-ATPase) (277); 5.5 nM[b] (157), 25 nM[b] (214) (bovine heart MF_1-ATPase); 21 nM[b] (bovine heart SMP-ATPase) (157); noncatalytic sites 0.2 μM[c] and catalytic sites < 0.001, 0.023, 1.39 μM[c] (EF_1-ATPase) (429)
TNP-ADP	15–20 nM[a] (bovine heart MF_1-ATPase) (277); 8 nM[b] (214), 10 nM[b] (157) (bovine heart MF_1-ATPase); 1.3 μM[b] (bovine heart SMP-ATP synthesis) (157); noncatalytic sites 6.5 μM[c] and catalytic sites 0.008, 1.3, 1.3 μM[c] (EF_1-ATPase) (429)
TNP-Ado	33 μM[b] (bovine heart MF_1-ATPase) (214)
Lin-benzo-ADP	16 μM[b] (bovine heart MF_1-ATPase) (199); 0.2 μM[c] (EF_1-ATPase) (424); <10 nM[c] and 1–2 μM[c] (bovine heart MF_1-ATPase) (428)
AP_4A	18 μM[a] (bovine heart MF_1-ATPase) (417)
AP_5A	~60% inhibition at 520 μM in 10 min (bovine heart MF_1-ATPase) (417); no inhibition up to 100 μM (bovine heart MF_1-ATPase) (325)
AP_6A	~80% inhibition at 520 μM in 80 min (bovine heart MF_1-ATPase) (417)
AMP-PNP	0.5 μM[b] (37), 0.33 μM[b] (306), 0.32 μM[b] (361), 14 nM[b] (84) (bovine heart MF_1-ATPase); 0.16 μM[b] (bovine heart SMP-ATPase) (306); 0.92 μM[b] (255), 0.3 μM[b] (361) (rat liver MF_1-ATPase); 1.3 μM[b] (rat liver SMP-ATPase) (255); 0.6[b] (EF_1-ATPase) (436)
GMP-PNP	12.3 μM[b] (bovine heart MF_1-ATPase) (37); 300 μM[b] (rat liver MF_1-ATPase) (361)
IMP-PNP	105 μM[b] with bicarbonate (bovine heart MF_1-ATPase) (362)
$AMP(CH_2)P$	K_m, 2.8 μM in the presence of 1 mM inhibitor from 0.85 μM in its absence (pea SMP-ATP synthesis) (254)
RhATP	Bi- and tridentate RhATP, 300 μM[b] (bovine heart MF_1-ATPase) (383)
CrATP or $Cr(NH_3)_4ATP$	Monodentate CrATP, 78 μM[b] (bovine heart MF_1-ATPase) (383); monodentate $Cr(NH_3)_4ATP$, 500 μM[b] (bovine heart MF_1-ATPase) (383); bidentate CrATP, 1 mM[b] (bovine heart MF_1-ATPase) (383) and 170 μM[b] (*S. cerevisiae* MF_1-ATPase) (432); bidentate $Cr(NH_3)_4ATP$, 100 μM[b] (bovine heart MF_1-ATPase) (383); tridentate CrATP, 150 μM[b] (*S. cerevisiae* MF_1-ATPase) (432)
$Co(NH_3)_4ATP$	Bidentate $Co(NH_3)_4ATP$, 400 μM[b] (bovine heart MF_1-ATPase) (384)
3′-*O*-Acetyl-ATP	400 nM[b] (bovine heart MF_1-ATPase) (394)
3′-*O*-Acetyl-ADP	55.3–85 μM[a] (bovine heart SMP, oxidative phosphorylation) (355, 356)
3′-*O*-Caproyl-ADP	1.7 μM[a] (bovine heart SMP-oxidative phosphorylation) (355)
3′-*O*-Enanthyl-ADP	2.7 μM[a] (bovine heart SMP-oxidative phosphorylation) (355)
3′-*O*-Caprylyl-ADP	1.7 μM[a] (bovine heart SMP-oxidative phosphorylation) (355)
DMAN-ADP/F-ADP	0.25 μM[a] (bovine heart SMP-oxidative phosphorylation) (356); 40 nM[b] (bovine heart SMP-oxidative phosphorylation) (356); 9.8 μM[b] (bovine heart SMP-uncoupled ATPase) (356); 50 nM[c] (bovine heart MF_1-ATPase) (397)
F-ATP	2.1 μM[a] (bovine heart SMP-oxidative phosphorylation) (356); 0.3 μM[b] (bovine heart SMP, oxidative phosphorylation) (356); 12–27 μM[b] (bovine heart SMP-uncoupled ATPase) (356)
3′-*O*-(1-Naphthoyl)-ADP/N-ADP	300–350 nM[a] (bovine heart SMP-oxidative phosphorylation) (355, 356); 4.6 μM[b] (bovine MF_1-ATPase) (240); 9 μM[b] (bovine heart SMP-ATPase) (240); 48 nM[b] (bovine heart SMP-oxidative phosphorylation) (355); 20–50 nM[c] (bovine MF_1-ATPase) (397)
3′-*O*-(1-Naphthoyl)-ATP	2.0 μM[a] (bovine heart SMP-oxidative phosphorylation) (356)
3′-*O*-(2-Naphthoyl)-ADP	5.0 μM[a] (bovine heart SMP-oxidative phosphorylation) (356)
BzATP	0.85 μM[b] (bovine heart MF_1-ATPase) (3); ~6 μM[b] (TF_1-ATPase) (8); 1.6 μM[c] (bovine heart MF_1-ATPase) (3)
BzADP	0.72 μM[b] (bovine heart MF_1-ATPase) (3)
t-butylacetyl-ADP	1.5 μM[a] (bovine heart SMP-oxidative phosphorylation) (355)
3′-*O*-Phenylacetyl-ADP	3.2–3.6 μM[a] (bovine heart SMP-oxidative phosphorylation) (355, 356)
3′-*O*-Phenylbutyryl-ADP	1.3–4.6 μM[a] (bovine heart SMP-oxidative phosphorylation) (355, 356); 0.2 μM[b] (bovine heart SMP-oxidative phosphorylation) (355)
3′-*O*-Benzoyl-ADP	6.0 μM[a] (bovine heart SMP-oxidative phosphorylation) (355, 356)
3′-*O*-[*N*-(2-Nitrophenyl)-γ−aminobutyryl]-ADP	0.55 μM[a] (bovine heart SMP-oxidative phosphorylation) (356)
3′-*O*-[*N*-(4-Nitrophenyl)-γ−aminobutyryl]-ADP	0.76 μM[a] (bovine heart SMP-oxidative phosphorylation) (356)
3′-*O*-(1-Naphthylacetyl)-ADP	0.8 μM[a] (bovine heart SMP-oxidative phosphorylation) (356)
3′-*O*-(2-Naphthylacetyl)-ADP	0.8 μM[a] (bovine heart SMP-oxidative phosphorylation) (356)
3′-*O*-(1-Anthranoyl)-ADP	0.56 μM[a] (bovine heart SMP-oxidative phosphorylation) (356)
3′-*O*-(9-Anthranoyl)-ADP	5.9 μM[a] (bovine heart SMP-oxidative phosphorylation) (355, 356, 397); 1.1 μM[b] (bovine heart SMP-oxidative phosphorylation) (355)
FSBI	0.5 mM[c] for reversible binding (bovine heart MF_1-ATPase) (49)
FSBA	45% (1 h) and 65% (2 h) inhibition at 0.8 mM (bovine heart SMP-ATPase) (51); 0.23 mM[c] for reversible binding (pig heart MF_1-ATPase) (101)
FSBεA	250 μM[c] (bovine heart MF_1-ATPase) (414)
AP_2-PL	~150 μM[c] (α subunit of EF_1-ATPase) (326); 30% inhibition at 50 μM (EF_1-ATPase) (288)
AP_3-PL	18 μM[a] (EF_1-ATPase) (288); 2.5 μM[a] with Mg^{2+} and 10 μM[a] without Mg^{2+} (EF_1-ATPase) (184)
AP_4-PL	18 μM[a] (EF_1-ATPase) (288)
oATP	10 mM[b] (*M. phlei* F_1-ATPase) (219); 1.05 mol/mol of ATPase[a] (ox heart MF_1-ATPase) (239); 40% inhibition at 1 mol/mol ATPase without ADP and 60 min incubation (ox heart MF_1-ATPase) (239)
oADP	80 μM[c] (bovine heart MF_1-ATPase) (217)
oAMP	90% inhibition at 3 mM (bovine heart MF_1-ATPase) (95)
Cibacron blue	600 μM[a] (rat liver MF_1-ATPase) (28)
BzAF	50 μM[b] in the dark (bovine heart MF_1-ATPase) (297); 58 μM[c] (bovine heart MF_1-ATPase) (297)

[a] I_{50}.
[b] K_i.
[c] K_d.

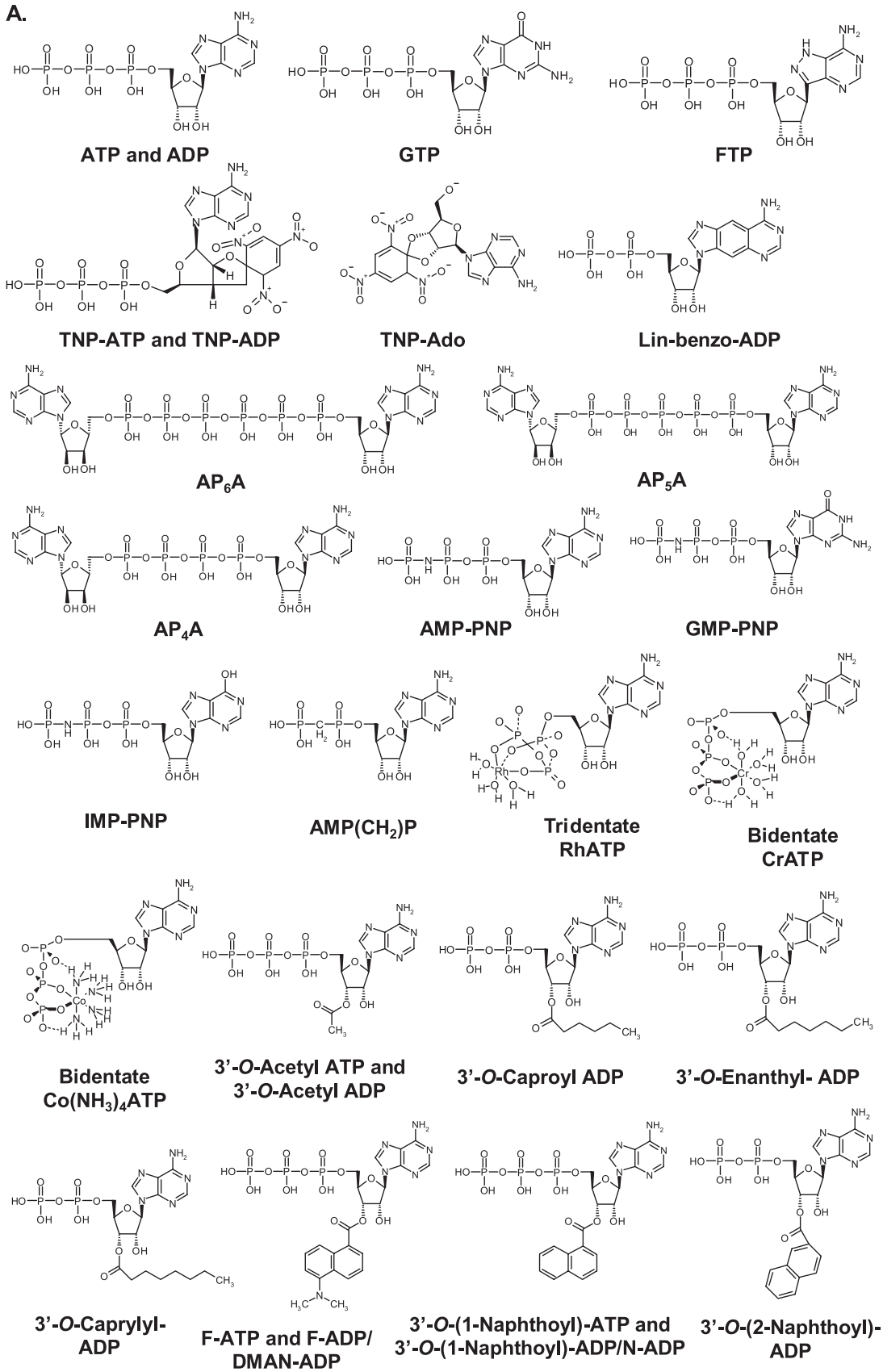

FIG. 9. Structures of purine nucleotides and nucleotide analogs. (A) Nucleotides and nucleotide analogs. (B) Azidonucleotides.

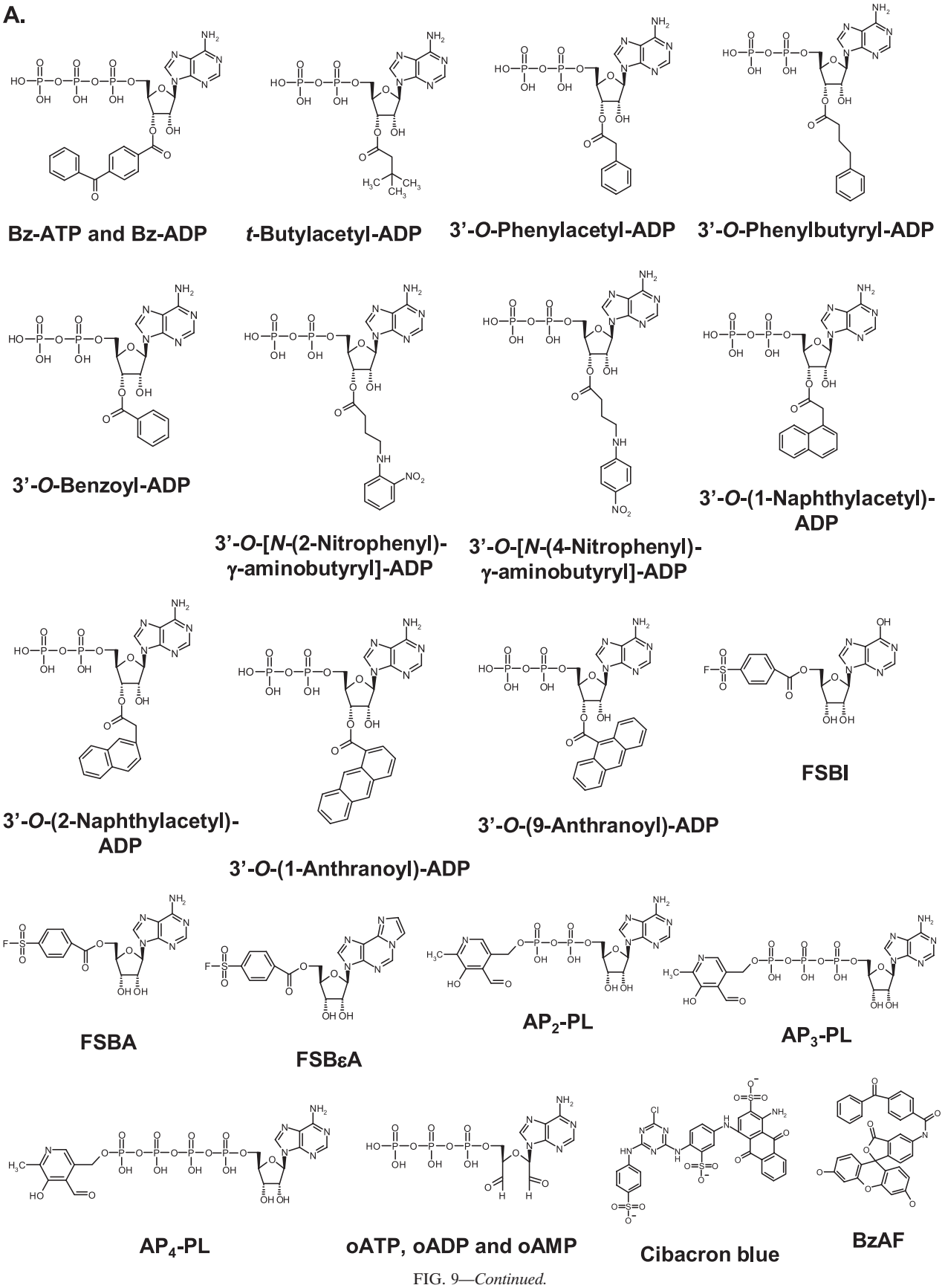

FIG. 9—*Continued.*

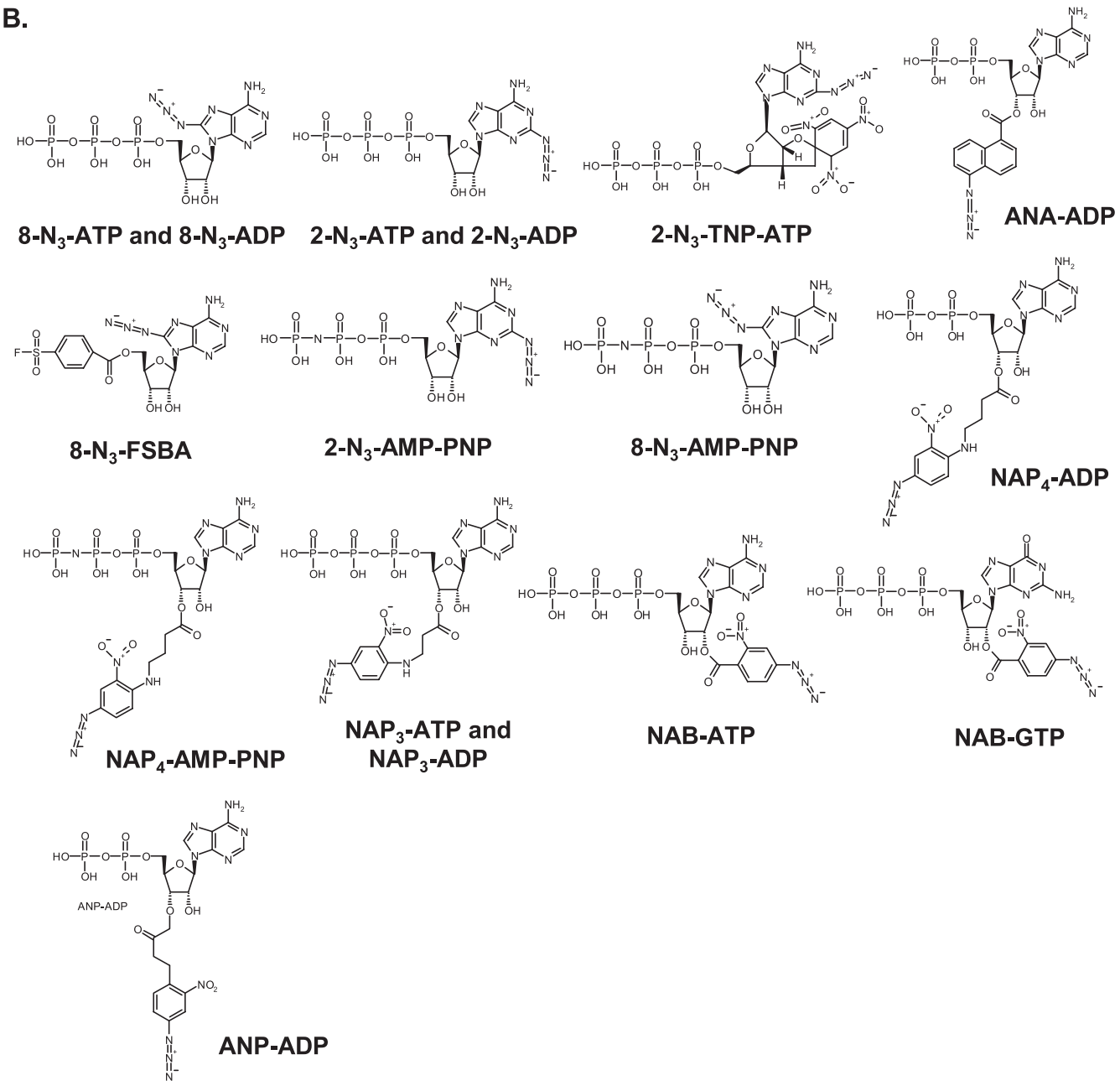

FIG. 9—*Continued.*

thesis and exhibit a much stronger inhibition of ATP synthesis than of ATP hydrolysis (356, 397). F-ADP binds to three sites in bovine heart MF_1 with K_d values of 50 nM for all sites, whereas the N-ADP binds to two sites with K_d values of 20 to 50 nM (397). F-ADP binds approximately 10 times more strongly than F-ATP (3′-*O*-[1-(5-dimethylamino)-naphthoyl]ATP), whereas F-AMP (3′-*O*-[1-(5-dimethylamino)-naphthoyl]AMP) is not inhibitory (356). ANA-ADP (3′-*O*-[5-azidonaphthoyl]-ADP) is a photoreactive analog of N-ADP (Fig. 9B and Table 18). It binds to the same site as N-ADP but with a lower affinity, i.e., about 2.5 times lower than the K_i of N-ADP for bovine heart MF_1. Upon illumination, ANA-ADP rapidly photoinactivates F_1 (240).

3′-*O*-(4-Benzoyl)benzoyladenosine 5′-triphosphate (BzATP) and BzADP are ribose-modified photoactivatable analogs of ATP and ADP in which a photoreactive (4-benzoyl)benzoyl group is attached to the 3′ hydroxyls of ribose (Fig. 9A) (435). BzATP binds to the ATP synthase β subunits both isolated and complexed but binds only to isolated α subunits (33). BzATP and BzADP bind to the catalytic site as competitive and reversible inhibitors in the absence of illumination. However, under actinic illumination, BzATP and

TABLE 18. Azidonucleotides

Name	Molecular formula	Other names	Inhibitory potency (reference)
8-Azido-ATP	$C_{10}H_{15}N_8O_{13}P_3$	8-Azidoadenosine 5′-triphosphate	1 mM[b] (bovine heart SMP, phosphorylation) (371); 1 mM[b] (bovine heart SMP-ATPase) (371); 88% inhibition at 1.7 mM (bovine heart MF_1-ATPase) (419); complete inhibition at 2 inhibitor bound mol/mol F_1 (bovine heart MF_1-ATPase) (110, 420)
8-Azido-ADP	$C_{10}H_{14}N_8O_{10}P_2$	8-Azidoadenosine 5′-diphosphate	86% inhibition at 1.7 mM (bovine heart MF_1-ATPase) (419); full inhibition at 1.9–2 mol bound inhibitor/mol F_1 (134, 419)
2-Azido-ATP	$C_{10}H_{15}N_8O_{13}P_3$	2-Azidoadenosine 5′-triphosphate	52% inhibition at 1.8 (0.8 covalent) inhibitor mol/mol F_1 (EF_1-ATPase) (425); complete inhibition at 0.92 inhibitor bound mol/mol F_1 (bovine heart MF_1-ATPase) (408)
2-Azido-ADP	$C_{10}H_{14}N_8O_{10}P_2$	2-Azidoadenosine 5′-diphosphate; 1-azidoadenosine-3′,5′-bisphosphate	5 μM[c] in the dark (bovine heart MF_1-ATPase) (45); full inhibition at 1.9–2 mol bound inhibitor/mol F_1 (45, 134)
2-Azido-TNP-ATP	$C_{17}H_{20}N_{11}O_{18}P_3$	2-N_3-TNP-ATP	
ANA-ADP	$C_{21}H_{17}N_8O_{11}P_2$	3′-*O*-[5-Azidonaphthoyl]-ADP	11 μM[b] in the dark (bovine heart MF_1-ATPase) (240); total inactivation at 2 mol/mol F_1 (bovine heart MF_1-ATPase) (240)
8-Azido-FSBA	$C_{17}H_{15}FN_8O_7S$	5′-*p*′-Fluorosulfonylbenzoyl-8-azidoadenosine; 8-N_3-FSBA	0.47 mM[c] in the dark (bovine heart MF_1-ATPase) (453)
2-Azido-AMP-PNP	$C_{10}H_{15}N_9O_{12}P_3$	2-Azidoadenyl-5′-yl imidodiphosphate	4 μM[b] (bovine heart MF_1-ATPase) (109)
8-Azido-AMP-PNP	$C_{10}H_{15}N_9O_{12}P_3$	8-Azidoadenyl-5′-yl imidodiphosphate	460 μM[b] (bovine heart MF_1-ATPase) (109)
NAP_4-ADP	$C_{20}H_{24}N_{10}O_{13}P_2$	*N*-4-Azido-2-nitrophenyl-γ−aminobutyryl-ADP	2.0 μM[a] (bovine heart SMP-oxidative phosphorylation) (355); 0.6 mM[b] in the dark (bovine heart MF_1-ATPase) (244); 0.5 μM[b] (bovine heart SMP-oxidative phosphorylation) (355)
NAP_4-AMP-PNP	$C_{20}H_{23}N_{11}O_{15}P_3$	Nap_4-PPNHP; NAP_4-AdoPP[NH]P; *N*-4-azido-2-nitrophenyl γ−aminobutyryl-5-adenylyl imidodiphosphate; *N*-4-Azido-2-nitrophenyl-γ-aminobutyryl-AdoPP[NH]P	3 μM[c] in the dark (bovine heart MF_1-ATPase) (247)
NAP_3-ATP	$C_{19}H_{23}N_{10}O_{16}P_3$	3′-*O*-{3-[*N*-(4-Azido-2-nitrophenyl) amino]propionyl}adenosine 5′-triphosphate; arylazido aminopropionyl ATP	43% maximum inhibition at 36 μM with 15 min photoreaction (bovine heart MF_1-ATPase) (341)
NAP_3-ADP	$C_{19}H_{22}N_{10}O_{13}P_2$	3′-*O*-[3-[*N*-(Azido-2-nitrophenyl) amino]propionyl]adenosine 5′-diphosphate; arylazido-β-alanyl-ADP; arylazido aminopropionyl ADP	80% inhibition at 50 μM in the dark (pig heart MF_1-ATPase) (117)
NAB-ATP	$C_{17}H_{18}N_9O_{16}P_3$	3′(2′)-*O*-(2-Nitro-4-azidobenzoyl)adenosine 5′-triphosphate	K_m of 0.85 mM, maximal 40–45% modification (bovine heart MF_1-ATPase) (216)
NAB-GTP	$C_{17}H_{18}N_9O_{17}P_3$	3′(2′)-*O*-(2-Nitro-4-azidobenzoyl)guanosine 5′-triphosphate	Maximal 40–45% modification (bovine heart MF_1-ATPase) (216)
ANP-ADP	$C_{19}H_{27}N_9O_{13}P_2$	3′-*O*-[3-(4-Azido-2-nitrophenyl)propionyl]-ADP	1.3 μM[a] (bovine heart SMP-oxidative phosphorylation) (355); 50 μM[b] (bovine heart MF_1-ATPase) (426); 0.2 μM[b] (bovine heart SMP-oxidative phosphorylation) (355, 426); full inhibition at 3 mol/mol F_1 (bovine heart MF_1-ATPase) (426)

[a] I_{50}.
[b] K_i.
[c] K_d.

BzADP inactivate F_1 irreversibly by covalently modifying the catalytic site (3, 8, 435).

Other 3′-*O*-substituted adenine nucleotides include 3′-*O*-phenylacetyl-ADP, 3′-*O*-phenylbutyryl-ADP, 3′-*O*-benzoyl-ADP, 3′-*O*-[*N*-(2-nitrophenyl)-γ-aminobutyryl]-ADP, 3′-*O*-[*N*-(4-nitrophenyl)-γ-aminobutyryl]-ADP, 3′-*O*-naphthoyl-(1)-ADP, 3′-*O*-naphthoyl-(1)-ATP, 3′-*O*-naphthoyl-(2)-ADP, 3′-*O*-naphthyl-(1)-acetyl-ADP, 3′-*O*-naphthyl-(2)-acetyl-ADP, 3′-

O-5-dimethylaminonaphthoyl-(1)-ADP, 3′-*O*-5-dimethylaminonaphthoyl-(1)-ATP, 3′-*O*-anthranoyl-(1)-ADP, and 3′-*O*-anthranoyl-(9)-ADP (356). These inhibitors inhibit oxidative phosphorylation in bovine heart SMP with K_i values in the range of 0.3 to 5.9 μM (Table 17).

The fluorosulfonylbenzoyl nucleotides 5′-*p*-fluorosulfonylbenzoylinosine (FSBI), 5′-*p*-fluorosulfonylbenzoyladenosine (FSBA), and 5′-*p*-fluorosulfonylbenzoylethenoadenosine (FSBεA) bind to F_1 and inactivate the enzyme by modifying amino acid side chains of α and/or β subunits. FSBI binds to the β subunit reversibly and reacts covalently with a Tyr residue. The inactivation follows pseudo-first-order kinetics, and the residues modified are βTyr345 in bovine heart MF_1 (49, 57) and βTyr364 in F_1 from thermophilic bacterium PS3 (50). The modification of a Tyr residue in a single β subunit is sufficient to inactivate F_1 completely (49).

FSBA binds reversibly to a single binding site on the β subunit of MF_1 (101). This inactivates F_1 irreversibly by forming a covalent bond via a process that follows pseudo-first-order kinetics (51, 101). The modified residues are αTyr244, αTyr300, and either βTyr368 or βHis427 (51, 56, 114, 407). The complete inactivation of F_1-ATPase by FSBA requires the modification of all three copies of the β subunits, in contrast to that by FSBI (49). 8-azido-FSBA (5′-*p*-fluorosulfonylbenzoyl-8-azidoadenosine) binds to MF_1 in the absence of light and inhibits ATPase activity. Upon illumination of the dark-inactivated F_1, 8-azido-FSBA induces in high yield cross-linking between βHis427 and βTyr345 within the same β subunit (453).

FSBεA binds to αTyr244 of MF_1, inactivating ATPase activity with pseudo-first-order kinetics (152, 414). Maximal inactivation is achieved when FSBεA modifies αTyr244 in one or two copies of the subunit. Inactivation of F_1 by both FSBA and FSBεA is stimulated by high concentrations of phosphate, whereas inactivation by FSBI is not greatly affected. Prior modification of F_1 with FSBA completely prevents modification of αTyr244 by FSBεA, while prior inactivation with FSBI allows considerable modification.

Adenosine oligophospho-pyridoxal compounds (AP_xPL) contain a chain of phosphoryl groups linking adenosine and pyridoxal moieties. Adenosine triphospho-pyridoxal (AP_3-PL) binds to the catalytic sites of EF_1 and inhibits hydrolytic activity by modifying α and β subunits. The stoichiometric ratio of binding of AP_3-PL for complete inactivation of F_1 is about 1 mol of AP_3-PL per 1 mol F_1 (288). Addition of Mg^{2+} increases the inhibitory potencies of AP_3-PL and also causes a change in the ratio of modification of α and β subunits by AP_3-PL from 4:1 in the absence of Mg^{2+} to 1:3 in its presence (184). The residues modified by AP_3-PL are αLys201, βLys155, and βLys201 (184, 281, 390). Adenosine tetraphospho-pyridoxal (AP_4-PL) binds to EF_1 with the same concentration for half-maximal inactivation as AP_3-PL and shows essentially the same absorption spectrum and binding kinetics (288). Adenosine diphospho-pyridoxal (AP_2-PL or PLP-AMP) is a weak inhibitor compared to AP_3-PL (288). It binds to αLys201 in the isolated α subunit from *E. coli* with a maximal stoichiometry of approximately 1 mol/mol (K_d of ~150 μM). It also impairs the reconstitution of α subunits with β and γ subunits.

The 2′,3′-dialdehydes of ATP, ADP, and AMP (oATP, oADP, and oAMP) are periodate-oxidized derivatives of ATP, ADP, and AMP in which the ribose ring is opened (Fig. 9A). In the presence of Mg^{2+}, oATP is a substrate and acts as a competitive inhibitor of ATP hydrolysis. Prolonged incubation of the enzyme with oATP inactivates F_1-ATPase activity irreversibly with pseudo-first-order kinetics by modifying both α and β subunits (95, 219, 239). Similar inactivation kinetics are also observed with oADP, but the kinetics of inactivation are the same whether Mg^{2+} is present or absent (95). The type of subunits and stoichiometry for the binding of oADP to F_1 are somewhat controversial; the binding of oADP to both α and β subunits with a stoichiometry of 2 to 3 mol oADP/mol F_1 (95, 239) and the binding of oADP only to α subunits with a stoichiometry of 0.9 to 1 mol oADP/mol F_1 (217) both have been proposed. oAMP also inactivates F_1, while AMP is not a substrate for F_1. Finally, both oADP and oAMP inactivate F_1 more efficiently than does oATP (Table 17).

Cibacron blue and 4-benzoyl(benzoyl)-1-amidofluorescein (BzAF) are structural analogs of purine nucleotides. They bind to MF_1 and inhibit ATPase activity (28, 297). BzAF contains a benzophenone moiety on one side of the molecule that is excitable by irradiation at ~340 to 366 nm, and the irradiation of BzaF leads to the covalent insertion of BzAF into F_1. BzAF also contains a fluorescein moiety on the other side of the molecule that fluoresces at >515 nm upon excitation at ~460 to 490 nm. BzAF inhibits mitochondrial ATP synthase as a catalytic site-specific covalent modifying agent (297). Like BzATP, BzAF binds to F_1 competitively with respect to ATP in the absence of illumination and forms a covalent bond with F_1 upon actinic irradiation. The photoinactivation of F_1 by BzAF follows pseudo-first-order kinetics.

8-Azido-ATP and 8-azido-ADP are adenine-modified analogs of ATP and ADP in which an azido group is attached to the carbon 8 of adenine (Fig. 9B). 8-Azido-ATP is a substrate of F_1 and is hydrolyzed slowly by F_1 in the dark (420). The K_m for 8-azido-ATP is similar to that for ATP, but the V_{max} of hydrolysis with 8-azido-ATP is only 6% of that observed with ATP (bovine heart MF_1) (371). On irradiation at 350 to 360 nm, the 8-azido-ATP inactivates F_1-ATPase by binding covalently to F_1, where both α and β subunits are modified. About 2.5 to 3 times more 8-azido-ATP is bound to β than to α subunits in MF_1 (175, 371), whereas almost equal amounts are bound at these two subunits in CF_1 (421). The modified residues in the β subunit of bovine heart F_1 are Lys301, Ile304, and Tyr311 (175). F_1-ATPase activity is completely inhibited when 2 mol 8-azido-ATP binds per mol F_1. Moreover, Mg^{2+} is not required for the binding (420). Interestingly, 8-azido-ADP is phosphorylated by ATP synthase in SMP at a very low rate in the dark. The K_i for 8-azido-ADP is about 1 mM for mitochondrial F_0F_1 from bovine heart, whereas the K_i for ADP is ~20 nM for MF_1 from the same source (371). Photolysis at 350 nm leads to the inactivation of ATP synthase, as the 8-azido-ADP preferentially binds to β subunits (133, 371). The ATPase activity of F_1 is completely inhibited at 2 mol of 8-azido-ADP bound per 1 mol F_1 (419). In the presence of fluoroaluminate, 8-azido-ADP modifies βTyr-345 (133).

2-Azido-ATP and -ADP are also adenine-modified analogs of ATP and ADP in which an azido group is attached to carbon 2 of adenine. 2-Azido-ADP photolabels β subunits exclusively upon photoirradiation, in contrast to 8-azido-

ADP or -ATP, which modify both α and β subunits (86, 89, 419, 421). 2-Azido-ADP binds to F_1 with an affinity similar to the affinity of ADP (45), and upon irradiation it modifies βLeu342, βIle344, βTyr345, βPro346, or βTyr368 (bovine heart MF_1) (111, 132).

2- and 8-Azidoadenyl-5′-imidodiphosphate (2-azido-AMP-PNP and 8-azido-AMP-PNP) are derivatives of AMP-PNP. They bind to F_1 at what appear to be both catalytic and noncatalytic sites (109). Under nonphotolytic conditions, 2-azido-AMP-PNP has a much higher inhibitory potency (K_i = 4 μM) than 8-azido-AMP-PNP (K_i = 460 μM).

3′-Arylazido butyryl ADP (NAP_4-ADP) is a photoreactive derivative of ADP in which a photosensitive *N*-4-azido-2-nitrophenylaminobutyryl group is attached to the adenine ring of ADP (244). NAP_4-ADP is a competitive inhibitor with respect to ATP, with a K_i value of 0.6 mM (bovine heart MF_1). NAP_4-ADP is a moderate inhibitor in the dark. However, upon photoirradiation with visible light, it inactivates F_1 by binding covalently to both α and β subunits. NAP_4-AMP-PNP (or NAP_4-AdoPP[NH]P) is an analog of NAP_4-ATP containing an NH group that replaces oxygen at the position of the terminal bridge oxygen of the triphosphate chain. NAP_4-AMP-PNP binds to F_1 with high affinity, and upon illumination, it inactivates F_1 by covalently modifying α and β subunits (247). NAP_4-AMP-PNP preferentially modifies the α subunit(s) at low concentrations, whereas it modifies α and β subunits equally at high concentrations.

3′-*O*-[3-[*N*-(Azido-2-nitrophenyl)amino]propionyl]ATP (NAP_3-ATP) and NAP_3-ADP are analogs of ATP and ADP in which a photoreactive *N*-4-azido-2-nitrophenylaminopropionyl group is attached to the adenine ring. NAP_3-ATP acts as a substrate in the dark and shows photodependent inhibition associated with covalent modification of F_1 upon illumination (117, 341). In contrast, NAP_3-ADP, just like ADP, induces hysteretic inhibition of soluble F_1 and membrane-bound F_1, with the latter being more sensitive (117). The kinetics of inhibition is biphasic. Preincubation of MF_1 from pig heart with NAP_3-ADP in the dark inhibits ATPase activity about 80%, a value that is increased to 87% upon photoirradiation (117).

3′(2′)-*O*-(2-Nitro-4-azidobenzoyl)ATP (NAB-ATP) and NAB-GTP are 3′(2′)-*O*-(2-nitro-4-azidobenzoyl)-derivatives of ATP and GTP in which a 2-nitro-4-azidobenzoyl group is attached to the 2′ hydroxyls of ribose. NAB-ATP binds to the catalytic site of F_1 and is hydrolyzed to NAB-ADP and inorganic phosphate (216). After hydrolysis, NAB-ADP remains bound to F_1, whereas phosphate is dissociated. The $F_1 \cdot$ NAD-ADP complex is inactive, but in the presence of ATP, the bound NAB-ADP is released, resulting in the reactivation of ATPase activity. Illumination (300 to 380 nm) of F_1 inhibited with NAB-ADP leads to its covalent binding to the enzyme. NAB-GTP has an inhibitory activity similar to that of NAB-ATP.

3′-*O*-[3-(4-Azido-2-nitrophenyl)propionyl]-ADP (ANP-ADP) is a photoreactive analog of ADP in which a 4-azido-2-nitrophenyl propionyl group is attached to the 3′ hydroxyls of ribose (Fig. 9B). ANP-ADP binds to nucleotide binding sites on F_1, inhibiting both ATP hydrolysis and ATP synthesis (355, 426). Inhibition of F_1 by ANP-ADP is competitive with ADP in the dark, but upon illumination, ANP-ADP inactivates F_1 by covalently modifying α and β subunits. The stoichiometry for complete photoinactivation of F_1 is 3 mol of ANP-ADP/mol of F_1. The inhibition of F_1 by the photolabeling is reversed by mild alkaline treatment due to the hydrolysis of the 3′-ester bond and release of the ADP moiety of the inhibitor (426).

AMINO ACID MODIFIERS

Amino Group Modifiers

Phenylglyoxal and butanedione are dicarbonylic Arg residue modifiers. They inactivate both membrane-bound and isolated F_1 (Fig. 10A and Table 19) (43, 128, 129, 162, 248, 375, 381, 385). Inactivation by these agents follows pseudo-first-order kinetics (67, 128, 129, 248). Although the rate of inactivation is decreased in the presence of ADP and ATP (67, 128, 398), it is not significantly influenced by the presence of phosphate (398). Phenylglyoxal and butanedione also inhibit ATP↔ P_i exchange activity (43, 128, 162, 248, 385). Only one molecule of reagent per F_1 active site is required for inactivation, with the binding site(s) believed to be located at or near this active site (128, 248).

1-Fluoro-2,4-dinitrobenzene is a Lys residue modifier that inhibits the hydrolytic activity of MF_1 (11, 194, 250, 399). It modifies Lys162 (bovine sequence) in the P loop, the same residue to which the nitrobenzene (NBD) group migrates at pH 9 (194). Inhibition of ATPase activity follows first-order kinetics (399), with about four 2,4-dinitrophenyl labels required for 96% inhibition (194). Inhibition is reversed nearly 50% by dithiothreitol (11) and is protected effectively by ATP or P_i and slightly by ADP (399).

Dansyl chloride is an acyl chloride of 5-dimethylamino-1-naphthalenesulfonic acid. It modifies reactive amino groups of proteins. Dansyl chloride binds to MF_1 and inhibits both ATP synthesis and membrane-bound ATPase activity to approximately the same extent (250).

Carboxyl Group Modifiers

Carbodiimides are compounds containing a N=C=C functional group. Some inhibit ATP synthase by modifying carboxyl residues residing within F_1, F_0, or both (Fig. 10B). DCCD and *N*-(2,2,6,6-tetramethylpeperidyl-1-oxyl)-*N*-(cyclohexyl)carbodiimide (NCCD) are lipid-soluble carbodiimides. DCCD binds to both F_1 and F_0 of ATP synthases from mitochondria and some bacteria (137, 204, 400, 441) (Table 20). F_1 from some bacteria, such as *Helicobacter pylori*, are insensitive to DCCD (36). DCCD reacts covalently with DCCD-sensitive F_1 via a Glu residue in the β subunit. In F_1 from *E. coli*, βGlu192 binds DCCD, while in bovine MF_1, βGlu199, corresponding to *E. coli* βGlu192, is modified. In F_1 from thermophilic *Bacillus*, βGlu181 (*E. coli* sequence) rather than βGlu192 is modified (137, 400, 441). Incorporation of 1 mol of DCCD into 1 mol of F_1 results in 95% inhibition of the ATPase activity of EF_1, and 2 mol of DCCD/mol F_1 leads to complete inhibition (400). In the crystal structure of the F_1-DCCD complex from bovine heart mitochondria, one molecule of DCCD is bound per F_1 (137). In this structure, the βGlu199 of β_{DP} located at the interface between β_{DP} and α_{DP} is modified. The covalently

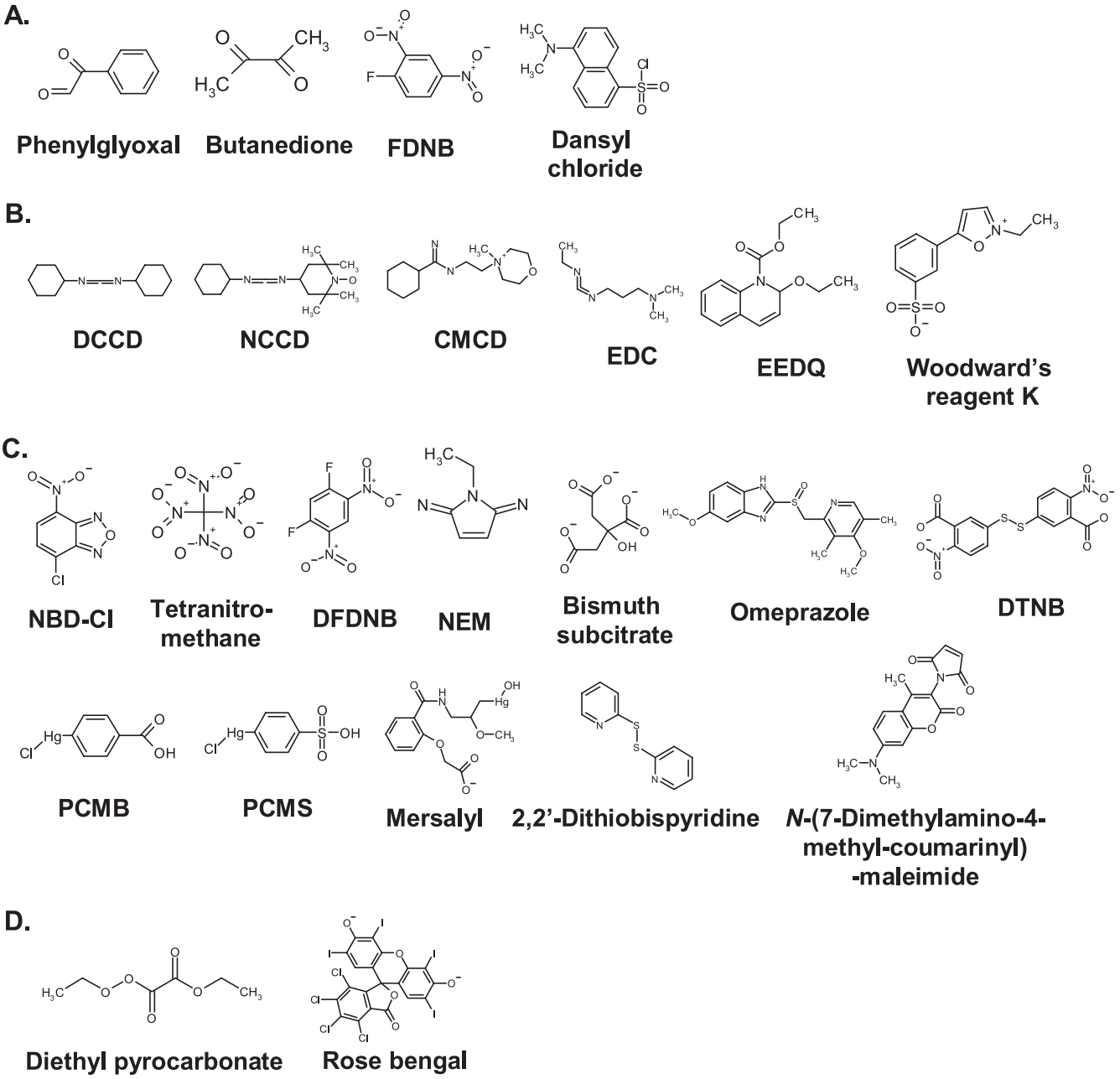

FIG. 10. Structures of amino acid residue modifiers. (A) Amino group modifiers. FDNB, 1-fluoro-2,4-dinitrobenzene. (B) Carboxyl group modifiers. CMCD, 1-cyclohexyl-3-(2-morpholinoethyl)carbodiimide metho-*p*-toluenesulfonate. (C) Cys/Tyr residue modifiers. DTNB, 5,5′-dithiobis(2-nitrobenzoic acid). (D) His residue modifiers.

modified DCCD (dicyclohexyl-*N*-acylurea) is bound in a hydrophobic cleft with one face exposed to the solvent. Residues βVal164, βMet167, βVal420 and βPhe424 contribute to the binding of DCCD, and the steric hindrance involved is believed to inhibit F_1 by blocking a conformational change from β_{DP} to β_E.

DCCD, by binding F_0 (35), also inhibits F_0-mediated proton translocation and the ATPase activity of the coupled F_0F_1 complex. Here, DCCD is bound covalently to an essential carboxyl residue of subunit *c* at position 61 (*E. coli* sequence) (68, 122, 364). The stoichiometries for the maximal inhibition of function are 1 mol of DCCD/mol of F_0, i.e., modification of 1 subunit *c*/F_0 for inhibiting ATPase activity of ATP synthase and 2 mol of DCCD/mol F_0 for inhibiting proton translocation (140, 171, 213).

NCCD is a lipid-soluble spin-labeled inhibitor of ATP synthase that targets the F_0 of ATP synthase (23, 24). The binding site for NCCD is believed to be the same as that for DCCD, i.e., Asp61 of subunit *c*, as NCCD's binding to the ATP synthase is prevented by DCCD (24). Moreover, the mutant of

TABLE 19. Amino group modifiers

Name or abbreviation	Molecular formula	Other names	Inhibitory potency, I_{50} (reference)
Phenylglyoxal	$C_8H_6O_2$	Benzoylcarboxaldehyde; phenylglyoxal; benzoylformaldehyde; phenylethanedione; α-oxobenzeneacetaldehyde	25% inhibition at 2.7 μmol/mg protein (bovine heart SMP-ATPase) (162); 47.5% inhibition at 3 mM (*E. coli* F_0F_1-ATPase after F_0 modification) (381); 33.5% inhibition at 20 mM (*E. coli* F_0-liposome proton uptake) (381)
Butanedione	$C_4H_6O_2$	Diacetyl; dimethyl glyoxal; 2,3-butanedione; dimethyl diketone; butadione	0.63 μmol/mg protein and ~100% inhibition at 1.7 μmol/mg protein (bovine heart SMP-ATPase) (162)
FDNB	$C_6H_3FN_2O_4$	1-Fluoro-2,4-dinitrobenzene; dinitrofluorobenzene; 2,4-DNFB; 2,4-dinitro-1-fluorobenzene; 2,4-dinitrofluorobenzene; fluoro-1,3-dinitrobenzene; Sanger's reagent	96% inhibition at about four 2,4-dinitrophenyl labels (bovine heart MF_1-ATPase) (194)
Dansyl chloride	$C_{12}H_{12}ClNO_2S$	5-(Dimethylamino)-naphthalene-1-sulfonyl chloride; 1-chlorosulfonyl-5-dimethylaminonaphthalene; 1-dimethylaminonaphthalene-5-sulfonyl chloride; dansyl; DNS chloride	

Ala25 in subunit *c*, which is near Asp61, shows a greatly reduced inhibitory activity with NCCD (138).

1-Cyclohexyl-3-(2-morpholinoethyl)carbodiimide metho-*p*-toluenesulfonate and ethyldimethylaminopropyl carbodiimide (EDC) are water-soluble carbodiimides that modify a carboxyl group(s) in F_1. 1-Cyclohexyl-3-(2-morpholinoethyl)carbodiimide metho-*p*-toluenesulfonate binds to F_1 reversibly and likely modifies carboxyl groups near the catalytic sites (186). EDC inhibits F_1 after modifying several carboxyl groups in β subunits. The inhibition by EDC is greatly reduced by Mg^{2+} (236). Incorporation of about 13 mol of EDC/mol F_1 (*E. coli*) leads to 95% inhibition of ATPase activity. Here, two-thirds of the bound EDC is bound to β subunits, where it modifies multiple sites in a short segment (residues 162 to 194) (*E. coli* sequence) (236). EDC also promotes formation of intersubunit cross-links between subunits β and ε. The residues involved are βGlu381 and likely εSer108 (90).

N-Ethoxycarboxyl-2-ethoxy-1,2-dihydroquinoline (EEDQ) inhibits both MF_1 and BF_1 (Fig. 10B and Table 20) (204, 222, 250, 320, 322, 399). The inactivation by EEDQ is both pH and temperature dependent and also time and concentration dependent (204, 322). One mole of EEDQ binds to one mole of F_1. The inactivation follows pseudo-first-order kinetics until 90 to 95% inactivation occurs (322). Inhibitions by EEDQ and DCCD are additive, suggesting that the binding sites of EEDQ and DCCD are either the same (204, 222) or located close to each other (320).

Woodward's reagent K inhibits both F_1 and F_0 (204, 381). The chemical modification of the β subunit of F_1 from *Rhodospirillum rubrum* with this reagent results in loss of both phosphate and ATP binding capacities (203). However, ADP binding sites remain active. Chemical modification of F_0 from *E. coli* by Woodward's reagent K inhibits both proton translocation and total ATPase activity (381).

Cys and Tyr Residue Modifiers

4-Chloro-7-nitrobenzofurazan (NBD-Cl) is a fluorescent adenine analog that labels Tyr or Cys residues (Fig. 10C and Table 21). It inhibits both the synthetic and hydrolytic activities of ATP synthases from bacteria, chloroplasts, and mitochondria by modifying an essential residue (βTyr311, bovine sequence) at the catalytic site(s) of F_1 (12, 70, 119, 120, 245, 388, 415). Depending on the experimental conditions, other subunits, particularly the α subunit, are also modified by NBD-Cl (96, 121, 146, 283). In F_1 modified by NBD-Cl, the Tyr-*O*-NBD linkage is unstable at alkaline pH. The NBD group from βTyr311 migrates to βLys162 in the P-loop at pH 9 as a consequence of O-to-N migration (13, 14, 121). The resulting NBD-*N*-Lys derivative of F_1 is also catalytically inactive (14, 121). In a crystal structure of bovine MF_1 covalently modified by NBD-Cl, the NBD-Cl is found in only one of three β subunits, β_E (292). The βTyr311 residues in the β_{TP} and β_{DP} subunits are buried at the α-β subunit interfaces and are inaccessible to NBD-Cl. The NBD binding pocket is positioned in the central nucleotide binding domain with no hydrogen bonds between the NBD ring and the protein. NBD-Cl appears to inhibit F_1 by preventing β_E from undergoing a conformational change (292).

Tetranitromethane and 1,5-difluoro-2,4-dinitrobenzene (DFDNB) modify Tyr residues. Tetranitromethane nitrates the Tyr residue of ATP synthase subunit *c* of the thermophilic bacterium PS3 and inhibits the proton conduction of TF_0 (375). In contrast, tetranitromethane inhibits neither proton translocation nor ATPase activity of *E. coli* ATP synthase (381). However, DFDNB does inhibit the ATPase activity of MF_1 (7, 55), with a molar ratio of 3 for complete inhibition. Here, inhibition is reversed by dithiothreitol. (7). Inactivation of F_1 by DFDNB is believed to be due to modification of either βTyr311 (55) or another Tyr residue (7).

Thiol group reagents, *N*-ethylmaleimide (NEM), bismuth subcitrate, omeprazole, 5,5′-dithiobis(2-nitrobenzoic acid), *p*-chloromercuribenzoate (PCMB), *p*-chloromercuribenzene sulfonate (PCMS), mersalyl, 2,2′-dithiobispyridine, and *N*-(7-dimethylamino-4-methyl-coumarinyl)-maleimide inhibit ATP synthase by modifying Cys residues. Specifically, NEM inhibits the ATPase activity of F_1s from fungi, some bacteria such as *Vibrio parahaemolyticus*, and some mito-

TABLE 20. Carboxyl group modifiers

Name or abbreviaion	Molecular formula	Other names	Inhibitory potency (reference)
DCCD	$C_{13}H_{22}N_2$	1,3-Dicyclohexylcarbodiimide; *N,N′*-dicyclohexylcarbodiimide; bis(cyclohexyl)carbodiimide; carbodicyclohexylimide; *N,N′*-methanetetraylbiscyclo-hexaamine	1.2 μg of inhibitor/mg protein[a] (*S. cerevisiae* SMP-ATPase) (150); 1–5 μg of inhibitor/mg protein[a] (*T. pyriformis* SMP-ATPase) (404); 200 μM[a] in less than 5 min and at ~40 μM[a] in 30 min (*R. rubrum* F_1-ATPase) (204); 1.9 μg/mg protein[a] (*C. fasciculata* SMP-ATPase) (439); 95% inhibition with 1 mol DCCD/mol F_1 (EF_1-ATPase) (400); maximal 70–80% inhibition at 30 μM (membrane-bound EF_0F_1-ATPase) (171); 47% inhibition at 5 μM (*C. thermoaceticum* membrane-bound F_0F_1-ATPase) (190); 97% inhibition with 2 mol inhibitor bound/mol F_1 (bovine heart MF_1-ATPase) (250); maximal inhibition at 1 mol inhibitor/mol F_0 (bovine heart SMP-ATPase) (140); maximal inhibition at 2 mol inhibitor/mol F_0 (bovine heart H^+-translocation) (140); maximal inhibition at 1 mol inhibitor/mol F_0 (*E. coli* membrane H^+-translocation) (171)
NCCD	$C_{16}H_{28}N_3O$	*N*-(2,2,6,6-Tetramethylpeperidyl-1-oxyl)-*N*(cyclohexyl)carbodiimide; *N*-(2,2,6,6-tetramethyl-1-oxypiperid-4-yl)-*N′*-cyclohexylcarbodiimide	0.65 nmol/mg protein[a] (bovine heart SMP-ATPase) (24); 85% inhibition at 1 nmol NCCD/mg protein (bovine heart SMP-ATPase) (23)
CMCD	$C_{14}H_{28}N_3O \cdot C_7H_8O_3S$	1-Cyclohexyl-3-(2-morpholinoethyl) carbodiimidemetho-*p*-toluenesulfonate; *N*-cyclohexyl-*N′*-2-morpholinoethyl-carbodiimide-methyl-4-toluolsulfonate	200 μM[b] (bovine heart MF_1-ATPase) (186)
EDC	$C_8H_{17}N_3$	Ethyldimethylaminopropyl carbodiimide; 1-ethyl-3-[3-(dimethylamino)propyl] carbodiimide; (3-(dimethylamino) propyl)ethylcarbodiimide	95% inhibition at 13 mol of EDC/mol F_1 (EF_1-ATPase) (236)
EEDQ	$C_{14}H_{17}NO_3$	*N*-Ethoxycarboxyl-2-ethoxy-1,2-dihydroquinoline	200 μM[a] in less than 5 min and at ~40 μM[a] in 30 min (*R. rubrum* F_1-ATPase) (204); 70% inhibition at 400–600 μM (bovine heart MF_1-ATPase) (250, 320); 75% inhibition at 400 μM (*E. coli* F_1-ATPase) (320)
Woodward's reagent K	$C_{11}H_{11}NO_4S$	2-Ethyl-5-phenylisoxazolium-3′-sulfonate; *N*-ethyl-5-phenylisoxazolium-3′-sulfonate	88% inhibition at 15 mM (*E. coli* F_0-liposome proton uptake) (162)

[a] I_{50}.
[b] K_d.

chondria, i.e., those from *S. cerevisiae* and *Schizosaccharomyces pombe* (115, 145, 344). The inactivation of F_1 by NEM in sensitive cases is irreversible and protected by nucleotides (115). In contrast, the F_1s from *E. coli* and bovine heart mitochondria are resistant to NEM (344, 366). NEM also binds various F_0 polypeptides, inhibiting proton conduction (445). For example, NEM inhibits mitochondrial F_0 from bovine heart while labeling 25-, 11-, and 9-kDa polypeptides (445).

Bismuth subcitrate and omeprazole are antiulcer drugs. They bind to sulfhydryl groups of F_1 and form stable complexes (36). They inhibit the ATPase activity of F_1 from *Helicobacter pylori* via a reaction that can be prevented and also reversed by mercaptan glutathione. At low pH, omeprazole is converted into a cyclic sulfonamide, and this form inhibits the ATPase activity of *H. pylori* F_1 more potently than the form without acid activation (I_{50} = 43 μM when acid activated, compared to 90 μM without acid activation).

Regarding other sulfhydryl reactive agents, 5,5′-dithiobis(2-nitrobenzoic acid) inhibits the ATPase activity of nucleotide-depleted F_1 (392). In contrast, it is inhibitory neither to native F_1 nor to nucleotide-depleted F_1 in the presence of either ADP or ATP.

PCMB, PCMS, and mersalyl are polar organic mercurials that target F_0 of mitochondrial ATP synthase. Both PCMB and PCMS inhibit the ATP synthesis and ATPase activities of bovine heart ATP synthase. Thiols modified by the mercurials are different from those modified by NEM (438). In contrast to the case for NEM, inhibition by mercurials is reversed almost completely (PCMB) or partially (PCMS) by addition of dithiothreitol. Moreover, the binding of mercurials protects the ATP synthase from irreversible inhibition by DCCD. Mersalyl also inhibits proton conductivity by F_0 from bovine heart mitochondria. Here, the inhibition is much more potent than that observed with PCMB and PCMS (445). Although mersalyl has no inhibitory effect at concentration of up to ≤50 μM, it inhibits proton conduction at higher concentrations (~70% inhibition at 130 μM).

The sulfhydryl-reactive agents 2,2′-dithiobispyridine and *N*-(7-dimethylamino-4-methyl-coumarinyl)-maleimide also inhibit proton conductivity by F_0 from bovine heart mitochondria (445). *N*-(7-Dimethylamino-4-methyl-coumarinyl)-maleimide has stronger inhibitory potencies than 2,2′-dithiobispyridine and NEM. *N*-(7-dimethylamino-4-methyl-coumarinyl)-maleimide shows no inhibition up to a concentration of 200 μM and inhibits proton conduction by 60% at 400 μM.

TABLE 21. Cys/Tyr residue modifiers

Name or abbreviation	Molecular formula	Other names	Inhibitory potency, I_{50} (reference)
NBD-Cl	$C_6H_2ClN_3O_3$	NBF-Cl; 7-chloro-4-nitrobenzofurazan; 4-chloro-7-nitrobenzofurazan; 7-chloro-4-nitrobenzofurazan; 4-chloro-7-nitro-2,1,3-benzoxadiazole; 7-chloro-4-nitrobenzo-2-oxa-1,3-diazole; 4-chloro-7-nitrobenzo-2-oxa-1,3-diazole	4.5 μg of inhibitor/mg protein (*T. pyriformis* SMP-ATPase) (404); 68% inhibition at 50 μM (*C. thermoaceticum* F_1-ATPase) (190); complete inhibition at 1 mol inhibitor bound/mol F_1 (bovine heart F_1-ATPase) (246); >90% inhibition at 1.4 mol inhibitor bound/mol F_1 (TF_1-ATPase) (415)
Tetranitromethane	CN_4O_8	Tetan	130 nmol/mg protein and ~100% inhibition at 210 nmol/mg protein (bovine heart SMP-ATPase) (162); 2.5 mM (TF_0 vesicle, proton conduction) (375); almost complete inhibition at 8 mM (TF_0 vesicle, proton conduction) (375)
DFDNB	$C_6H_2F_2N_2O_4$	1,5-Difluoro-2,4-dinitrobenzene; 4,6-difluoro-1,3-dinitrobenzene	Complete inhibition at 3 mol inhibitor/mol F_1 (bovine heart MF_1-ATPase) (7)
NEM	$C_6H_7N_1O_2$	*N*-Ethylmaleimide; maleic acid *N*-ethylimide	~0.6 mM (*S. pombe* MF_1-ATPase) (115); 74% inhibition at 1 mM (*V. parahaemolyticus* F_1-ATPase) (344)
Bismuth subcitrate	$C_6H_8O_7Bi$	CBS; colloidal bismuth subcitrate; tripotassium dicitratobismuthate	73 μM (*H. pylori* F_1-ATPase) (36)
Omeprazole[a]	$C_{17}H_{19}N_3O_3S$	5-Methoxy-2-(((4-methoxy-3,5-dimethyl-2-pyridyl)methyl)sulfinyl)benzimidazole; Audazol; Omepral	90 μM (without acid activation) and 43 μM (with acid activation) (*H. pylori* F_1-ATPase) (36)
DTNB	$C_{14}H_8N_2O_8S_2$	5,5′-Dithiobis(2-nitrobenzoic acid); dithionitrobenzoic acid; 2,2′-dinitro-5,5′-dithiodibenzoic acid; 3,3′-dithiobis(6-nitrobenzoic acid); dithiobisnitrobenzoic acid; Ellman's Reagent	39% inhibition at 0.4 mM and 46% inhibition at 1.3 mM (bovine heart MF_1-ATPase) (392)
PCMB	$C_7H_5ClHgO_2$	*p*-Chloromercuribenzoic acid; 4-carboxyphenylmercuric chloride; 4-chloromercuribenzoic acid	~90% inhibition at 4.5 mM (bovine heart SMP-ATPase) (438)
PCMS	$C_6H_5ClHgO_3S$	*p*-Chloromercuribenzene sulfonate; 4-chloromercuribenzenesulfonate; PCMBS	6 mM (bovine heart SMP-ATPase) (438)
Mersalyl	$C_{13}H_{16}HgNO_6.Na$	*O*-((3-Hydroxymercuri-2-methoxypropyl)carbamoyl)phenoxy-acetic acid; (3-((2-(carboxymethoxy)benzoyl)amino)-2-methoxypropyl)hydroxymercury; mercuramide; mercusal; mersalyl acid	70% inhibition at 130 μM (bovine heart MF_0, proton conductivity) (445)
2,2′-Dithiobispyridine	$C_{10}H_8N_2S_2$	2,2′-Dithiodipyridine; 2,2′-dipyridyl disulfide; 2PDS; bis(2-pyridinyl) disulfide	55% inhibition at 1 mM (bovine heart MF_0, proton conductivity) (445)
N-(7-Dimethylamino-4-methyl-coumarinyl)-maleimide	$C_{16}H_{14}N_2O_4$	*N*-(4-Methyl-7-dimethylamino-3-coumarinyl)maleimide	60% inhibition at 400 μM (bovine heart MF_0, proton conductivity) (445)

[a] Omeprazole is converted to a cyclic sulfenamide with acid-activation.

His Residue Modifiers

Diethyl pyrocarbonate and Rose bengal are His residue-modifying reagents (Fig. 10D and Table 22). Diethyl pyrocarbonate modifies the ATP synthase β subunit, completely preventing the binding of phosphate. It also blocks the binding of ATP to a Mg^{2+}-dependent low-affinity site (203, 381, 445). In contrast, the ADP binding capacity of the β subunit is not

TABLE 22. His and other amino acid residue modifiers

Name	Molecular formula	Other names	Inhibitory potency, I_{50} (reference)
Diethyl pyrocarbonate	$C_6H_{10}O_5$	Baycovin; diethyl dicarbonate; diethyl oxydiformate; pyrocarbonic acid diethyl ester	>50% inhibition at 3 mM (*E. coli* F_0, liposome proton uptake) (381)
Rose bengal	$C_{20}H_2Cl_4I_4Na_2O_5$	Bengal rose	75–85% inhibition at 0.2 μM (bovine heart F_1-ATPase) (139)
Iodine	I_2		40 μM (rat liver MF_1-ATPase) (314)

TABLE 23. Physical inhibitory factors

Factor	Inhibitory potency (reference)
Hydrostatic pressure	850 bars[a] (bovine heart SMP-ATPase, 0.02 mg/ml) (105)
Far-UV irradiation	~80% inhibition within 15 min at 254 nm (bovine heart SMP-ATPase) (75)
Cold temp	15–60 min[b] at 4°C (324), 4–40 min[a] at 0°C with different prepn (bovine heart MF_1-ATPase) (308, 309)

[a] I_{50}.
[b] Half-life.

affected by modification with diethyl pyrocarbonate (203). Diethyl pyrocarbonate also modifies F_0 from *E. coli*, inducing inhibition of proton uptake (381).

Rose bengal photooxidizes His residues of β subunits, causing conformational instability in F_1 (139). About 60% of the His residues are photooxidized, causing 50% inactivation. This photochemical damage is prevented by various phenanthroline compounds.

Others

Iodine is an electron-dense heavy atom that reacts with and inactivates F_1 (314). It behaves like a typical covalent inhibitor in its modification of amino acid residues. MgATP, MgADP, and phosphate fail to protect F_1 from inhibition by iodine. Iodine preferentially labels the ATP synthase β subunit, although it also labels α and γ subunits to some extent. About 10 atoms of iodine are incorporated per F_1 (rat liver mitochondria) under conditions where the labeling proceeds in a linear fashion. About two atoms of iodine are incorporated per β subunit.

PHYSICAL INHIBITORY FACTORS

High Hydrostatic Pressure

High hydrostatic pressure of above 60 to 80 MPa inactivates both F_1 and the complete ATP synthase (F_0F_1) (Table 23) (105, 310, 377). At below 60 to 80 MPa, the hydrostatic pressure shows stimulatory effects on ATPase activity. However, both membrane-bound and isolated F_0F_1 from mitochondria are inhibited reversibly at high hydrostatic pressure, while soluble F_1-ATPase is inactivated irreversibly due to reassociation with an altered hydrodynamic radius after decompression (105). In contrast to the case for the isolated mitochondrial ATP synthase, the inhibition of the isolated ATP synthase from chloroplasts is irreversible, showing no restoration after decompression (377). The inactivation is dependent on protein concentration (377). Inhibition by high hydrostatic pressure is believed to be associated with dissociation that impairs contacts essential for transmission of conformational information between those subunits needed for rotational catalysis (105, 377).

UV Irradiation

Mitochondrial ATPase activity is inhibited also by far-UV irradiation. UV light at 254 nm results in a time-dependent inhibition of both membrane-bound and soluble F_1. Inhibition reaches its maximum level within 15 min after exposure of SMP to UV (75). This also induces the release of tightly bound adenine nucleotides from F_1. Succinate, a substrate for the electron transport chain, partially protects against the detrimental effects of UV. Inhibition by UV is due to the photochemical modification of the essential Tyr residue located at the active site of F_1 that induces subsequent structural changes in F_1.

Low Temperature

The F_1"catalytic" moiety of the ATP synthase (F_0F_1) is cold labile (308, 309, 324). Its ATPase activity decrease rapidly upon incubation at low temperature. The rate of inactivation is first order, and the half-life varies between 15 and 60 min with different preparations (324). The inactivation is not protected by ATP, ADP, or Mg^{2+} and is reversed by rewarming the enzyme solution under appropriate conditions (309). The inactivation by cold temperature is associated with the dissociation of the enzyme complex into subunits (309).

MISCELLANEOUS INHIBITORS

Polyborates are boron cluster compounds with a unique molecular structure and unusual chemical properties. Among the polyborates, dodecaborates ($[B_{12}H_{12}]^{2-}$) and dicarbononaborates ($[C_2B_9H_{11}]^-$) inhibit ATPase activity of MF_1, and dicarbononaborates have much stronger inhibitory potencies than dodecaborates (Fig. 11) (104). One of the dicarbononaborates, dichlorodicarbononaborate ($[Cl_2C_2B_9H_{10}]^-$), that contains two chlorides inhibits competitively with respect to ATP the ATPase activities of both membrane-bound and soluble F_1. The inhibition is due to a direct interaction of the reagent with the catalytic F_1 moiety (104).

Almitrine is a piperazine-like agent that is known to be a respiratory stimulant that enhances respiration by acting as an agonist of peripheral chemoreceptors located on the carotid bodies. This agent inhibits mitochondrial ATP synthase in an uncompetitive manner (336). Also, it does not destroy the electrochemical proton gradient across the mitochondrial membrane that normally drives ATP synthesis (333–335). Thus, mitochondria treated with this agent remain intact despite the fact that this agent has debilitated their ATP synthase.

5-Hydroxynaphthalenedicarboxylic anhydride (HNA) inhibits the mitochondrial ATPase activity induced by 2,4-dinitrophenol and the ATPase activity of SMP induced by Mg^{2+} (165). HNA also inhibits the ATP-energized mitochondrial volume change. The inhibitory effects of HNA are similar to those of rutamycin.

R207910 is a diarylquinoline drug that has antimycobacterial activity. It inhibits mycobacterial ATP synthase and targets subunit *c* in F_0 (15, 215, 313). The site of action of R207910 seems to be located close to an essential carboxyl residue, Asp61 of subunit *c* (*E. coli* sequence), as the mutations Asp32Val (*Mycobacterium smegmatis*) and Ala63Pro (*M. tuber-*

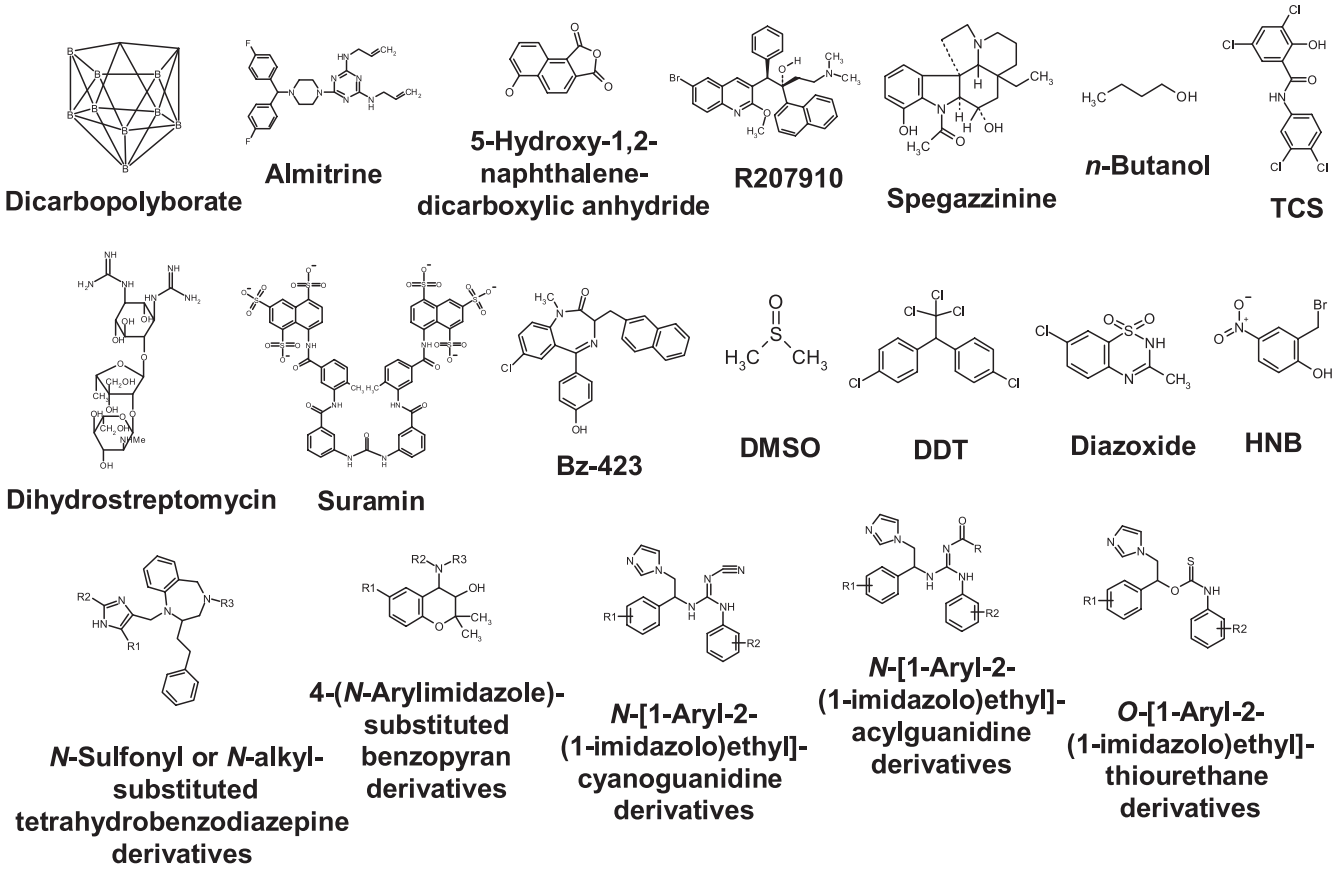

FIG. 11. Miscellaneous inhibitors. TCS, tetrachlorosalicylanilide.

culosis) confer resistance to the drug. Also, the mycobacterial species naturally resistant to R207910 contains Met at position 63 in place of a conserved Ala in all sensitive mycobacteria (15, 181, 313). R207910 is an enantiomeric compound with two chiral centers. It adopts the lowest-energy conformation with the carbon alpha relative to the quinoline moiety R and the carbon beta S (135). The binding of the inhibitor to the binding site in ATP synthase is stereoselective, and its (*S*,*R*) stereoisomer is 2 orders of magnitude less inhibitory than R207910 (215). R207910 appears to act specifically on mycobacteria, and the range of MICs of R207910 is 0.03 to 0.12 μg/ml for 99% inhibition of the growth of *M. tuberculosis* strains (15). The killing effect of *M. tuberculosis* by R207910 is time dependent rather than concentration dependent (15), and R207910 acts synergically when combined with other tuberculous drugs (183, 237, 238).

Spegazzinine is a dihydroindole alkaloid from *Aspidosperma chakensis* Spegazzini (103). It inhibits uncompetitively the ATPase activities of both membrane-bound and isolated CF_1 from spinach (10). Spegazzinine inhibits both cyclic and noncyclic photophosphorylation of isolated spinach chloroplasts. It also inhibits the mitochondrial ATPase activity of *S. pombe* (234) and slightly inhibits the mitochondrial ATPase activity of *Tetrahymena pyriformis* ST (404). In contrast, spegazzinine has no inhibitory effects on the ATPase activities of ATP synthases from *Clostridium pasteurianum* (78), *Tritrichomonas foetus* (235), and mitochondria of *Crithidia fasciculata* (439).

n-Butanol inhibits the ATPase activities of both membrane-bound and soluble MF_1 (406). It inhibits the isolated F_1 at the same or lower concentrations as it inhibits membrane-bound F_1. Inhibition is temperature dependent. *N*-Butanol also shows partial inhibition of ATP synthesis.

Tetrachlorosalicylanilide is a lipophilic weak acid known as an H^+ conductor. It inhibits the ATPase activities of both isolated F_1 and F_0F_1 from *Vibrio parahaemolyticus* (290, 344). The concentration of tetrachlorosalicylanilide for 50% inhibition of F_0F_1-ATPase activity from *V. parahaemolyticus* is about 9 to 10 μM (290).

Dihydrostreptomycin is a polycationic aminoglycoside antibiotic drug produced from *Streptomyces humidus*. It significantly stimulates the ATPase activity of membrane-bound ATP synthase from bovine heart mitochondria in the concentration range of 1 to 5 mM. The stimulation is followed by inhibition at higher concentrations (161). Dihydrostreptomycin also inhibits the ATPase activity of isolated F_1, but the stimulation of the ATPase activity observed in the inhibition of membrane-bound F_1 at low concentrations of dihydrostreptomycin is not observed in the inhibition of isolated F_1. The inhibition of ATPase activity of F_1 by dihydrostreptomycin is noncompetitive. Dihydrostreptomycin also exhibits partial inhibition of proton conductivity of F_0 in the ATP synthase devoid of its catalytic F_1 moiety.

Suramin, a synthetic antiparasitic drug, is an inhibitor of various proteins in different cell types and also inhibits the

binding of some growth factors to their receptors. Suramin also binds to ATP synthase and inhibits both F_1-ATPase and membrane-bound F_0F_1-ATPase from mitochondria (28, 173). Suramin acts as a noncompetitive inhibitor of the membrane-bound ATPase and as a strictly competitive inhibitor of purified F_1-ATPase (173). Half-maximal inhibition of rat liver F_1-ATPase occurs at 40 μM suramin.

Bz-423 is an 1,4-benzodiazepine derivative known as a cytotoxic immunomodulatory drug that suppresses disease in lupus-prone mice by inducing apoptosis in autoreactive B and T lymphocytes (193). Bz-423 binds to the OSCP subunit of ATP synthase and inhibits both synthetic and hydrolytic activities of the enzyme. The inhibition of the ATPase activity of ATP synthase by Bz-423 leads to rapid generation of superoxide (O_2^-) from the respiratory chain within mitochondria and the initiation of apoptosis by the reactive oxygen species. Bz-423 affects both the V_{max} and K_m of the ATPase activity of ATP synthase and inhibits ATP synthesis in a concentration-dependent fashion.

Dimethyl sulfoxide (DMSO) inhibits the hydrolytic activities of BF_1 and MF_1 strongly at concentrations of above 30 to 40% (9, 345, 440). Inhibition by DMSO is reversible, affecting V_{max} without a significant change in the K_m (9, 440). In contrast, the synthesis of ATP by soluble F_1 is promoted in the presence of DMSO (94, 197, 346). The effect of DMSO on the promotion of ATP synthesis by isolated F_1 is considered to be due to an increase in affinity of F_1 for phosphate at the catalytic site (197, 345).

Hypochlorous acid (HOCl) is a strong oxidant that is produced as a microbicide in activated neutrophils and monocytes by myeloperoxidase-catalyzed peroxidation of chloride ion (182). HOCl inhibits the ATPase activity of F_1 in a biphasic fashion. The ATPase activity falls rapidly to 20 to 30% at low concentrations of HOCl and then slowly to zero at high concentrations (29). The biphasic mode of inhibition is attributed to two different inhibitory activities of HOCl: oxidative modification of intact F_1 and subunit dissociation of F_1 due to more extensive oxidation (29, 167). The target sites for HOCl are believed to be amino acid residues within nucleophilic side chains (167).

4,4′-Dichlorodiphenyltrichloroethane (DDT) is a synthetic organic insecticide and affects sodium ion channels in the neurons of DDT-sensitive insects, causing repetitive discharge by the increase and prolongation of membrane's negative afterpotential, leading to spasms and eventual death. DDT binds to an unidentified 23-kDa protein in the F_0 of mitochondrial ATP synthase and inhibits the ATPase activity of the enzyme (442, 443). The 23-kDa protein is present in DDT-sensitive insects but not in DDT-tolerant insects and mammals, and the prepared DDT-sensitive ATP synthase devoid of the 23-kDa protein is not inhibited by DDT (442, 443).

Diazoxide, a mitochondrial potassium channel activator, is a cardioprotective drug for short-term treatment of malignant hypertension. Diazoxide also binds to MF_1 and potentiates the binding of IF_1 to F_1, inhibiting the ATPase activity of ATP synthase (79, 80). The inhibition by diazoxide is reversible, and the binding of one equivalent of diazoxide to F_1 is sufficient to inhibit the F_1-ATPase activity. The inhibitory effect of diazoxide is ATP dependent, and no inhibition is observed without Mg^{2+}-ATP. The binding site of diazoxide is believed to be located within the nucleotide binding domain of the β subunit.

2-Hydroxy-5-nitrobenzyl bromide (HNB) stimulates the hydrolytic activity of F_1 from bovine heart mitochondria at below 0.5 mM but exhibits a concentration-dependent inhibition of F_1 from the same source at above 0.5 mM (26, 27). HNB is a Trp-modifying reagent. Its capacity to activate catalytic activity at below 0.5 mM is attributed to its covalent interaction with a single Trp residue in the ε subunit of F_1 (26). In contrast, HNB's inhibitory effect at above 0.5 mM appears to be due to noncovalent, reversible, aspecific binding to F_1. About 50% of the hydrolytic activity is inhibited at 2.5 mM.

A series of derivatives of benzodiazepine, 4-(*N*-arylimidazole)-substituted benzopyran, and *N*-[1-aryl-2-(1-imidazolo) ethyl]-guanidine have been synthesized and tested for the treatment of ischemic heart disease as cardioprotective agents (Table 24) (20, 21, 166). During ischemia, ATP is hydrolyzed by mitochondrial ATP synthase, leading to depletion of ATP. To prevent the ATP wastage in ischemia, the ATPase activity of ATP synthase should be inhibited selectively without affecting the ATP synthesis activity of the enzyme. Several inhibitors were proposed as potential compounds for drug design for ischemia.

N-Sulfonyl- or *N*-alkyl-substituted tetrahydrobenzodiazepine derivatives inhibit the mitochondrial ATPase activity of ATP synthase (166). The inhibition of ATP synthesis by these derivatives is much less potent than their inhibition of ATP hydrolysis. The derivatives with an *N*-sulfonyl moiety seem to have stronger inhibitory potencies than those with an *N*-alkyl moiety.

4-(*N*-Arylimidazole)-substituted benzopyran derivatives are inhibitors of ATP hydrolysis of mitochondrial ATP synthase (21, 156). The inhibition of ATP synthesis by these derivatives is about an order of magnitude less potent than that of ATP hydrolysis (21). Both the *N*-arylimidazole ring and benzopyran seem to be required for inhibition, since the removal of either from the structure causes a dramatic loss of inhibitory potency. BMS-199264 has been tested as a cardioprotective agent in ischemic rat hearts and showed selective inhibition of ATP hydrolase activity with no effect on ATP synthesis (156). It conserved ATP during ischemia, while it had no influence on preischemic ATP concentrations and cardiac function.

Cyano- and acylguanidine derivatives containing imidazoloethyl and aryl groups also inhibit the hydrolytic activity of mitochondrial ATP synthase (20). Inhibition by derivatives of *N*-[1-aryl-2-(1-imidazolo)ethyl]-cyanoguanidine and *N*-[1-aryl-2-(1-imidazolo)ethyl]-acylguanidine is selective for ATPase activity. No inhibition of ATP synthesis is observed up to 100 μM. In cyanoguanidine derivatives, the number and position of the chloride in aryl groups are believed to be important for their inhibitory activities. For example, the 2,4-dichloro analog is more potent than 2,3-dichloro and monochloro analogs in inhibiting the ATPase activity of F_1. Two symmetrical enantiomers with an identical chemical composition also have different inhibitory potencies. For instance, one entiomer of *N*-[(*Z*)-[(4-chlorophenyl)amino]{[1-(2,4-dichlorophenyl)-2-(1*H*-imidazol-1-yl)ethyl]amino}methylidene]-3-cyanobenzamide inhibits the ATPase activity of bovine mitochondrial ATP synthase (F_0F_1) with an I_{50} of 18 nM, whereas

TABLE 24. Miscellaneous inhibitors

Name or abbreviation	Molecular formula	Other names	Inhibitory potency (reference)
Dicarbopolyborate	$C_2B_9H_{11}$ (Dicarbononaborate)		Mercapto and chloro derivatives of dicarbononaborates, ~95% inhibition at 500–800 μM (rat liver MF_1-ATPase) (104); dichlorodicarbononaborate, 170 μM[b] (rat liver MF_1-ATPase) (104)
Almitrine	$C_{26}H_{29}F_2N_7$	6-(4-(Bis(4-fluorphenyl)methyl)-1-piperazinyl)-*N,N′*-di-2-propenyl-1,3,5-triazin-2,4-diamin; 2,4-bis(allylamino)-6-(4-(bis(*p*-fluorophenyl)methyl)-1-piperazinyl)-s-triazine	30 μM[a] (*S. cerevisiae* mitochondria, ATPase) (336)
5-Hydroxy-1,2-naphthalene dicarboxylic anhydride	$C_{12}H_6O_4$	6-Hydroxynaphtho(1,2-c)furan-1,3-dione; 5-hydroxynaphthalenedicarboxylic anhydride	Complete inhibition of ATPase induced by gramicidin at 30 μM (rat liver SMP-ATPase) (165)
R207910	$C_{32}H_{31}BrN_2O_2$	1-(6-Bromo-2-methoxy-quinolin-3-yl)-4-dimethylamino-2-naphthalen-1-yl-1-phenyl-butan-2-ol; TMC207; compound J	2.5 nM[a] (*M. smegmatis* membrane vesicles, ATP synthesis) (215); 99% inhibition in the range of 0.03–0.12 μg/ml (*M. tuberculosis*, growth) (15)
Spegazzinine	$C_{21}H_{28}N_2O_3$		18.5–24 μg inhibitor/mg protein[a] (*S. pombe* ATPase activity of cell extracts) (234); 100 μM[a] (spinach CF_1-ATPase) (10); 80 μM[a] (spinach chloroplasts, photophosphorylation) (10)
n-Butanol	$C_4H_{10}O$	1-Butanol; propyl carbinol; *n*-butyl alcohol; 1-hydroxybutane; butyl hydroxide; Hemostyp; methylolpropane; propylcarbinol; propylmethanol	160 mM[a] (bovine heart MF_1-ATPase) (406)
TCS	$C_{13}H_7Cl_4NO_2$	TCSA; tetrachlorosalicylanilide; 3,3′,4′,5-tetrachlorosalicylanilide; 3,5-dichlorosalicyl 3,4-dichloroanilide; 3,5-dichloro-*N*-(3,4-dichlorophenyl)-2-hydroxy-benzamide	9–10 μM[a] (F_0F_1-ATPase from *V. parahaemolyticus*) (290); 71% inhibition at 25 μM (*V. parahaemolyticus* F_1-ATPase) (344)
Dihydrostreptomycin	$C_{21}H_{41}N_7O_{12}$	Abiocine; Vibriomycin	38 mM[b] (bovine heart SMP- and isolated MF_1-ATPase) (161)
Suramin	$C_{51}H_{40}N_6O_{23}S_6$	Belganyl; Naganol	40 μM[a] (rat liver MF_1-ATPase) (28); 0.7 μg/ml[a] (*C. fasciculata* MF_1-ATPase) (173)
Bz-423	$C_{27}H_{21}ClN_2O_2$	Bz-48	5 μM[a] (Ramos cells, ATP synthesis) (193)
DMSO	C_2H_6OS	Dimethyl sulfoxide	> 95% inhibition at 40% DMSO (vol/vol) (EF_1-ATPase) (9); ~60% inhibition at 50% DMSO (TF_1-ATPase) (440)
Hypochlorous acid	HOCl		75% inhibition at 125 μM HOCl/g cells (EF_1-ATPase) (167); 50 μmol inhibitor/g cells[a] (EF_1-ATPase) (29)
DDT	$C_{14}H_9C_{15}$	4, 4′-Dichlorodiphenyltri-chloroethane; 4, 4′-DDT; *p,p′*-DDT; 1,1′-(2,2,2-trichloroethylidene)bis (4-chlorobenzene); Agritan; Chlorophenothan; 1,1,1-trichloro-2,2-bis(4,4′-dichlorodiphenyl) ethane; Detoxan	50% lethal dose of 11 μg/mg (*A. melllifera*)
Diazoxide	$C_8H_7ClN_2O_2S$	7-Chloro-3-methyl-2*H*-1,2,4-benzothiadiazine 1,1-dioxide; Eudemine; Hyperstat; Hypertonalum	K_d of IF_1 to F_1, 250 nM with 1 diazoxide equivalent/F_1 from 760 nM without diazoxide (bovine MF_1-ATPase) (80)

Continued on following page

TABLE 24—*Continued*

Name or abbreviation	Molecular formula	Other names	Inhibitory potency (reference)
HNB	$C_7H_6BrNO_3$	2-Hydroxy-5-nitrobenzyl bromide; Koshland's reagent I; 2-bromomethyl-4-nitrophenol; α-bromo-4-nitro-*o*-cresol	2.5 mM[a] (bovine heart MF_1-ATPase) (27)
N-Sulfonyl or *N*-alkyl-substituted tetrahydrobenzodiazepine derivatives	$C_{28}H_{30}N_4O_3S$	1-(1*H*-Imidazol-4-ylmethyl)-4-[(4-methoxyphenyl)sulfonyl]-2-(2-phenylethyl)-2,3,4,5-tetrahydro-1*H*-1,4-benzodiazepine	77 nM[a] (bovine heart MF_0F_1-ATPase) (166)
	$C_{22}H_{23}F_3N_4O_2S$	1-(1*H*-Imidazol-4-ylmethyl)-2-(2-phenylethyl)-4-[(trifluoromethyl)sulfonyl]-2,3,4,5-tetrahydro-1*H*-1,4-benzodiazepine	77 nM[a] (bovine heart MF_0F_1-ATPase) (166)
	$C_{31}H_{36}N_4O_2S$	4-[(4-*tert*-Butylphenyl)sulfonyl]-1-(1*H*-imidazol-4-ylmethyl)-2-(2-phenylethyl)-2,3,4,5-tetrahydro-1*H*-1,4-benzodiazepine	8 nM[a] (bovine heart MF_0F_1-ATPase) (166)
	$C_{32}H_{38}N_4O_2S$	4-[(4-*tert*-Butylphenyl)sulfonyl]-1-[(5-methyl-1*H*-imidazol-4-yl)methyl]-2-(2-phenylethyl)-2,3,4,5-tetrahydro-1*H*-1,4-benzodiazepine	77 nM[a] (bovine heart MF_0F_1-ATPase) (166)
	$C_{28}H_{28}Cl_2N_4O_2S$	4-[(3,4-Dichlorophenyl)sulfonyl]-1-[(5-methyl-1*H*-imidazol-4-yl)methyl]-2-(2-phenylethyl)-2,3,4,5-tetrahydro-1*H*-1,4-benzodiazepine	22 nM[a] (bovine heart MF_0F_1-ATPase) (166)
4-(*N*-Arylimidazole)-substituted benzopyran derivatives	$C_{22}H_{21}ClN_4O_2$	4-[(4-Chlorophenyl)(1*H*-imidazol-2-ylmethyl)amino]-3-hydroxy-2,2-dimethyl-3,4-dihydro-2*H*-chromene-6-carbonitrile	*3R, 4S* enantiomer, 0.48 μM[a] (rat heart MF_0F_1-ATPase) (21) and 4 μM[a] (rat heart SMP-ATP synthesis) (21); *3S, 4R* enantiomer, 0.24 μM[a] (rat heart SMP-ATPase) (21) and 3.8 μM[a] (rat heart SMP-ATP synthesis) (21);
	$C_{26}H_{31}ClN_4O_4S$	4-[(4-Chlorophenyl)(1*H*-imidazol-2-ylmethyl)amino]-2,2-dimethyl-6-(piperidin-1-ylsulfonyl)-3,4-dihydro-2*H*-chromen-3-ol	*3R, 4S* enantiomer (BMS-199264), 0.48 μM[a] (rat heart SMP-ATPase) (21), 18 μM[a] (rat heart SMP-ATP synthesis) (21); ~42% inhibition at 3 μM (ischemic rat heart SMP-ATPase) (156)
N-[1-Aryl-2-(1-imidazolo)ethyl]-cyanoguanidine derivatives	$C_{19}H_{14}Cl_4N_6$	2-Cyano-1-(2,4-dichlorophenyl)-3-[1-(2,4-dichlorophenyl)-2-(1*H*-imidazol-1-yl)ethyl]guanidine	0.6 μM[a] (bovine MF_0F_1-ATPase) (20)
	$C_{21}H_{14}Cl_2F_6N_6$	1-{1-[2,5-Bis(trifluoromethyl)phenyl]-2-(1*H*-imidazol-1-yl)ethyl}-2-cyano-3-(2,4-dichlorophenyl)guanidine	0.71 μM[a] (bovine MF_0F_1-ATPase) (20)
N-[1-Aryl-2-(1-imidazolo)ethyl]-acylguanidine derivatives	$C_{26}H_{19}Cl_3N_6O$	*N*-[(*Z*)-[(4-Chlorophenyl)amino]{[1-(2,4-dichlorophenyl)-2-(1*H*-imidazol-1-yl)ethyl]amino}methylidene]-3-cyanobenzamide	Racemic mixture, 33 nM[a] (bovine MF_0F_1-ATPase) (20); one enantiomer. 18 nM[a] (bovine MF_0F_1-ATPase) (20); the other enantiomer, >100 nM[a] (bovine MF_0F_1-ATPase) (20)
	$C_{25}H_{19}Cl_4N_5O$	4-Chloro-*N*-[(*Z*)-[(4-chlorophenyl)amino]{[1-(2,4-dichlorophenyl)-2-(1*H*-imidazol-1-yl)ethyl]amino}methylidene]benzamide	Racemic mixture, 82 nM[a] (bovine MF_0F_1-ATPase) (20)
O-[1-Aryl-2-(1-imidazolo)ethyl]-thiourethane derivatives	$C_{18}H_{14}Cl_3N_3OS$	*O*-[1-(2,4-Dichlorophenyl)-2-(1*H*-imidazol-1-yl)ethyl] (4-chlorophenyl)carbamothioate	0.43 μM[a] (bovine heart MF_0F_1-ATPase) (20); >300 μM[a] (bovine heart MF_0F_1, ATP synthesis) (20)
	$C_{18}H_{13}Cl_4N_3OS$	*O*-[1-(2,4-Dichlorophenyl)-2-(1*H*-imidazol-1-yl)ethyl] (2,4-dichlorophenyl)carbamothioate	30 nM[a] (bovine heart MF_0F_1-ATPase) (20)
Dio-9 complex	Unknown (a mixture of at least 9 compounds)		0.7 μg inhibitor/mg protein[a] (*T. pyriformis* SMP-ATPase) (404); ~500 μg inhibitor/mg protein[a] (*S. faecalis* F_1-ATPase) (169); 6.6 μg/mg protein[a] (*C. fasciculata* SMP-ATPase) (439)
Ethanol	C_2H_5OH	Ethyl alcohol	60% inhibition at about 7 μM (*V. parahaemolyticus* F_0F_1-ATPase) (290)
Zinc	Zn^{2+}		~100 μM[a] (*V. parahaemolyticus* F_0F_1-ATPase) (290)

[a] I_{50}.
[b] K_i.

the other entiomer has no inhibitory activity on the ATPase activity of the same enzyme (20).

O-[1-Aryl-2-(1-imidazolo)ethyl]-thiourethane derivatives also inhibit the ATPase activity of mitochondrial ATP synthase. Similar to the derivatives of *N*-[1-aryl-2-(1-imidazolo) ethyl]-cyanoguanidine and *N*-[1-aryl-2-(1-imidazolo)ethyl]-acylguanidine, the *O*-[1-aryl-2-(1-imidazolo)ethyl]-thiourethane derivatives also maintain selectivity for inhibition of ATPase activity of ATP synthase over ATP synthesis. For example, substitutions in the 1-aryl-2-imidazoloethyl and aniline moieties affect the inhibitory potencies of the derivatives, and halogen substitution in these moieties also seems to be favorable for promoting inhibition.

Dio-9 is a mixture of at least nine compounds, two of which have antibiotic properties (232). Dio-9 inhibits both ATPase and ATP synthase activities of mitochondria, chloroplasts, and bacteria (124, 125, 163, 169, 431). There is still much to be learned about the structures and chemical actions of the class of compounds comprising Dio-9.

Ethanol inhibits the ATPase activity of F_0F_1 from *V. parahaemolyticus* at concentrations of above 4% (290). In contrast, ethanol exhibits stimulatory effects on the ATPase activity of F_1.

Zinc strongly inhibits the ATPase activities of both purified and membrane-bound F_0F_1 from *V. parahaemolyticus* (267, 290). The site of action of the zinc ion is considered to be located within F_0 (290).

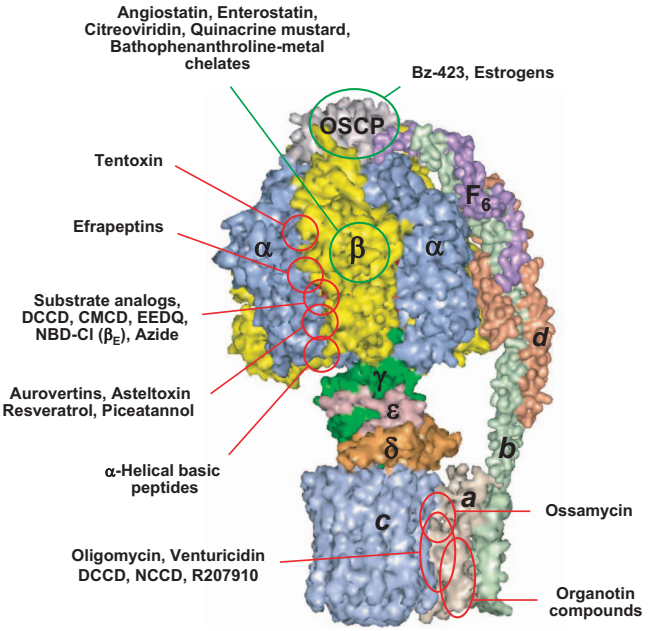

FIG. 12. Inhibitory sites of ATP synthase. The inhibitor binding sites in the ATP synthase as revealed by biochemical/structural studies are indicated by red circles, and the binding subunits in which the binding sites have not been completely clarified are indicated by green circles. The coordinates of each subunit in the structural model are the same as in Fig. 1.

CONCLUSIONS

ATP synthase was previously considered to be located only in the mitochondrial inner membrane, the bacterial plasma membrane, and the chloroplast thylakoid membrane. It was also considered to be involved only in the synthesis of ATP or in the generation of a proton gradient. Now, however, significant evidence has accumulated that the ATP synthase is also present on the surfaces of multiple animal cell types and serves as a receptor for various ligands, participating in a number of cellular processes, including angiogenesis, lipid metabolism, the regulation of intercellular pH, and the cytolytic pathway of tumor cells (17, 38, 39, 72, 91, 202, 269). As the multiple roles of the cell surface ATP synthase are now beginning to be understood, this pivotal enzyme complex both at this location and its mitochondrial location is emerging as a molecular target for the treatment of various diseases.

The use of ATP synthase as a molecular target has multiple advantages. First, as it is indispensable for energy metabolism, if selectively targeted, it may be possible to eradicate some types of cancer. It may also provide an ideal target for controlling a number of other diseases because of its complex subunit composition. For example, it has been demonstrated already that a lupus drug, Bz-423, targets the OSCP of F_0, whereas an antimycobacterial drug, R207910, binds to subunit *c* of F_0 (15, 193, 313). In addition, it has been shown that resveratrol and piceatannol, potential antiangiogenesis agents, block tumor growth by binding to the β subunit of F_1 (143, 449). Lastly, the high inhibitory specificity of ATP synthase inhibitors also suggests that this complex is an excellent target for the development of new insecticidal or herbicidal agents. For example, tentoxin is a strong inhibitor of CF_1-ATPase from certain sensitive species such as spinach, potato, and lettuce, but it has little or no inhibitory effect on the same enzyme from insensitive species such as corn, tobacco, and radish, even though they exhibit high sequence and structural similarity (380). In addition, slight structural modifications of tentoxin can cause dramatic effects on the properties and inhibitory potencies of the inhibitor (316, 351). Finally, the drug R207910, developed for the treatment of tuberculosis, also shows a narrow selectivity in its inhibition of the ATP synthase in mycobacterial species (15).

The mitochondrial ATP synthase contains a number of supernumerary subunits that are absent in bacterial or chloroplast counterparts. The plasma membrane ATP synthase found in various types of animal cells also includes more subunit types than the bacterial and chloroplast ATP synthases. The roles of the supernumerary subunits are currently unknown or poorly defined, but evidence is accumulating that these "extra" subunits are also involved in cellular processes other than ATP synthesis. Thus, subunit F_6 has been reported to be associated with regulating blood pressure. Additionally, subunit *e* has been reported to be involved in the regulation of the expression of the gene for subunit *g* of the ATP synthase (18) and also for that of the c-*myc* proto-oncogene (177, 226). The expression level of subunit *e* has also been shown to be highly sensitive to diverse physiologic changes and stresses. Although the detailed regulatory roles of subunits F_6 and *e* and the roles of other supernumerary subunits require further investigation, it seems likely that they will be implicated in a multitude of cellular processes that will result in future use of the ATP synthase as a drug target.

In this review, we have provided detailed information about

most natural and synthetic inhibitors of ATP synthases reported to date. Figure 12 summarizes the known or proposed sites of these ATP synthase inhibitors. About 270 inhibitors are described here and need further investigations to identify clearly or confirm their sites of actions and inhibitory mechanisms. When this mammoth task is accomplished, it will further heighten consideration of ATP synthase as a major target for new therapies for human and animal diseases and likely contribute also to the discovery of novel agents that may prove valuable in agriculture and other areas. In addition, the rich source of structures and other knowledge about ATP synthase inhibitors already provided in this review will likely prove invaluable as scaffolds for new drug discoveries in the near future.

ACKNOWLEDGMENTS

P.L.P. is supported for work on ATP synthase by National Institutes of Health grants 5R01 CA10951 and 5P01 HL081427.

REFERENCES

1. **Abad, M. C., R. K. Arni, D. K. Grella, F. J. Castellino, A. Tulinsky, and J. H. Geiger.** 2002. The X-ray crystallographic structure of the angiogenesis inhibitor angiostatin. J. Mol. Biol. **318:**1009–1017.
2. **Abrahams, J. P., S. K. Buchanan, M. J. Van Raaij, I. M. Fearnley, A. G. Leslie, and J. E. Walker.** 1996. The structure of bovine F_1-ATPase complexed with the peptide antibiotic efrapeptin. Proc. Natl. Acad. Sci. USA **93:**9420–9424.
3. **Ackerman, S. H., C. Grubmeyer, and P. S. Coleman.** 1987. Evidence for catalytic cooperativity during ATP hydrolysis by beef heart F_1-ATPase. Kinetics and binding studies with the photoaffinity label BzATP. J. Biol. Chem. **262:**13765–13772.
4. **Agarwal, N., and V. K. Kalra.** 1984. Studies on the mechanism of action of local anesthetics on proton translocating ATPase from *Mycobacterium phlei*. Biochim. Biophys. Acta **764:**316–323.
5. **Ahmad, Z., and A. E. Senior.** 2006. Inhibition of the ATPase activity of *Escherichia coli* ATP synthase by magnesium fluoride. FEBS Lett. **580:**517–520.
6. **Ahmad, Z., and A. E. Senior.** 2004. Mutagenesis of residue βArg-246 in the phosphate-binding subdomain of catalytic sites of *Escherichia coli* F_1-ATPase. J. Biol. Chem. **279:**31505–31513.
7. **Akhrem, A. A., M. A. Kisel, I. A. Kozlov, I. S. Tsybovsky, and E. N. Vulfson.** 1985. The inhibition of mitochondrial F_1-ATPase by 1,5-difluoro-2,4-dinitrobenzene. FEBS Lett. **187:**249–252.
8. **Aloise, P., Y. Kagawa, and P. S. Coleman.** 1991. Comparative Mg^{2+}-dependent sequential covalent binding stoichiometries of 3′-*O*-(4-benzoyl) benzoyl adenosine 5′-diphosphate of MF_1, TF_1, and the $\alpha_3\beta_3$ core complex of TF_1. The binding change motif is independent of the F_1 γδε subunits. J. Biol. Chem. **266:**10368–10376.
9. **Al-Shawi, M. K., and A. E. Senior.** 1992. Effects of dimethyl sulfoxide on catalysis in *Escherichia coli* F_1-ATPase. Biochemistry **31:**886–891.
10. **Andreo, C. S.** 1978. Inhibition of energy-transducing functions of chloroplasts by spegazzinine. Arch. Biochem. Biophys. **186:**416–421.
11. **Andrews, W. W., and W. S. Allison.** 1981. 1-Fluoro-2,4-dinitrobenzene modifies a tyrosine residue when it inactivates the bovine mitochondrial F_1-ATPase. Biochem. Biophys. Res. Commun. **99:**813–819.
12. **Andrews, W. W., F. C. Hill, and W. S. Allison.** 1984. Identification of the essential tyrosine residue in the β subunit of bovine heart mitochondrial F_1-ATPase that is modified by 7-chloro-4-nitro[^{14}C]benzofurazan. J. Biol. Chem. **259:**8219–8225.
13. **Andrews, W. W., F. C. Hill, and W. S. Allison.** 1984. Identification of the lysine residue to which the 4-nitrobenzofurazan group migrates after the bovine mitochondrial F_1-ATPase is inactivated with 7-chloro-4-nitro[^{14}C]benzofurazan. J. Biol. Chem. **259:**14378–14382.
14. **Andrews, W. W., M. Yoshida, F. C. Hill, and W. S. Allison.** 1984. Identification of an essential lysine residue in the β subunit of the F_1-ATPase from the thermophilic bacterium, PS3, using 7-chloro-4-nitro[^{14}C]benzofurazan. Biochem. Biophys. Res. Commun. **123:**1040–1046.
15. **Andries, K., P. Verhasselt, J. Guillemont, H. W. Gohlmann, J. M. Neefs, H. Winkler, J. Van Gestel, P. Timmerman, M. Zhu, E. Lee, P. Williams, D. de Chaffoy, E. Huitric, S. Hoffner, E. Cambau, C. Truffot-Pernot, N. Lounis, and V. Jarlier.** 2005. A diarylquinoline drug active on the ATP synthase of *Mycobacterium tuberculosis*. Science **307:**223–227.
16. **Arakaki, N., T. Kita, H. Shibata, and T. Higuti.** 2007. Cell-surface H^+-ATP synthase as a potential molecular target for anti-obesity drugs. FEBS Lett. **581:**3405–3409.
17. **Arakaki, N., T. Nagao, R. Niki, A. Toyofuku, H. Tanaka, Y. Kuramoto, Y. Emoto, H. Shibata, K. Magota, and T. Higuti.** 2003. Possible role of cell surface H^+-ATP synthase in the extracellular ATP synthesis and proliferation of human umbilical vein endothelial cells. Mol. Cancer Res. **1:**931–939.
18. **Arnold, I., K. Pfeiffer, W. Neupert, R. A. Stuart, and H. Schagger.** 1998. Yeast mitochondrial F_1F_0-ATP synthase exists as a dimer: identification of three dimer-specific subunits. EMBO J. **17:**7170–7178.
19. **Arntzen, C. J.** 1972. Inhibition of photophosphorylation by tentoxin, a cyclic tetrapeptide. Biochim. Biophys. Acta **283:**539–542.
20. **Atwal, K. S., S. Ahmad, C. Z. Ding, P. D. Stein, J. Lloyd, L. G. Hamann, D. W. Green, F. N. Ferrara, P. Wang, W. L. Rogers, L. M. Doweyko, A. V. Miller, S. N. Bisaha, J. B. Schmidt, L. Li, K. J. Yost, H. J. Lan, and C. S. Madsen.** 2004. *N*-[1-Aryl-2-(1-imidazolo)ethyl]-guanidine derivatives as potent inhibitors of the bovine mitochondrial F_1F_0 ATP hydrolase. Bioorg. Med. Chem. Lett. **14:**1027–1030.
21. **Atwal, K. S., P. Wang, W. L. Rogers, P. Sleph, H. Monshizadegan, F. N. Ferrara, S. Traeger, D. W. Green, and G. J. Grover.** 2004. Small molecule mitochondrial F_1F_0 ATPase hydrolase inhibitors as cardioprotective agents. Identification of 4-(*N*-arylimidazole)-substituted benzopyran derivatives as selective hydrolase inhibitors. J. Med. Chem. **47:**1081–1084.
22. **Avron, M., and N. Shavit.** 1965. Inhibitors and uncouplers of photophosphorylation. Biochim. Biophys. Acta **109:**317–331.
23. **Azzi, A., M. A. Bragadin, G. Neri, G. Farnia, and A. M. Tamburro.** 1973. A spin-label carbodiimide as a probe for mitochondrial ATPase. FEBS Lett. **30:**249–252.
24. **Azzi, A., M. A. Bragadin, A. M. Tamburro, and M. Santato.** 1973. Site-directed spin labeling of the mitochondrial membrane. Synthesis and utilization of the adenosine triphosphatase inhibitor (*N*-(2,2,6,6-tetramethyl-piperidyl-1-oxyl)-*N*′-(cyclohexyl)-carbodiimide). J. Biol. Chem. **248:**5520–5526.
25. **Bald, D., T. Amano, E. Muneyuki, B. Pitard, J. L. Rigaud, J. Kruip, T. Hisabori, M. Yoshida, and M. Shibata.** 1998. ATP synthesis by F_0F_1-ATP synthase independent of noncatalytic nucleotide binding sites and insensitive to azide inhibition. J. Biol. Chem. **273:**865–870.
26. **Baracca, A., S. Barogi, G. Lenaz, and G. Solaini.** 1993. Interactions and effects of 2-hydroxy-5-nitrobenzyl bromide on the bovine heart mitochondrial F_1-ATPase. Int. J. Biochem. **25:**1269–1275.
27. **Baracca, A., D. Menegatti, G. Parenti Castelli, C. A. Rossi, and G. Solaini.** 1990. Does 2-hydroxy-5-nitrobenzyl bromide react with the ε-subunit of the mitochondrial F_1-ATPase? Biochem. Int. **21:**1135–1142.
28. **Barret, J. M., A. P. Ernould, M. H. Rouillon, G. Ferry, A. Genton, and J. A. Boutin.** 1993. Studies of the potency of protein kinase inhibitors on ATPase activities. Chem. Biol. Interact. **86:**17–27.
29. **Barrette, W. C., Jr., D. M. Hannum, W. D. Wheeler, and J. K. Hurst.** 1989. General mechanism for the bacterial toxicity of hypochlorous acid: abolition of ATP production. Biochemistry **28:**9172–9178.
30. **Barta, I., P. Smerak, Z. Polivkova, H. Sestakova, M. Langova, B. Turek, and J. Bartova.** 2006. Current trends and perspectives in nutrition and cancer prevention. Neoplasma **53:**19–25.
31. **Barzu, O., F. Guerrieri, R. Scarfo, G. Capozza, and S. Papa.** 1989. Effect of cetyltrimethylammonium on ATP hydrolysis and proton translocation in the F_0-F_1 H^+-ATP synthase of mitochondria. J. Bioenerg. Biomembr. **21:**403–414.
32. **Bar-Zvi, D., and N. Shavit.** 1982. Modulation of the chloroplast ATPase by tight ADP binding. Effect of uncouplers and ATP. J. Bioenerg. Biomembr. **14:**467–478.
33. **Bar-Zvi, D., M. Yoshida, and N. Shavit.** 1996. Modification of domains of α and β subunits of F_1-ATPase from the thermophylic bacterium PS3, in their isolated and associated forms, by 3′-*O*-(4-benzoyl)benzoyl adenosine 5′-triphosphate (BzATP). J. Bioenerg. Biomembr. **28:**471–481.
34. **Baubichon, H., C. Godinot, A. Di Pietro, and D. C. Gautheron.** 1981. Competition between ADP and nucleotide analogues to occupy regulatory sites(s) related to hysteretic inhibition of mitochondrial F_1-ATPase. Biochem. Biophys. Res. Commun. **100:**1032–1038.
35. **Beechey, R. B., A. M. Roberton, C. T. Holloway, and I. G. Knight.** 1967. The properties of dicyclohexylcarbodiimide as an inhibitor of oxidative phosphorylation. Biochemistry **6:**3867–3879.
36. **Beil, W., C. Birkholz, S. Wagner, and K. F. Sewing.** 1995. Bismuth subcitrate and omeprazole inhibit *Helicobacter pylori* F_1-ATPase. Pharmacology **50:**333–337.
37. **Belda, F. J., F. G. Carmona, F. G. Canovas, J. C. Gomez-Fernandez, and J. A. Lozano.** 1983. A kinetic study of the interaction between mitochondrial F_1 adenosine triphosphatase and adenylyl imidodiphosphate and guanylyl imidodiphosphate. Biochem. J. **210:**727–735.
38. **Berger, K., U. Sivars, M. S. Winzell, P. Johansson, U. Hellman, C. Rippe, and C. Erlanson-Albertsson.** 2002. Mitochondrial ATP synthase—a possible target protein in the regulation of energy metabolism in vitro and in vivo. Nutr. Neurosci. **5:**201–210.
39. **Berger, K., M. S. Winzell, J. Mei, and C. Erlanson-Albertsson.** 2004. Enterostatin and its target mechanisms during regulation of fat intake. Physiol. Behav. **83:**623–630.

40. **Bernardes, C. F., J. R. Meyer-Fernandes, O. B. Martins, and A. E. Vercesi.** 1997. Inhibition of succinic dehydrogenase and F_0F_1-ATP synthase by 4,4′-diisothiocyanatostilbene-2,2′-disulfonic acid (DIDS). Z. Naturforsch. C **52:** 799–806.
41. **Blatt, N. B., J. J. Bednarski, R. E. Warner, F. Leonetti, K. M. Johnson, A. Boitano, R. Yung, B. C. Richardson, K. J. Johnson, J. A. Ellman, A. W. Opipari, Jr., and G. D. Glick.** 2002. Benzodiazepine-induced superoxide signals B cell apoptosis: mechanistic insight and potential therapeutic utility. J. Clin. Investig. **110**:1123–1132.
42. **Borghese, R., P. Turina, L. Lambertini, and B. A. Melandri.** 1998. The atpIBEXF operon coding for the F_0 sector of the ATP synthase from the purple nonsulfur photosynthetic bacterium Rhodobacter capsulatus. Arch. Microbiol. **170:**385–388.
43. **Bossard, M. J., and S. M. Schuster.** 1981. Catalysis of partial reactions of ATP synthesis by beef heart mitochondrial adenosine triphosphatase. J. Biol. Chem. **256:**1518–1521.
44. **Bossard, M. J., and S. M. Schuster.** 1981. Structural preferences for the binding of chromium nucleotides by beef heart mitochondrial ATPase. J. Biol. Chem. **256:**6617–6622.
45. **Boulay, F., P. Dalbon, and P. V. Vignais.** 1985. Photoaffinity labeling of mitochondrial adenosinetriphosphatase by 2-azidoadenosine 5′-[α-^{32}P]diphosphate. Biochemistry **24:**7372–7379.
46. **Bowler, M. W., M. G. Montgomery, A. G. Leslie, and J. E. Walker.** 2006. How azide inhibits ATP hydrolysis by the F-ATPases. Proc. Natl. Acad. Sci. USA **103:**8646–8649.
47. **Boyer, P. D.** 2000. Catalytic site forms and controls in ATP synthase catalysis. Biochim. Biophys. Acta **1458:**252–262.
48. **Braig, K., R. I. Menz, M. G. Montgomery, A. G. Leslie, and J. E. Walker.** 2000. Structure of bovine mitochondrial F_1-ATPase inhibited by Mg^{2+} ADP and aluminium fluoride. Structure Fold Des. **8:**567–573.
49. **Bullough, D. A., and W. S. Allison.** 1986. Inactivation of the bovine heart mitochondrial F_1-ATPase by 5′-*p*-fluorosulfonylbenzoyl[^{3}H]inosine is accompanied by modification of tyrosine 345 in a single β subunit. J. Biol. Chem. **261:**14171–14177.
50. **Bullough, D. A., and W. S. Allison.** 1988. Inactivation of the F_1-ATPase from the thermophilic bacterium PS3 by 5′-*p*-fluorosulfonylbenzoylinosine at 65 °C is accompanied by modification of β-tyrosine-364. Biochim. Biophys. Acta **934:**397–400.
51. **Bullough, D. A., and W. S. Allison.** 1986. Three copies of the β subunit must be modified to achieve complete inactivation of the bovine mitochondrial F_1-ATPase by 5′-*p*-fluorosulfonylbenzoyladenosine. J. Biol. Chem. **261:** 5722–5730.
52. **Bullough, D. A., E. A. Ceccarelli, D. Roise, and W. S. Allison.** 1989. Inhibition of the bovine-heart mitochondrial F_1-ATPase by cationic dyes and amphipathic peptides. Biochim. Biophys. Acta **975:**377–383.
53. **Bullough, D. A., E. A. Ceccarelli, J. G. Verburg, and W. S. Allison.** 1989. Localization of sites modified during inactivation of the bovine heart mitochondrial F_1-ATPase by quinacrine mustard using [3H]aniline as a probe. J. Biol. Chem. **264:**9155–9163.
54. **Bullough, D. A., M. Kwan, P. K. Laikind, M. Yoshida, and W. S. Allison.** 1985. The varied responses of different F_1-ATPases to chlorpromazine. Arch. Biochem. Biophys. **236:**567–575.
55. **Bullough, D. A., J. G. Verburg, M. Yoshida, and W. S. Allison.** 1987. Evidence for functional heterogeneity among the catalytic sites of the bovine heart mitochondrial F_1-ATPase. J. Biol. Chem. **262:**11675–11683.
56. **Bullough, D. A., M. Yoshida, and W. S. Allison.** 1986. Sequence of the radioactive tryptic peptide obtained after inactivating the F_1-ATPase of the thermophilic bacterium PS3 with 5′-*p*-fluorosulfonylbenzoyl[^{3}H]adenosine at 65 °C. Arch. Biochem. Biophys. **244:**865–871.
57. **Bullough, D. A., S. Q. Zhuo, and W. S. Allison.** 1991. Separate β subunits are derivatized with ^{14}C and ^{3}H when the bovine heart mitochondrial F_1-ATPase is doubly labeled with 7-chloro-4-nitro[^{14}C]benzofurazan and 5′-*p*-fluorosulfonylbenzoyl[^{3}H]inosine. Biochim. Biophys. Acta **1057:**208–214.
58. **Burrell, H. E., B. Wlodarski, B. J. Foster, K. A. Buckley, G. R. Sharpe, J. M. Quayle, A. W. Simpson, and J. A. Gallagher.** 2005. Human keratinocytes release ATP and utilize three mechanisms for nucleotide interconversion at the cell surface. J. Biol. Chem. **280:**29667–29676.
59. **Burwick, N. R., M. L. Wahl, J. Fang, Z. Zhong, T. L. Moser, B. Li, R. A. Capaldi, D. J. Kenan, and S. V. Pizzo.** 2005. An inhibitor of the F_1 subunit of ATP synthase (IF_1) modulates the activity of angiostatin on the endothelial cell surface. J. Biol. Chem. **280:**1740–1745.
60. **Cabezon, E., P. J. Butler, M. J. Runswick, R. J. Carbajo, and J. E. Walker.** 2002. Homologous and heterologous inhibitory effects of ATPase inhibitor proteins on F-ATPases. J. Biol. Chem. **277:**41334–41341.
61. **Cabezon, E., M. G. Montgomery, A. G. Leslie, and J. E. Walker.** 2003. The structure of bovine F_1-ATPase in complex with its regulatory protein IF_1. Nat. Struct. Biol. **10:**744–750.
62. **Capozza, G., O. Dmitriev, I. A. Krasnoselskaya, S. Papa, and V. P. Skulachev.** 1991. The effect of F_0 inhibitors on the *Vibrio alginolyticus* membrane ATPase. FEBS Lett. **280:**274–276.
63. **Carlsson, C., and L. Ernster.** 1981. Uncoupler-reversible inhibition of mitochondrial ATPase by metal chelates of bathophenanthroline. I. General features. Biochim. Biophys. Acta **638:**345–357.
64. **Carlsson, C., and L. Ernster.** 1981. Uncoupler-reversible inhibition of mitochondrial ATPase by metal chelates of bathophenanthroline. II. Comparison with other inhibitors. Biochim. Biophys. Acta **638:**358–364.
65. **Carlsson-Skwirut, C., and L. Ernster.** 1982. Bathophenanthroline-ruthenium chelate, a fluorescent inhibitor of F_1-ATPase. FEBS Lett. **145:**77–81.
66. **Cataldi de Flombaum, M. A., and A. O. Stoppani.** 1986. Effects of ethidium bromide on the mitochondrial adenosine triphosphatase from *Trypanosoma cruzi*. Biochem. Int. **12:**513–519.
67. **Cataldi de Flombaum, M. A., and A. O. Stoppani.** 1982. Phenylglyoxal inactivation of the mitochondrial adenosine triphosphatase from *Trypanosoma cruzi*. Mol. Biochem. Parasitol. **5:**371–379.
68. **Cattell, K. J., C. R. Lindop, I. G. Knight, and R. B. Beechey.** 1971. The identification of the site of action of *NN*′-dicyclohexylcarbodi-imide as a proteolipid in mitochondrial membranes. Biochem. J. **125:**169–177.
69. **Cavelier, F., C. Enjalbal, J. Santolini, F. Haraux, C. Sigalat, J. Verducci, and F. Andre.** 1997. Analogs of tentoxin: tools for mechanistic investigations. Lett. Peptide Sci. **4:**283–288.
70. **Ceccarelli, E. A., J. G. Verburg, S. Q. Zhuo, and W. S. Allison.** 1989. Selectivity of modification when latent and activated forms of the chloroplast F_1-ATPase are inactivated by 7-chloro-4-nitrobenzofurazan. Arch. Biochem. Biophys. **272:**400–411.
71. **Cerrini, S., D. Lamba, A. Scatturin, and G. Ughetto.** 1989. The crystal and molecular structure of the α-helical nonapeptide antibiotic leucinostatin A. Biopolymers **28:**409–420.
72. **Champagne, E., L. O. Martinez, X. Collet, and R. Barbaras.** 2006. Ecto-F_1F_O ATP synthase/F_1 ATPase: metabolic and immunological functions. Curr. Opin. Lipidol. **17:**279–284.
73. **Chandrasekaran, K., K. Hatanpaa, S. I. Rapoport, and D. R. Brady.** 1997. Decreased expression of nuclear and mitochondrial DNA-encoded genes of oxidative phosphorylation in association neocortex in Alzheimer disease. Brain Res. Mol. Brain Res. **44:**99–104.
74. **Chang, T., and H. S. Penefsky.** 1973. Aurovertin, a fluorescent probe of conformational change in beef heart mitochondrial adenosine triphosphatase. J. Biol. Chem. **248:**2746–2754.
75. **Chavez, E., and A. Cuellar.** 1984. Inactivation of mitochondrial ATPase by ultraviolet light. Arch. Biochem. Biophys. **230:**511–516.
76. **Chazotte, B., G. Vanderkooi, and D. Chignell.** 1982. Further studies on F_1-ATPase inhibition by local anesthetics. Biochim. Biophys. Acta **680:**310–316.
77. **Chen, C., A. K. Saxena, W. N. Simcoke, D. N. Garboczi, P. L. Pedersen, and Y. H. Ko.** 2006. Mitochondrial ATP synthase. Crystal structure of the catalytic F_1 unit in a vanadate-induced transition-like state and implications for mechanism. J. Biol. Chem. **281:**13777–13783.
78. **Clarke, D. J., F. M. Fuller, and J. G. Morris.** 1979. The proton-translocating adenosine triphosphatase of the obligately anaerobic bacterium *Clostridium pasteurianum*. 1. ATP phosphohydrolase activity. Eur. J. Biochem. **98:**597–612.
79. **Comelli, M., G. Metelli, and I. Mavelli.** 2007. Downmodulation of mitochondrial F_0F_1 ATP synthase by diazoxide in cardiac myoblasts: a dual effect of the drug. Am. J. Physiol. Heart Circ. Physiol. **292:**H820–H829.
80. **Contessi, S., G. Metelli, I. Mavelli, and G. Lippe.** 2004. Diazoxide affects the IF_1 inhibitor protein binding to F_1 sector of beef heart F_0F_1ATPsynthase. Biochem. Pharmacol. **67:**1843–1851.
81. **Crane, R. K., and F. Lipmann.** 1953. The effect of arsenate on aerobic phosphorylation. J. Biol. Chem. **201:**235–243.
82. **Crosby, B., M. Boutry, and A. Goffeau.** 1979. Inhibition of soluble yeast mitochondria ATPase by ethidium-bromide. Biochem. Biophys. Res. Commun. **88:**448–455.
83. **Cross, R. L., and W. E. Kohlbrenner.** 1978. The mode of inhibition of oxidative phosphorylation by efrapeptin (A23871). Evidence for an alternating site mechanism for ATP synthesis. J. Biol. Chem. **253:**4865–4873.
84. **Cross, R. L., and C. M. Nalin.** 1982. Adenine nucleotide binding sites on beef heart F_1-ATPase. Evidence for three exchangeable sites that are distinct from three noncatalytic sites. J. Biol. Chem. **257:**2874–2881.
85. **Cunningham, C. C., and D. T. George.** 1975. The relationship between the bovine heart mitochondrial adenosine triphosphatase, lipophilic compounds, and oligomycin. J. Biol. Chem. **250:**2036–2044.
86. **Czarnecki, J. J., M. S. Abbott, and B. R. Selman.** 1982. Photoaffinity labeling with 2-azidoadenosine diphosphate of a tight nucleotide binding site on chloroplast coupling factor 1. Proc. Natl. Acad. Sci. USA **79:**7744–7748.
87. **Dabbeni-Sala, F., and P. Palatini.** 1990. Mechanism of local anesthetic effect. Involvement of F_0 in the inhibition of mitochondrial ATP synthase by phenothiazines. Biochim. Biophys. Acta **1015:**248–252.
88. **Dabbeni-Sala, F., G. Schiavo, and P. Palatini.** 1990. Mechanism of local anesthetic effect on mitochondrial ATP synthase as deduced from photolabelling and inhibition studies with phenothiazine derivatives. Biochim. Biophys. Acta **1026:**117–125.
89. **Dalbon, P., F. Boulay, and P. V. Vignais.** 1985. Exploration of nucleotide

binding sites in the mitochondrial membrane by 2-azido-[α-^{32}P]ADP. FEBS Lett. **180:**212–218.
90. **Dallmann, H. G., T. G. Flynn, and S. D. Dunn.** 1992. Determination of the 1-ethyl-3-[(3-dimethylamino)propyl]-carbodiimide-induced cross-link between the β and ε subunits of *Escherichia coli* F_1-ATPase. J. Biol. Chem. **267:**18953–18960.
91. **Das, B., M. O. Mondragon, M. Sadeghian, V. B. Hatcher, and A. J. Norin.** 1994. A novel ligand in lymphocyte-mediated cytotoxicity: expression of the β subunit of H^+ transporting ATP synthase on the surface of tumor cell lines. J. Exp. Med. **180:**273–281.
92. **De Gomez-Puyou, M. T., A. Gomez-Puyou, and M. Beigel.** 1976. On the mechanism of action of alkylguanidines in oxidative phosphorylation: their action on soluble F_1. Arch. Biochem. Biophys. **173:**326–331.
93. **De Meirleir, L., S. Seneca, W. Lissens, E. Schoentjes, and B. Desprechins.** 1995. Bilateral striatal necrosis with a novel point mutation in the mitochondrial ATPase 6 gene. Pediatr. Neurol. **13:**242–246.
94. **de Meis, L.** 1989. Role of water in the energy of hydrolysis of phosphate compounds—energy transduction in biological membranes. Biochim. Biophys. Acta **973:**333–349.
95. **de Melo, D. F., M. Satre, and P. V. Vignais.** 1984. Inactivation of beef heart mitochondrial F_1-ATPase by the 2′,3′-dialdehyde derivatives of adenine nucleotides. FEBS Lett. **169:**101–106.
96. **Deters, D. W., E. Racker, N. Nelson, and H. Nelson.** 1975. Partial resolution of the enzymes catalyzing photophosphorylation. XV. Approaches to the active site of coupling factor I. J. Biol. Chem. **250:**1041–1047.
97. **Devenish, R. J., M. Prescott, G. M. Boyle, and P. Nagley.** 2000. The oligomycin axis of mitochondrial ATP synthase: OSCP and the proton channel. J. Bioenerg. Biomembr. **32:**507–515.
98. **de Vicente, J. I., P. del Valle, F. Busto, D. de Arriaga, and J. Soler.** 1991. Inhibition by excess of free ATP, and free Mg^{2+} ions of the mitochondrial F_1-ATPase moiety from *Phycomyces blakesleeanus*. Biochem. Int. **24**:339–347.
99. **de Vries, D. D., B. G. van Engelen, F. J. Gabreels, W. Ruitenbeek, and B. A. van Oost.** 1993. A second missense mutation in the mitochondrial ATPase 6 gene in Leigh's syndrome. Ann. Neurol. **34**:410–412.
100. **Di Pietro, A., C. Godinot, M.-L. Bouillant, and D. C. Gautheron.** 1975. Pig heart mitochondrial ATPase: properties of purified and membrane-bound enzyme. Effects of flavonoids. Biochemie **57:**959–967.
101. **Di Pietro, A., C. Godinot, J.-C. Martin, and D. C. Gautheron.** 1979. Affinity labeling of catalytic and regulatory sites of pig heart mitochondrial F_1-ATPase by 5′-*p*-fluorosulfonylbenzoyladenosine. Biochemistry **18:**1738–1745.
102. **Di Pietro, A., F. Penin, C. Godinot, and D. C. Gautheron.** 1980. "Hysteretic" behavior and nucleotide binding sites of pig heart mitochondrial F_1 adenosine 5′-triphosphatase. Biochemistry **19:**5671–5678.
103. **Djerassi, C., H. W. Brewer, H. Budzikiewicz, O. O. Orazi, and R. A. Corral.** 1962. The structure of the aspidosperma alkaloids spegazzinine and spegazzinidine. J. Am. Chem. Soc. **84:**3480–3485.
104. **Drahota, Z., V. Mares, H. Rauchova, P. Saf, and M. Kalous.** 1994. Inhibition of mitochondrial ATPase by dicarbopolyborate, a new enzyme inhibitor. J. Bioenerg. Biomembr. **26:**583–586.
105. **Dreyfus, G., H. Guimaraes-Motta, and J. L. Silva.** 1988. Effect of hydrostatic pressure on the mitochondrial ATP synthase. Biochemistry **27:**6704–6710.
106. **Du, Z. Y., and P. D. Boyer.** 1990. On the mechanism of sulfite activation of chloroplast thylakoid ATPase and the relation of ADP tightly bound at a catalytic site to the binding change mechanism. Biochemistry **29:**402–407.
107. **Dupuis, A., J. P. Issartel, and P. Vignais.** 1989. Direct identification of the fluoroaluminate and fluoroberyllate species responsible for inhibition of the mitochondrial F_1-ATPase. FEBS Lett. **255:**47–52.
108. **Ebel, R. E., and H. A. Lardy.** 1975. Influence of aurovertin on mitochondrial ATPase activity. J. Biol. Chem. **250:**4992–4995.
109. **Eckhardt, U., and W. G. Hanstein.** 1993. Beef heart mitochondrial F_1-ATPase: inhibition by azidoadenyl-5′-yl imidodiphosphates and cooperative binding of substrate. Biochim. Biophys. Acta **1144:**419–425.
110. **Edel, C. M., A. F. Hartog, and J. A. Berden.** 1993. Identification of an exchangeable non-catalytic site on mitochondrial F_1-ATPase which is involved in the negative cooperativity of ATP hydrolysis. Biochim. Biophys. Acta **1142:**327–335.
111. **Edel, C. M., A. F. Hartog, and J. A. Berden.** 1992. Inhibition of mitochondrial F_1-ATPase activity by binding of (2-azido-) ADP to a slowly exchangeable non-catalytic nucleotide binding site. Biochim. Biophys. Acta **1101:**329–338.
112. **Edwards, D. L., and B. W. Unger.** 1978. Nuclear mutations conferring oligomycin resistance in *Neurospora crassa*. J. Biol. Chem. **253:**4254–4258.
113. **Emaus, R. K., R. Grunwald, and J. J. Lemasters.** 1986. Rhodamine 123 as a probe of transmembrane potential in isolated rat-liver mitochondria: spectral and metabolic properties. Biochim. Biophys. Acta **850:**436–448.
114. **Esch, F. S., and W. S. Allison.** 1978. Identification of a tyrosine residue at a nucleotide binding site in the β subunit of the mitochondrial ATPase with *p*-fluorosulfonyl[^{14}C]-benzoyl-5′-adenosine. J. Biol. Chem. **253:**6100–6106.
115. **Falson, P., A. Di Pietro, and D. C. Gautheron.** 1986. Chemical modification of thiol groups of mitochondrial F_1-ATPase from the yeast *Schizosaccharomyces pombe*. Involvement of α- and γ-subunits in the enzyme activity. J. Biol. Chem. **261:**7151–7159.
116. **Feldman, R. I., and D. S. Sigman.** 1985. Membrane-specific inhibitors of the bovine heart mitochondrial ATPase. Biochim. Biophys. Acta **806:**277–282.
117. **Fellous, G., C. Godinot, H. Baubichon, A. Di Pietro, and D. C. Gautheron.** 1984. Photolabeling on β subunit of the nucleotide site related to hysteretic inhibition of mitochondrial F_1-ATPase. Biochemistry **23:**5294–5299.
118. **Ferguson, S. J., and P. John.** 1977. The inhibitor-sensitivity of the plasma-membrane adenosine triphosphatase of *Paracoccus denitrificans*: comparison with the mitochondrial adenosine triphosphatase. Biochem. Soc. Trans. **5:**1525–1527.
119. **Ferguson, S. J., P. John, W. J. Lloyd, G. K. Radda, and F. R. Whatley.** 1974. Selective and reversible inhibition of the ATPase of *Micrococcus denitrificans* by 7-chloro-4-nitrobenzo-2-oxa-1,3 diazole. Biochim. Biophys. Acta **357:**457–461.
120. **Ferguson, S. J., W. J. Lloyd, M. H. Lyons, and G. K. Radda.** 1975. The mitochondrial ATPase. Evidence for a single essential tyrosine residue. Eur. J. Biochem. **54:**117–126.
121. **Ferguson, S. J., W. J. Lloyd, and G. K. Radda.** 1975. The mitochondrial ATPase. Selective modification of a nitrogen residue in the β subunit. Eur. J. Biochem. **54:**127–133.
122. **Fillingame, R. H.** 1975. Identification of the dicyclohexylcarbodiimide-reactive protein component of the adenosine 5′-triphosphate energy-transducing system of *Escherichia coli*. J. Bacteriol. **124:**870–883.
123. **Fillingame, R. H., M. Oldenburg, and D. Fraga.** 1991. Mutation of alanine 24 to serine in subunit *c* of the *Escherichia coli* F_1F_0-ATP synthase reduces reactivity of aspartyl 61 with dicyclohexylcarbodiimide. J. Biol. Chem. **266:**20934–20939.
124. **Fisher, R. R., and R. J. Guillory.** 1968. The action of Dio-9: energy-linked swelling of rat-liver mitochondria. Biochim. Biophys. Acta **162:**182–194.
125. **Fisher, R. R., and R. J. Guillory.** 1967. Inhibition of the energy conservation reactions of *Rhodospirillum rubrum* by Dio-9. Biochim. Biophys. Acta **143:**654–656.
126. **Fitin, A. F., E. A. Vasilyeva, and A. D. Vinogradov.** 1979. An inhibitory high affinity binding site for ADP in the oligomycin-sensitive ATPase of beef heart submitochondrial particles. Biochem. Biophys. Res. Commun. **86:**434–439.
127. **Frasch, A. C., J. J. Cazzulo, and A. O. Stoppani.** 1978. Solubilization and some properties of the Mg^{2+}-activated adenosine triphosphatase from *Trypanosoma cruzi*. Comp. Biochem. Physiol. B **61:**207–212.
128. **Frigeri, L., Y. M. Galante, W. G. Hanstein, and Y. Hatefi.** 1977. Effects of arginine binding reagents on ATPase and ATP-P_i exchange activities of mitochondrial ATP synthetase complex (complex V). J. Biol. Chem. **252:**3147–3152.
129. **Frigeri, L., Y. M. Galante, and Y. Hatefi.** 1978. Interaction of complex V and F_1-ATPase with [^{14}C]phenylglyoxal. J. Biol. Chem. **253:**8935–8940.
130. **Futai, M., P. C. Sternweis, and L. A. Heppel.** 1974. Purification and properties of reconstitutively active and inactive adenosinetriphosphatase from *Escherichia coli*. Proc. Natl. Acad. Sci. USA **71:**2725–2729.
131. **Galanis, M., J. R. Mattoon, and P. Nagley.** 1989. Amino acid substitutions in mitochondrial ATP synthase subunit 9 of *Saccharomyces cerevisiae* leading to venturicidin or ossamycin resistance. FEBS Lett. **249:**333–336.
132. **Garin, J., F. Boulay, J. P. Issartel, J. Lunardi, and P. V. Vignais.** 1986. Identification of amino acid residues photolabeled with 2-azido[α-^{32}P]adenosine diphosphate in the β subunit of beef heart mitochondrial F_1-ATPase. Biochemistry **25:**4431–4437.
133. **Garin, J., L. Michel, A. Dupuis, J. P. Issartel, J. Lunardi, J. Hoppe, and P. Vignais.** 1989. Photolabeling of the phosphate binding site of mitochondrial F_1-ATPase by [^{32}P]azidonitrophenyl phosphate. Identification of the photolabeled amino acid residues. Biochemistry **28:**1442–1448.
134. **Garin, J., M. Vincon, J. Gagnon, and P. Vignais.** 1994. Photolabeling of mitochondrial F_1-H^+ATPase by 2-azido[^{3}H]ADP and 8-azido[^{3}H]ADP entrapped as fluorometal complexes into the catalytic sites of the enzyme. Biochemistry **33:**3772–3777.
135. **Gaurrand, S., S. Desjardins, C. Meyer, P. Bonnet, J. M. Argoullon, H. Oulyadi, and J. Guillemont.** 2006. Conformational analysis of R207910, a new drug candidate for the treatment of tuberculosis, by a combined NMR and molecular modeling approach. Chem. Biol. Drug Des. **68:**77–84.
136. **Gause, E. M., M. A. Buck, and M. G. Douglas.** 1981. Binding of citreoviridin to the β subunit of the yeast F_1-ATPase. J. Biol. Chem. **256:**557–559.
137. **Gibbons, C., M. G. Montgomery, A. G. Leslie, and J. E. Walker.** 2000. The structure of the central stalk in bovine F_1-ATPase at 2.4 A resolution. Nat. Struct. Biol. **7:**1055–1061.
138. **Girvin, M. E., and R. H. Fillingame.** 1994. Hairpin folding of subunit *c* of F_1F_O ATP synthase: ^{1}H distance measurements to nitroxide-derivatized aspartyl-61. Biochemistry **33:**665–674.
139. **Glaser, E., E. Cadenas, S. Andell, and L. Ernster.** 1988. Inhibition of the mitochondrial F_1-ATPase by Rose Bengal mediated photooxidation. Interaction of the Fe^{2+} chelate of bathophenanthroline with the sensitizer. Acta Chem. Scand. B **42:**175–182.
140. **Glaser, E., B. Norling, J. Kopecky, and L. Ernster.** 1982. Comparison of the

effects of oligomycin and dicyclohexylcarbodiimide on mitochondrial ATPase and related reactions. Eur. J. Biochem. **121:**525–531.
141. **Gledhill, J. R., M. G. Montgomery, A. G. Leslie, and J. E. Walker.** 2007. How the regulatory protein, IF_1, inhibits F_1-ATPase from bovine mitochondria. Proc. Natl. Acad. Sci. USA **104:**15671–15676.
142. **Gledhill, J. R., M. G. Montgomery, A. G. Leslie, and J. E. Walker.** 2007. Mechanism of inhibition of bovine F_1-ATPase by resveratrol and related polyphenols. Proc. Natl. Acad. Sci. USA **104:**13632–13637.
143. **Gledhill, J. R., and J. E. Walker.** 2005. Inhibition sites in F_1-ATPase from bovine heart mitochondria. Biochem. J. **386:**591–598.
144. **Gomez-Fernandez, J. C., and D. A. Harris.** 1978. A thermodynamic analysis of the interaction between the mitochondrial coupling adenosine triphosphatase and its naturally occurring inhibitor protein. Biochem. J. **176:**967–975.
145. **Gregory, R., and B. Hess.** 1981. The sulphydryl content of yeast mitochondrial F_1-ATPase and the stoichiometry of subunits. FEBS Lett. **129:**210–214.
146. **Gregory, R., D. Recktenwald, and B. Hess.** 1981. The interaction of nucleotides with F_1-ATPase inactivated with 4-chloro-7-nitrobenzofurazan. Biochim. Biophys. Acta **635:**284–294.
147. **Gresser, M. J., S. Beharry, and D. M. Moennich.** 1984. Inhibition of mitochondrial F_1-ATPase by adenylyl imidodiphosphate. Curr. Top. Cell. Regul. **24:**365–378.
148. **Griffiths, D. E.** 1997. Cation adducts of mitochondrial ATPase subunit *c*: is subunit *c* a proton/cation exchanger? Biochem. Soc. Trans. **25**:388S.
149. **Griffiths, D. E.** 1994. Dibutyltin-3-hydroxyflavone titrates a dissociable component (cofactor) of ATP synthase: an energy transfer component linked to the ubiquinone pool. Biochem. Soc. Trans. **22**:225S.
150. **Griffiths, D. E., and R. L. Houghton.** 1974. Studies on energy-linked reactions: modified mitochondrial ATPase of oligomycin-resistant mutants of *Saccharomyces cerevisiae*. Eur. J. Biochem. **46:**157–167.
151. **Griffiths, D. E., R. L. Houghton, W. E. Lancashire, and P. A. Meadows.** 1975. Studies on energy-linked reactions: isolation and properties of mitochondrial venturicidin-resistant mutants of *Saccharomyces cerevisiae*. Eur. J. Biochem. **51:**393–402.
152. **Grodsky, N. B., C. Dou, and W. S. Allison.** 1998. Mutations in the nucleotide binding domain of the α subunits of the F_1-ATPase from thermophilic *Bacillus* PS3 that affect cross-talk between nucleotide binding sites. Biochemistry **37:**1007–1014.
153. **Groth, G.** 2002. Structure of spinach chloroplast F_1-ATPase complexed with the phytopathogenic inhibitor tentoxin. Proc. Natl. Acad. Sci. USA **99:**3464–3468.
154. **Groth, G., D. A. Mills, E. Christiansen, M. L. Richter, and B. Huchzermeyer.** 2000. Characterization of a phosphate binding domain on the α-subunit of chloroplast ATP synthase using the photoaffinity phosphate analogue 4-azido-2-nitrophenyl phosphate. Biochemistry **39:**13781–13787.
155. **Groth, G., and E. Pohl.** 2001. The structure of the chloroplast F_1-ATPase at 3.2 A resolution. J. Biol. Chem. **276:**1345–1352.
156. **Grover, G. J., K. S. Atwal, P. G. Sleph, F. L. Wang, H. Monshizadegan, T. Monticello, and D. W. Green.** 2004. Excessive ATP hydrolysis in ischemic myocardium by mitochondrial F_1F_0-ATPase: effect of selective pharmacological inhibition of mitochondrial ATPase hydrolase activity. Am. J. Physiol. Heart Circ. Physiol. **287:**H1747–H1755.
157. **Grubmeyer, C., and H. S. Penefsky.** 1981. The presence of two hydrolytic sites on beef heart mitochondrial adenosine triphosphatase. J. Biol. Chem. **256:**3718–3727.
158. **Gruys, K. J., J. L. Urbauer, and S. M. Schuster.** 1985. Metal-nucleotide structural characteristics during catalysis by beef heart mitochondrial F_1. J. Biol. Chem. **260:**6533–6540.
159. **Guerrero, K. J., L. L. Ehler, and P. D. Boyer.** 1990. Guanosine and formycin triphosphates bind at non-catalytic nucleotide binding sites of CF_1 ATPase and inhibit ATP hydrolysis. FEBS Lett. **270:**187–190.
160. **Guerrero, K. J., Z. X. Xue, and P. D. Boyer.** 1990. Active/inactive state transitions of the chloroplast F_1 ATPase are induced by a slow binding and release of Mg^{2+}. Relationship to catalysis and control of F_1 ATPases. J. Biol. Chem. **265:**16280–16287.
161. **Guerrieri, F., S. Micelli, C. Massagli, E. Gallucci, and S. Papa.** 1984. Interaction of the aminoglycoside antibiotic dihydrostreptomycin with the H^+-ATPase of mitochondria. Biochem. Pharmacol. **33:**2505–2510.
162. **Guerrieri, F., and S. Papa.** 1981. Effect of chemical modifiers of amino acid residues on proton conduction by the H^+-ATPase of mitochondria. J. Bioenerg. Biomembr. **13:**393–409.
163. **Guillory, R. J.** 1964. The action of Dio-9: an inhibitor and an uncoupler of oxidative phosphorylation. Biochim. Biophys. Acta **89:**197–207.
164. **Gupta, S., S. B. Krasnoff, D. W. Roberts, and J. A. A. A. Renwick.** 1992. Structure of efrapeptins from the fungus *Tolypocladium niveum*: peptide inhibitors of mitochondrial ATPase. J. Org. Chem. **57:**2306–2313.
165. **Hadler, H. I., and J. M. Demetriou.** 1975. A new inhibitor of coupled oxidative phosphorylation, 5-hydroxynaphthalenedicarboxylic anhydride, a derivative of a carcinogenic polynuclear hydrocarbon. Biochemistry **14:**5374–5378.
166. **Hamann, L. G., C. Z. Ding, A. V. Miller, C. S. Madsen, P. Wang, P. D. Stein, A. T. Pudzianowski, D. W. Green, H. Monshizadegan, and K. S. Atwal.** 2004. Benzodiazepine-based selective inhibitors of mitochondrial F_1F_0 ATP hydrolase. Bioorg. Med. Chem. Lett. **14:**1031–1034.
167. **Hannum, D. M., W. C. Barrette, Jr., and J. K. Hurst.** 1995. Subunit sites of oxidative inactivation of *Escherichia coli* F_1-ATPase by HOCl. Biochem. Biophys. Res. Commun. **212**:868–874.
168. **Hara, K. Y., Y. Kato-Yamada, Y. Kikuchi, T. Hisabori, and M. Yoshida.** 2001. The role of the βDELSEED motif of F_1-ATPase: propagation of the inhibitory effect of the ε subunit. J. Biol. Chem. **276:**23969–23973.
169. **Harold, F. M., J. R. Baarda, C. Baron, and A. Abrams.** 1969. Dio 9 and chlorhexidine: inhibitors of membrane-bound ATPase and of cation transport in *Streptococcus faecalis*. Biochim. Biophys. Acta **183:**129–136.
170. **Hase, Y., M. Tatsuno, T. Nishi, K. Kataoka, Y. Kabe, Y. Yamaguchi, N. Ozawa, M. Natori, H. Handa, and H. Watanabe.** 2008. Atrazine binds to F_1F_0-ATP synthase and inhibits mitochondrial function in sperm. Biochem. Biophys. Res. Commun. **366:**66–72.
171. **Hermolin, J., and R. H. Fillingame.** 1989. H^+-ATPase activity of *Escherichia coli* F_1F_0 is blocked after reaction of dicyclohexylcarbodiimide with a single proteolipid (subunit *c*) of the F_0 complex. J. Biol. Chem. **264:**3896–3903.
172. **Hicks, D. B., and T. A. Krulwich.** 1990. Purification and reconstitution of the F_1F_0-ATP synthase from alkaliphilic *Bacillus firmus* OF4. Evidence that the enzyme translocates H^+ but not Na^+. J. Biol. Chem. **265:**20547–20554.
173. **Higa, A. I., and J. J. Cazzulo.** 1981. Mg^{2+}-activated adenosine triphosphatase from *Crithidia fasciculata*: purification and inhibition by suramin and efrapeptin. Mol. Biochem. Parasitol. **3:**357–367.
174. **Hochman, Y., and C. Carmeli.** 1981. Correlation between the kinetics of activation and inhibition of adenosinetriphosphatase activity by divalent metal ions and the binding of manganese to chloroplast coupling factor 1. Biochemistry **20:**6287–6292.
175. **Hollemans, M., M. J. Runswick, I. M. Fearnley, and J. E. Walker.** 1983. The sites of labeling of the β-subunit of bovine mitochondrial F_1-ATPase with 8-azido-ATP. J. Biol. Chem. **258:**9307–9313.
176. **Hong, S., and P. L. Pedersen.** 2002. ATP synthase of yeast: structural insight into the different inhibitory potencies of two regulatory peptides and identification of a new potential regulator. Arch. Biochem. Biophys. **405:**38–43.
177. **Hong, S., and P. L. Pedersen.** 2003. Subunit E of mitochondrial ATP synthase: a bioinformatic analysis reveals a phosphopeptide binding motif supporting a multifunctional regulatory role and identifies a related human brain protein with the same motif. Proteins **51:**155–161.
178. **Horstman, L. L., and E. Racker.** 1970. Partial resolution of the enzyme catalyzing oxidative phosphorylation. XXII. Interaction between mitochondrial adenosine triphosphatase inhibitor and mitochondrial adenosine triphosphatase. J. Biol. Chem. **245:**1336–1344.
179. **Hu, N., D. A. Mills, B. Huchzermeyer, and M. L. Richter.** 1993. Inhibition by tentoxin of cooperativity among nucleotide binding sites on chloroplast coupling factor 1. J. Biol. Chem. **268:**8536–8540.
180. **Huang, T. C., H. Y. Chang, C. H. Hsu, W. H. Kuo, K. J. Chang, and H. F. Juan.** 2008. Targeting therapy for breast carcinoma by ATP synthase inhibitor aurovertin B. J. Proteome Res. **7:**1433–1444.
181. **Huitric, E., P. Verhasselt, K. Andries, and S. E. Hoffner.** 2007. In vitro antimycobacterial spectrum of a diarylquinoline ATP synthase inhibitor. Antimicrob. Agents Chemother. **51:**4202–4204.
182. **Hurst, J. K., and W. C. Barrette, Jr.** 1989. Leukocytic oxygen activation and microbicidal oxidative toxins. Crit. Rev. Biochem. Mol. Biol. **24**:271–328.
183. **Ibrahim, M., K. Andries, N. Lounis, A. Chauffour, C. Truffot-Pernot, V. Jarlier, and N. Veziris.** 2007. Synergistic activity of R207910 combined with pyrazinamide against murine tuberculosis. Antimicrob. Agents Chemother. **51:**1011–1015.
184. **Ida, K., T. Noumi, M. Maeda, T. Fukui, and M. Futai.** 1991. Catalytic site of F_1-ATPase of *Escherichia coli*. Lys-155 and Lys-201 of the β subunit are located near the γ-phosphate group of ATP in the presence of Mg^{2+}. J. Biol. Chem. **266:**5424–5429.
185. **Igarashi, K., K. Kashiwagi, H. Kobayashi, R. Ohnishi, T. Kakegawa, A. Nagasu, and S. Hirose.** 1989. Effect of polyamines on mitochondrial F_1-ATPase catalyzed reactions. J. Biochem. (Tokyo) **106:**294–298.
186. **Imeddize, E. A., I. A. Kozlov, V. A. Metel'skaia, and M. Mil'grom Ia.** 1978. Inhibition of mitochondrial ATPase by water-soluble carbodiimide. Biokhimiia **43**:1404–1413.
187. **Issartel, J. P., A. Dupuis, J. Lunardi, and P. V. Vignais.** 1991. Fluoroaluminum and fluoroberyllium nucleoside diphosphate complexes as probes of the enzymatic mechanism of the mitochondrial F_1-ATPase. Biochemistry **30:**4726–4733.
188. **Issartel, J. P., G. Klein, M. Satre, and P. V. Vignais.** 1983. Aurovertin binding sites on beef heart mitochondrial F_1-ATPase. Study with [^{14}C]aurovertin D of the binding stoichiometry and of the interaction between aurovertin and the natural ATPase inhibitor for binding to F_1. Biochemistry **22:**3492–3497.
189. **Issartel, J. P., and P. V. Vignais.** 1984. Evidence for a nucleotide binding site on the isolated β subunit from *Escherichia coli* F_1-ATPase. Interaction between nucleotide and aurovertin D binding sites. Biochemistry **23:**6591–6595.

190. **Ivey, D. M., and L. G. Ljungdahl.** 1986. Purification and characterization of the F_1-ATPase from *Clostridium thermoaceticum*. J. Bacteriol. **165:**252–257.
191. **Iwadate, M., T. Asakura, and M. P. Williamson.** 1998. The structure of the melittin tetramer at different temperatures. An NOE-based calculation with chemical shift refinement. Eur. J. Biochem. **257:**479–487.
192. **John, U. P., and P. Nagley.** 1986. Amino acid substitutions in mitochondrial ATPase subunit 6 of *Saccharomyces cerevisiae* leading to oligomycin resistance. FEBS Lett. **207:**79–83.
193. **Johnson, K. M., X. Chen, A. Boitano, L. Swenson, A. W. Opipari, Jr., and G. D. Glick.** 2005. Identification and validation of the mitochondrial F_1F_0-ATPase as the molecular target of the immunomodulatory benzodiazepine Bz-423. Chem. Biol. **12**:485–496.
194. **Joshi, V. K., and J. H. Wang.** 1987. Cross-linking study of the quaternary fine structure of mitochondrial F_1-ATPase. J. Biol. Chem. **262:**15721–15725.
195. **Kagawa, R., M. G. Montgomery, K. Braig, A. G. Leslie, and J. E. Walker.** 2004. The structure of bovine F_1-ATPase inhibited by ADP and beryllium fluoride. EMBO J. **23:**2734–2744.
196. **Kagawa, Y., and N. Nukiwa.** 1981. Conversion of stable ATPase to labile ATPase by acetylation, and the αβ and αγ subunit complexes during its reconstitution. Biochem. Biophys. Res. Commun. **100:**1370–1376.
197. **Kandpal, R. P., K. E. Stempel, and P. D. Boyer.** 1987. Characteristics of the formation of enzyme-bound ATP from medium inorganic phosphate by mitochondrial F_1 adenosinetriphosphatase in the presence of dimethyl sulfoxide. Biochemistry **26:**1512–1517.
198. **Kato-Yamada, Y., D. Bald, M. Koike, K. Motohashi, T. Hisabori, and M. Yoshida.** 1999. ε subunit, an endogenous inhibitor of bacterial F_1-ATPase, also inhibits F_0F_1-ATPase. J. Biol. Chem. **274:**33991–33994.
199. **Kauffman, R. F., H. A. Lardy, J. R. Barrio, M. C. Bario, and N. J. Leonard.** 1978. Dimensional probes of the enzyme binding sites of adenine nucleotides. Interaction of lin-benzoadenosine 5′-di- and triphosphate with mitochondrial ATP synthetase, purified ATPase, and the adenine nucleotide carrier. Biochemistry **17:**3686–3692.
200. **Kawai, K., H. Fukushima, and Y. Nozawa.** 1985. Inhibition of mitochondrial respiration by asteltoxin, a respiratory toxin from *Emericella variecolor*. Toxicol. Lett. **28:**73–77.
201. **Kayalar, C., J. Rosing, and P. D. Boyer.** 1977. An alternating site sequence for oxidative phosphorylation suggested by measurement of substrate binding patterns and exchange reaction inhibitions. J. Biol. Chem. **252:**2486–2491.
202. **Kenan, D. J., and M. L. Wahl.** 2005. Ectopic localization of mitochondrial ATP synthase: a target for anti-angiogenesis intervention? J. Bioenerg. Biomembr. **37:**461–465.
203. **Khananshvili, D., and Z. Gromet-Elhanan.** 1985. Evidence that the Mg-dependent low-affinity binding site for ATP and P_i demonstrated on the isolated β subunit of the $F_0 \cdot F_1$ ATP synthase is a catalytic site. Proc. Natl. Acad. Sci. USA **82:**1886–1890.
204. **Khananshvili, D., and Z. Gromet-Elhanan.** 1983. The interaction of carboxyl group reagents with the *Rhodospirillum rubrum* F_1-ATPase and its isolated β-subunit. J. Biol. Chem. **258:**3720–3725.
205. **Kihara, T., H. Kusakabe, G. Nakamura, T. Sakurai, and K. Isono.** 1981. Cytovaricin, a novel antibiotic. J. Antibiot. (Tokyo) **34:**1073–1074.
206. **Kim, B. W., H. J. Choo, J. W. Lee, J. H. Kim, and Y. G. Ko.** 2004. Extracellular ATP is generated by ATP synthase complex in adipocyte lipid rafts. Exp. Mol. Med. **36:**476–485.
207. **Kim, J. W., H. Adachi, K. Shin-ya, Y. Hayakawa, and H. Seto.** 1997. Apoptolidin, a new apoptosis inducer in transformed cells from *Nocardiopsis* sp. J. Antibiot. (Tokyo) **50:**628–630.
208. **Kim, S. H., R. Vlkolinsky, N. Cairns, and G. Lubec.** 2000. Decreased levels of complex III core protein 1 and complex V β chain in brains from patients with Alzheimer's disease and Down syndrome. Cell. Mol. Life Sci. **57:**1810–1816.
209. **Kirst, H. A., J. S. Mynderse, J. W. Martin, P. J. Baker, J. W. Paschal, J. L. Rios Steiner, E. Lobkovsky, and J. Clardy.** 1996. Structure of the spiroketalmacrolide ossamycin. J. Antibiot. (Tokyo) **49:**162–167.
210. **Ko, Y. H., M. Bianchet, L. M. Amzel, and P. L. Pedersen.** 1997. Novel insights into the chemical mechanism of ATP synthase. Evidence that in the transition state the γ-phosphate of ATP is near the conserved alanine within the P-loop of the β-subunit. J. Biol. Chem. **272:**18875–18881.
211. **Ko, Y. H., S. Hong, and P. L. Pedersen.** 1999. Chemical mechanism of ATP synthase. Magnesium plays a pivotal role in formation of the transition state where ATP is synthesized from ADP and inorganic phosphate. J. Biol. Chem. **274:**28853–28856.
212. **Konno, H., T. Murakami-Fuse, F. Fujii, F. Koyama, H. Ueoka-Nakanishi, C. G. Pack, M. Kinjo, and T. Hisabori.** 2006. The regulator of the F_1 motor: inhibition of rotation of cyanobacterial F_1-ATPase by the ε subunit. EMBO J. **25:**4596–4604.
213. **Kopecky, J., E. Glaser, B. Norling, and L. Ernster.** 1981. Relationship between the binding of dicyclohexylcarbodiimide and the inhibition of H^+-translocation in submitochondrial particles. FEBS Lett. **131:**208–212.
214. **Kormer, Z. S., I. A. Kozlov, Y. M. Milgrom, and I. Novikova.** 1982. Using 2′(3′)-*O*-trinitrophenyl derivatives of adenine nucleotides to study the structure and mechanism of functioning of soluble mitochondrial ATPase. Eur. J. Biochem. **121:**451–455.
215. **Koul, A., N. Dendouga, K. Vergauwen, B. Molenberghs, L. Vranckx, R. Willebrords, Z. Ristic, H. Lill, I. Dorange, J. Guillemont, D. Bald, and K. Andries.** 2007. Diarylquinolines target subunit *c* of mycobacterial ATP synthase. Nat. Chem. Biol. **3:**323–324.
216. **Kozlov, I. A., M. Milgrom Ya, M. B. Murataliev, and E. N. Vulfson.** 1985. The nucleotide binding site of F_1-ATPase which carries out uni-site catalysis is one of the alternating active sites of the enzyme. FEBS Lett. **189:**286–290.
217. **Kozlov, I. A., and Y. M. Milgrom.** 1980. The non-catalytic nucleotide-binding site of mitochondrial ATPase is localised on the α-subunit of factor F_1. Eur. J. Biochem. **106**:457–462.
218. **Krogmann, D. W., and M. L. Stiller.** 1962. A naturally occurring cofactor for photosynthetic phosphorylation. Biochem. Biophys. Res. Commun. **7:**46–49.
219. **Kumar, G., V. K. Kalra, and A. F. Brodie.** 1979. Affinity labeling of coupling factor-latent ATPase from *Mycobacterium phlei* with 2′,3′-dialdehyde derivatives of adenosine 5′-triphosphate and adenosine 5′-diphosphate. J. Biol. Chem. **254:**1964–1971.
220. **Laikind, P. K., and W. S. Allison.** 1983. Quinacrine mustard inactivates the bovine heart mitochondrial F_1-ATPase with the modification of the β subunit. J. Biol. Chem. **258:**11700–11704.
221. **Laikind, P. K., T. M. Goldenberg, and W. S. Allison.** 1982. On the mechanism of inhibition of the bovine heart F_1-ATPase by local anesthetics. Biochem. Biophys. Res. Commun. **109:**423–427.
222. **Laikind, P. K., F. C. Hill, and W. S. Allison.** 1985. The use of [^{3}H]aniline to identify the essential carboxyl group in the bovine mitochondrial F_1-ATPase that reacts with 1-(ethoxycarbonyl)-2-ethoxy-1,2-dihydroquinoline. Arch. Biochem. Biophys. **240:**904–920.
223. **Lang, D. R., and E. Racker.** 1974. Effect of quercetin and F_1 inhibitor on mitochondrial ATPase and energy-linked reactions in submitochondrial particles. Biochim. Biophys. Acta **333:**180–186.
224. **Lardy, H., P. Reed, and C. H. Lin.** 1975. Antibiotic inhibitors of mitochondrial ATP synthesis. Fed. Proc. **34:**1707–1710.
225. **Lardy, H. A., D. Johnson, and M. W. Mc.** 1958. Antibiotics as tools for metabolic studies. I. A survey of toxic antibiotics in respiratory, phosphorylative and glycolytic systems. Arch. Biochem. Biophys. **78:**587–597.
226. **Lauber, A. H., T. J. Barrett, M. Subramaniam, M. Schuchard, and T. C. Spelsberg.** 1997. A DNA-binding element for a steroid receptor-binding factor is flanked by dual nuclear matrix DNA attachment sites in the *c*-myc gene promoter. J. Biol. Chem. **272:**24657–24665.
227. **Lauquin, G., R. Pougeois, and P. V. Vignais.** 1980. 4-Azido-2-nitrophenyl phosphate, a new photoaffinity derivative of inorganic phosphate. Study of its interaction with the inorganic phosphate binding site of beef heart mitochondrial adenosine triphosphatase. Biochemistry **19:**4620–4626.
228. **Lebowitz, M. S., and P. L. Pedersen.** 1996. Protein inhibitor of mitochondrial ATP synthase: relationship of inhibitor structure to pH-dependent regulation. Arch. Biochem. Biophys. **330:**342–354.
229. **Lebowitz, M. S., and P. L. Pedersen.** 1993. Regulation of the mitochondrial ATP synthase/ATPase complex: cDNA cloning, sequence, overexpression, and secondary structural characterization of a functional protein inhibitor. Arch. Biochem. Biophys. **301:**64–70.
230. **Lee, R. S., J. Pagan, M. Satre, P. V. Vignais, and A. E. Senior.** 1989. Identification of a mutation in *Escherichia coli* F_1-ATPase β-subunit conferring resistance to aurovertin. FEBS Lett. **253:**269–272.
231. **Lee, R. S., J. Pagan, S. Wilke-Mounts, and A. E. Senior.** 1991. Characterization of *Escherichia coli* ATP synthase β-subunit mutations using a chromosomal deletion strain. Biochemistry **30:**6842–6847.
232. **Linnett, P. E., and R. B. Beechey.** 1979. Inhibitors of the ATP synthase system. Methods Enzymol. **55:**472–518.
233. **Linnett, P. E., A. D. Mitchell, M. D. Osselton, L. J. Mulheirn, and R. B. Beechey.** 1978. Citreoviridin, a specific inhibitor of the mitochondiral adenosine triphosphatase. Biochem. J. **170:**503–510.
234. **Lloyd, D., and S. W. Edwards.** 1976. Mitochondrial adenosine triphosphatase of the fission yeast, Schizosaccharomyces pombe 972H$^-$. Changes in activity and inhibitor-sensitivity in response to catabolite repression. Biochem. J. **160:**335–342.
235. **Lloyd, D., D. G. Lindmark, and M. Muller.** 1979. Adenosine triphosphatase activity of *Tritrichomonas foetus*. J. Gen. Microbiol. **115:**301–307.
236. **Lotscher, H. R., C. deJong, and R. A. Capaldi.** 1984. Inhibition of the adenosinetriphosphatase activity of *Escherichia coli* F_1 by the water-soluble carbodiimide 1-ethyl-3-[3-(dimethylamino)propyl]carbodiimide is due to modification of several carboxyls in the β subunit. Biochemistry **23:**4134–4140.
237. **Lounis, N., T. Gevers, J. Van Den Berg, and K. Andries.** 2008. Impact of the interaction of R207910 with rifampin on the treatment of tuberculosis studied in the mouse model. Antimicrob. Agents Chemother. **52:**3568–3572.
238. **Lounis, N., N. Veziris, A. Chauffour, C. Truffot-Pernot, K. Andries, and V. Jarlier.** 2006. Combinations of R207910 with drugs used to treat multidrug-

resistant tuberculosis have the potential to shorten treatment duration. Antimicrob. Agents Chemother. **50:**3543–3547.
239. **Lowe, P. N., and R. B. Beechey.** 1982. Interactions between the mitochondrial adenosinetriphosphatase and periodate-oxidized adenosine 5′-triphosphate, an affinity label for adenosine 5′-triphosphate binding sites. Biochemistry **21:**4073–4082.
240. **Lubben, M., U. Lucken, J. Weber, and G. Schafer.** 1984. Azidonaphthoyl-ADP: a specific photolabel for the high-affinity nucleotide-binding sites of F_1-ATPase. Eur. J. Biochem. **143:**483–490.
241. **Lucero, H., W. I. Lescano, and R. H. Vallejos.** 1978. Inhibition of energy conservation reactions in chromatophores of *Rhodospirillum rubrum* by antibiotics. Arch. Biochem. Biophys. **186:**9–14.
242. **Lucero, H. A., R. A. Ravizzine, and R. H. Vallejos.** 1976. Inhibition of spinach chloroplasts photophosphorylation by the antibiotics leucinostatin and efrapeptin. FEBS Lett. **68:**141–144.
243. **Lunardi, J., A. Dupuis, J. Garin, J. P. Issartel, L. Michel, M. Chabre, and P. V. Vignais.** 1988. Inhibition of H^+-transporting ATPase by formation of a tight nucleoside diphosphate-fluoroaluminate complex at the catalytic site. Proc. Natl. Acad. Sci. USA **85:**8958–8962.
244. **Lunardi, J., G. J. Lauquin, and P. V. Vignais.** 1977. Interaction of azidonitrophenylaminobutyryl-ADP, a photoaffinity ADP analog, with mitochondrial adenosine triphosphatase. Identification of the labeled subunits. FEBS Lett. **80:**317–323.
245. **Lunardi, J., M. Satre, M. Bof, and P. V. Vignais.** 1979. Reactivity of the β subunit of *Escherichia coli* adenosine triphosphatase with 4-chloro-7-nitrobenzofurazan. Biochemistry **18:**5310–5316.
246. **Lunardi, J., and P. V. Vignais.** 1979. Adenine nucleotide binding sites in chemically modified F_1-ATPase: inhibitory effect of 4-chloro-7-nitrobenzofurazan on photolabeling by arylazido nucleotides. FEBS Lett. **102:**23–28.
247. **Lunardi, J., and P. V. Vignais.** 1982. Studies of the nucleotide-binding sites on the mitochondrial F_1-ATPase through the use of a photoactivable derivative of adenylyl imidodiphosphate. Biochim. Biophys. Acta **682:**124–134.
248. **Marcus, F., S. M. Schuster, and H. A. Lardy.** 1976. Essential arginyl residues in mitochondrial adenosine triphosphatase. J. Biol. Chem. **251:**1775–1780.
249. **Matsui, T., E. Muneyuki, M. Honda, W. S. Allison, C. Dou, and M. Yoshida.** 1997. Catalytic activity of the $\alpha_3\beta_3\gamma$ complex of F_1-ATPase without noncatalytic nucleotide binding site. J. Biol. Chem. **272:**8215–8221.
250. **Matsuno-Yagi, A., and Y. Hatefi.** 1984. Inhibitory chemical modifications of F_1-ATPase: effects on the kinetics of adenosine 5′-triphosphate synthesis and hydrolysis in reconstituted systems. Biochemistry **23:**3508–3514.
251. **Matsuno-Yagi, A., T. Yagi, and Y. Hatefi.** 1985. Studies on the mechanism of oxidative phosphorylation: effects of specific F_0 modifiers on ligand-induced conformation changes of F_1. Proc. Natl. Acad. Sci. USA **82:**7550–7554.
252. **McEnery, M. W., and P. L. Pedersen.** 1986. Diethylstilbestrol. A novel F_0-directed probe of the mitochondrial proton ATPase. J. Biol. Chem. **261:**1745–1752.
253. **Melandri, A. B., E. Fabbri, and B. A. Melandri.** 1975. Energy transduction in photosynthetic bacteria. VIII. Activation of the energy-transducing ATPase by inorganic phosphate. Biochim. Biophys. Acta **376:**82–88.
254. **Melanson, D. L., and M. S. Spencer.** 1981. Kinetics of ATP synthesis in pea cotyledon submitochondrial particles. Plant Physiol. **68:**648–652.
255. **Melnick, R. L., J. T. De Sousa, J. Magiure, and L. Packer.** 1975. Action of the adenosine triphosphate analog, adenylyl imidodiphosphate in mitochondria. Arch. Biochem. Biophys. **166:**139–144.
256. **Menz, R. I., J. E. Walker, and A. G. Leslie.** 2001. Structure of bovine mitochondrial F_1-ATPase with nucleotide bound to all three catalytic sites: implications for the mechanism of rotary catalysis. Cell **106:**331–341.
257. **Meyer, W. L., L. F. Kuyper, R. B. Lewis, G. E. Templeton, and S. H. Woodhead.** 1974. The amino acid sequence and configuration of tentoxin. Biochem. Biophys. Res. Commun. **56:**234–240.
258. **Michel, L., J. Garin, G. Girault, and P. V. Vignais.** 1992. Photolabeling of the phosphate binding site of chloroplast coupling factor 1 with [^{32}P]azidonitrophenyl phosphate. FEBS Lett. **313:**90–93.
259. **Mikami, Y., K. Yazawa, K. Fukushima, T. Arai, S. Udagawa, and R. A. Samson.** 1989. Paecilotoxin production in clinical or terrestrial isolates of *Paecilomyces lilacinus* strains. Mycopathologia **108:**195–199.
260. **Minauro-Sanmiguel, F., C. Bravo, and J. J. Garcia.** 2002. Cross-linking of the endogenous inhibitor protein (IF_1) with rotor (γ, ε) and stator (α) subunits of the mitochondrial ATP synthase. J. Bioenerg. Biomembr. **34:**433–443.
261. **Minkov, I. B., A. F. Fitin, E. A. Vasilyeva, and A. D. Vinogradov.** 1979. Mg^{2+}-induced ADP-dependent inhibition of the ATPase activity of beef heart mitochondrial coupling factor F_1. Biochem. Biophys. Res. Commun. **89:**1300–1306.
262. **Minkov, I. B., and H. Strotmann.** 1989. The effect of azide on regulation of the chloroplast H^+-ATPase by ADP and phosphate. Biochim. Biophys. Acta **973:**7–12.
263. **Mitchell, P., and J. Moyle.** 1970. Influence of aurovertin on affinity of mitochondrial adenosine triphosphatase for ATP and ADP. FEBS Lett. **6:**309–311.
264. **Mitchell, R. A., B. F. Chang, C. H. Huang, and E. G. DeMaster.** 1971. Inhibition of mitochondrial energy-linked functions by arsenate. Evidence for a nonhydrolytic mode of inhibitor action. Biochemistry **10:**2049–2054.
265. **Mochimaru, M., and H. Sakurai.** 1997. Three kinds of binding site for tentoxin on isolated chloroplast coupling factor 1. FEBS Lett. **419:**23–26.
266. **Mori, Y., M. Suzuki, K. Fukushima, and T. Arai.** 1983. Structure of leucinostatin B, an uncoupler on mitochondria. J. Antibiot. (Tokyo) **36:**1084–1086.
267. **Moritani, C., Y. Sakai, M. Tsuda, H. Kanazawa, and T. Tsuchiya.** 1990. Characteristics of the H^+-translocating adenosine triphosphatase of *Vibrio parahaemolyticus*. Chem. Pharm. Bull. (Tokyo) **38:**164–167.
268. **Moriyama, Y., V. Patel, and M. Futai.** 1995. Quinacrine mustard and lipophilic cations inhibitory to both vacuolar H^+-ATPase and F_0F_1-ATP synthase. FEBS Lett. **359:**69–72.
269. **Moser, T. L., D. J. Kenan, T. A. Ashley, J. A. Roy, M. D. Goodman, U. K. Misra, D. J. Cheek, and S. V. Pizzo.** 2001. Endothelial cell surface F_1-F_0 ATP synthase is active in ATP synthesis and is inhibited by angiostatin. Proc. Natl. Acad. Sci. USA **98:**6656–6661.
270. **Moser, T. L., M. S. Stack, I. Asplin, J. J. Enghild, P. Hojrup, L. Everitt, S. Hubchak, H. W. Schnaper, and S. V. Pizzo.** 1999. Angiostatin binds ATP synthase on the surface of human endothelial cells. Proc. Natl. Acad. Sci. USA **96:**2811–2816.
271. **Moser, T. L., M. S. Stack, M. L. Wahl, and S. V. Pizzo.** 2002. The mechanism of action of angiostatin: can you teach an old dog new tricks? Thromb. Haemost. **87:**394–401.
272. **Moyle, J., and P. Mitchell.** 1975. Active/inactive state transitions of mitochondrial ATPase molecules influenced by Mg^{2+}, anions and aurovertin. FEBS Lett. **56:**55–61.
273. **Muneyuki, E., T. Hisabori, T. Sasayama, K. Mochizuki, and M. Yoshida.** 1996. The heterogeneous interaction of substoichiometric TNP-ATP and F_1-ATPase from *Escherichia coli*. J. Biochem. (Tokyo) **120:**940–945.
274. **Muneyuki, E., M. Makino, H. Kamata, Y. Kagawa, M. Yoshida, and H. Hirata.** 1993. Inhibitory effect of NaN_3 on the F_0F_1 ATPase of submitochondrial particles as related to nucleotide binding. Biochim. Biophys. Acta **1144:**62–68.
275. **Munter, K., M. Athanasiou, and C. Stournaras.** 1989. Inhibition of cellular activities by triethyllead. Role of glutathione and accumulation of triethyllead in vitro. Biochem. Pharmacol. **38:**3941–3945.
276. **Murataliev, M. B.** 1995. Interaction of mitochondrial F_1-ATPase with trinitrophenyl derivatives of ATP. Photoaffinity labeling of binding sites with 2-azido-2′,3′-*O*-(4,6-trinitrophenyl)adenosine 5′-triphosphate. Eur. J. Biochem. **232:**578–585.
277. **Murataliev, M. B., and P. D. Boyer.** 1994. Interaction of mitochondrial F_1-ATPase with trinitrophenyl derivatives of ATP and ADP. Participation of third catalytic site and role of Mg^{2+} in enzyme inactivation. J. Biol. Chem. **269:**15431–15439.
278. **Murataliev, M. B., Y. M. Milgrom, and P. D. Boyer.** 1991. Characteristics of the combination of inhibitory Mg^{2+} and azide with the F_1 ATPase from chloroplasts. Biochemistry **30:**8305–8310.
279. **Nadanaciva, S., J. Weber, and A. E. Senior.** 2000. New probes of the F_1-ATPase catalytic transition state reveal that two of the three catalytic sites can assume a transition state conformation simultaneously. Biochemistry **39:**9583–9590.
280. **Nagley, P., R. M. Hall, and B. G. Ooi.** 1986. Amino acid substitutions in mitochondrial ATPase subunit 9 of *Saccharomyces cerevisiae* leading to oligomycin or venturicidin resistance. FEBS Lett. **195:**159–163.
281. **Nakamoto, R. K., K. Shin, A. Iwamoto, H. Omote, M. Maeda, and M. Futai.** 1992. *Escherichia coli* F_0F_1-ATPase. Residues involved in catalysis and coupling. Ann. N. Y. Acad. Sci. **671:**335–344.
282. **Nakanishi-Matsui, M., S. Kashiwagi, H. Hosokawa, D. J. Cipriano, S. D. Dunn, Y. Wada, and M. Futai.** 2006. Stochastic high-speed rotation of *Escherichia coli* ATP synthase F_1 sector: the ε subunit-sensitive rotation. J. Biol. Chem. **281:**4126–4131.
283. **Nelson, N., B. I. Kanner, and D. L. Gutnick.** 1974. Purification and properties of Mg^{2+}-Ca^{2+} adenosinetriphosphatase from *Escherichia coli*. Proc. Natl. Acad. Sci. USA **71:**2720–2724.
284. **Nelson, N., H. Nelson, and E. Racker.** 1972. Partial resolution of the enzymes catalyzing photophosphorylation. XII. Purification and properties of an inhibitor isolated from chloroplast coupling factor 1. J. Biol. Chem. **247:**7657–7662.
285. **Nieuwenhuis, F. J., B. I. Kanner, D. L. Gutnick, P. W. Postma, and K. van Dam.** 1973. Energy conservation in membranes of mutants of *Escherichia coli* defective in oxidative phosphorylation. Biochim. Biophys. Acta **325:**62–71.
286. **Nishino, H., M. Murakoshi, X. Y. Mou, S. Wada, M. Masuda, Y. Ohsaka, Y. Satomi, and K. Jinno.** 2005. Cancer prevention by phytochemicals. Oncology **69**(Suppl. 1)**:**38–40.
287. **Noumi, T., M. Maeda, and M. Futai.** 1987. Mode of inhibition of sodium azide on H^+-ATPase of *Escherichia coli*. FEBS Lett. **213:**381–384.
288. **Noumi, T., M. Tagaya, K. Miki-Takeda, M. Maeda, T. Fukui, and M. Futai.**

1987. Loss of unisite and multisite catalyses by *Escherichia coli* F_1 through modification with adenosine tri- or tetraphosphopyridoxal. J. Biol. Chem. **262:**7686–7692.

289. **Nowak, K. F., V. Tabidze, and R. E. McCarty.** 2002. The C-terminal domain of the ε subunit of the chloroplast ATP synthase is not required for ATP synthesis. Biochemistry **41:**15130–15134.
290. **Ogawa, W., S. Izawa, Y. Sakai-Tomita, C. Moritani, M. Tsuda, K. Kinomura, S. Kitazawa, and T. Tsuchiya.** 1994. F_0F_1-ATPase of *Vibrio parahaemolyticus*: purification using new detergents and characterization. Biochim. Biophys. Acta **1188:**69–74.
291. **Oren, R., and Z. Gromet-Elhanan.** 1979. Coupling factor ATPase complex of *Rhodospirillum rubrum*. Purification and characterization of an oligomycin and *N,N′*-dicyclohexylcarbodiimide-sensitive (Ca^{2+} + Mg^{2+})-ATPase. Biochim. Biophys. Acta **548:**106–118.
292. **Orriss, G. L., A. G. Leslie, K. Braig, and J. E. Walker.** 1998. Bovine F_1-ATPase covalently inhibited with 4-chloro-7-nitrobenzofurazan: the structure provides further support for a rotary catalytic mechanism. Structure **6:**831–837.
293. **Osanai, T., K. Magota, M. Tanaka, M. Shimada, R. Murakami, S. Sasaki, H. Tomita, N. Maeda, and K. Okumura.** 2005. Intracellular signaling for vasoconstrictor coupling factor 6: novel function of β-subunit of ATP synthase as receptor. Hypertension **46:**1140–1146.
294. **Osanai, T., S. Okada, K. Sirato, T. Nakano, M. Saitoh, K. Magota, and K. Okumura.** 2001. Mitochondrial coupling factor 6 is present on the surface of human vascular endothelial cells and is released by shear stress. Circulation **104:**3132–3136.
295. **Pacheco-Moises, F., F. Minauro-Sanmiguel, C. Bravo, and J. J. Garcia.** 2002. Sulfite inhibits the F_1F_0-ATP synthase and activates the F_1F_0-ATPase of *Paracoccus denitrificans*. J. Bioenerg. Biomembr. **34:**269–278.
296. **Paik, S. R., J. M. Jault, and W. S. Allison.** 1994. Inhibition and inactivation of the F_1 adenosinetriphosphatase from *Bacillus* PS3 by dequalinium and activation of the enzyme by lauryl dimethylamine oxide. Biochemistry **33:** 126–133.
297. **Pal, P. K., and P. S. Coleman.** 1990. Detecting precatalytic conformational changes in F_1-ATPase with 4-benzoyl(benzoyl)-1-amidofluorescein, a novel fluorescent nucleotide site-specific photoaffinity label. J. Biol. Chem. **265:** 14996–15002.
298. **Palmer, D. N., G. Barns, D. R. Husbands, and R. D. Jolly.** 1986. Ceroid lipofuscinosis in sheep. II. The major component of the lipopigment in liver, kidney, pancreas, and brain is low molecular weight protein. J. Biol. Chem. **261:**1773–1777.
299. **Palmer, D. N., I. M. Fearnley, J. E. Walker, N. A. Hall, B. D. Lake, L. S. Wolfe, M. Haltia, R. D. Martinus, and R. D. Jolly.** 1992. Mitochondrial ATP synthase subunit *c* storage in the ceroid-lipofuscinoses (Batten disease). Am. J. Med. Genet. **42:**561–567.
300. **Papa, S., M. Tuena de Gomez-Puyou, and A. Gomez-Puyou.** 1975. On the mechanism of action of alkylguanidines on oxidative phosphorylation in mitochondria. Eur. J. Biochem. **55**:1–8.
301. **Park, M., L. Lin, S. Thomas, H. D. Braymer, P. M. Smith, D. H. Harrison, and D. A. York.** 2004. The F_1-ATPase β-subunit is the putative enterostatin receptor. Peptides **25:**2127–2133.
302. **Pedersen, P. L.** 1975. Adenosine triphosphatase from rat liver mitochondria: separate sites involved in ATP hydrolysis and in the reversible, high affinity binding of ADP. Biochem. Biophys. Res. Commun. **64:**610–616.
303. **Pedersen, P. L.** 2007. Transport ATPases into the year 2008: a brief overview related to types, structures, functions and roles in health and disease. J. Bioenerg. Biomembr. **39:**349–355.
304. **Pedersen, P. L., and L. M. Amzel.** 1993. ATP synthases. Structure, reaction center, mechanism, and regulation of one of nature's most unique machines. J. Biol. Chem. **268:**9937–9940.
305. **Pedersen, P. L., Y. H. Ko, and S. Hong.** 2000. ATP synthases in the year 2000: evolving views about the structures of these remarkable enzyme complexes. J. Bioenerg. Biomembr. **32:**325–332.
306. **Penefsky, H. S.** 1974. Differential effects of adenylyl imidodiphosphate on adenosine triphosphate synthesis and the partial reactions of oxidative phosphorylation. J. Biol. Chem. **249:**3579–3585.
307. **Penefsky, H. S.** 1977. Reversible binding of P_i by beef heart mitochondrial adenosine triphosphatase. J. Biol. Chem. **252:**2891–2899.
308. **Penefsky, H. S., M. E. Pullman, A. Datta, and E. Racker.** 1960. Partial resolution of the enzymes catalyzing oxidative phosphorylation. II. Participation of a soluble adenosine tolphosphatase in oxidative phosphorylation. J. Biol. Chem. **235:**3330–3336.
309. **Penefsky, H. S., and R. C. Warner.** 1965. Partial resolution of the enzymes catalyzing oxidative phosphorylation. VI. Studies on the mechanism of cold inactivation of mitochondrial adenosine triphosphatase. J. Biol. Chem. **240:** 4694–4702.
310. **Penniston, J. T.** 1971. High hydrostatic pressure and enzymic activity: inhibition of multimeric enzymes by dissociation. Arch. Biochem. Biophys. **142:**322–332.
311. **Perlin, D. S., L. R. Latchney, and A. E. Senior.** 1985. Inhibition of *Escherichia coli* H^+-ATPase by venturicidin, oligomycin and ossamycin. Biochim. Biophys. Acta **807:**238–244.
312. **Peter, H. W., M. R. Pinheiro, and M. Silva Lima.** 1981. Regulation of the F-ATPase from mitochondria of *Vigna sinensis* (L.) Savi cv. Pitiuba by spermine, spermidine, putrescine, Mg^{2+}, Na^+, and K^+. Can. J. Biochem. **59:**60–66.
313. **Petrella, S., E. Cambau, A. Chauffour, K. Andries, V. Jarlier, and W. Sougakoff.** 2006. Genetic basis for natural and acquired resistance to the diarylquinoline R207910 in mycobacteria. Antimicrob. Agents Chemother. **50:**2853–2856.
314. **Petrone, G., D. N. Garboczi, and P. L. Pedersen.** 1987. Mitochondrial ATP synthase complex: interaction of its F_1 adenosinetriphosphatase moiety with the heavy atom iodine. Biochemistry **26:**4016–4021.
315. **Phelps, D. C., K. Nordenbrand, B. D. Nelson, and L. Ernster.** 1975. Inhibition of purified mitochondiral ATPase (F_1) by bathophenanthroline and relief of the inhibition by uncouplers. Biochem. Biophys. Res. Commun. **63:**1005–1012.
316. **Pinet, E., F. Cavelier, J. Verducci, G. Girault, L. Dubart, F. Haraux, C. Sigalat, and F. Andre.** 1996. Synthesis, structure, and properties of MeSer1-tentoxin, a new cyclic tetrapeptide which interacts specifically with chloroplast F_1 H^+-ATPase differentiation of inhibitory and stimulating effects. Biochemistry **35:**12804–12811.
317. **Pinet, E., J. M. Gomis, G. Girault, F. Cavelier, J. Verducci, J. P. Noel, and F. Andre.** 1996. Tentoxin has at least two binding sites on CF_1 and ε-depleted CF_1 ATPases isolated from spinach chloroplast. FEBS Lett. **395:** 217–220.
318. **Pinet, E., J. M. Neumann, I. Dahse, G. Girault, and F. Andre.** 1995. Multiple interconverting conformers of the cyclic tetrapeptide tentoxin, [cyclo-(L-MeAla^1-L-Leu^2-MePhe[(Z)Δ]^3-Gly^4)], as seen by two-dimensional ^{1}H-nmr spectroscopy. Biopolymers **36:**135–152.
319. **Polgreen, K. E., J. Featherstone, A. C. Willis, and D. A. Harris.** 1995. Primary structure and properties of the inhibitory protein of the mitochondrial ATPase (H^+-ATP synthase) from potato. Biochim. Biophys. Acta **1229:**175–180.
320. **Pougeois, R.** 1983. EEDQ probably reacts with the Mg^{2+}-ATP catalytic sites of mitochondrial and bacterial F_1-ATPases. FEBS Lett. **154:**47–50.
321. **Pougeois, R., G. J. Lauquin, and P. V. Vignais.** 1983. Interaction of 4-azido-2-nitrophenyl phosphate, an inorganic phosphate photoreactive analogue, with chloroplast coupling factor 1. Biochemistry **22:**1241–1245.
322. **Pougeois, R., M. Satre, and P. Vignais.** 1978. *N*-Ethoxycarbonyl-2-ethoxy-1,2-dihydroquinoline, a new inhibitor of the mitochondrial F_1-ATPase. Biochemistry **17:**3018–3023.
323. **Price, K. E., A. Schlein, W. T. Bradner, and J. Lein.** 1963. Peliomycin, a new cytotoxic agent. II. Biological properties. Antimicrob. Agents Chemother. **161:**95–99.
324. **Pullman, M. E., H. S. Penefsky, A. Datta, and E. Racker.** 1960. Partial resolution of the enzymes catalyzing oxidative phosphorylation. I. Purification and properties of soluble dinitrophenol-stimulated adenosine triphosphatase. J. Biol. Chem. **235:**3322–3329.
325. **Quillen, E. E., G. C. Haslam, H. S. Samra, D. Amani-Taleshi, J. A. Knight, D. E. Wyatt, S. C. Bishop, K. K. Colvert, M. L. Richter, and P. A. Kitos.** 2006. Ectoadenylate kinase and plasma membrane ATP synthase activities of human vascular endothelial cells. J. Biol. Chem. **281:**20728–20737.
326. **Rao, R., D. Cunningham, R. L. Cross, and A. E. Senior.** 1988. Pyridoxal 5′-diphospho-5′-adenosine binds at a single site on isolated α-subunit from *Escherichia coli* F_1-ATPase and specifically reacts with lysine 201. J. Biol. Chem. **263:**5640–5645.
327. **Recktenwald, E., and B. Hess.** 1977. Allosteric influence of anions on mitochondrial ATPase of yeast. FEBS Lett. **76:**25–28.
328. **Reed, P. W., and H. A. Lardy.** 1975. Uncoupling and specific inhibition of phosphoryl transfer reactions in mitochondria by antibiotic A20668. J. Biol. Chem. **250:**3704–3708.
329. **Ren, H. M., and W. S. Allison.** 1997. Photoinactivation of the F_1-ATPase from spinach chloroplasts by dequalinium is accompanied by derivatization of methionine β183. J. Biol. Chem. **272:**32294–32300.
330. **Rhodes, A., K. H. Fantes, B. Boothroyd, M. P. McGonagle, and R. Crosse.** 1961. Venturicidin: a new antifungal antibiotic of potential use in agriculture. Nature **192**:952–954.
331. **Richter, M. L., R. Hein, and B. Huchzermeyer.** 2000. Important subunit interactions in the chloroplast ATP synthase. Biochim. Biophys. Acta **1458:** 326–342.
332. **Richter, M. L., W. J. Patrie, and R. E. McCarty.** 1984. Preparation of the ε subunit and ε subunit-deficient chloroplast coupling factor 1 in reconstitutively active forms. J. Biol. Chem. **259:**7371–7373.
333. **Rigoulet, M.** 1990. Control processes in oxidative phosphorylation: kinetic constraints and stoichiometry. Biochim. Biophys. Acta **1018:**185–189.
334. **Rigoulet, M., L. Fraisse, R. Ouhabi, B. Guerin, E. Fontaine, and X. Leverve.** 1990. Flux-dependent increase in the stoichiometry of charge translocation by mitochondrial ATPase/ATP synthase induced by almitrine. Biochim. Biophys. Acta **1018:**91–97.
335. **Rigoulet, M., X. Leverve, E. Fontaine, R. Ouhabi, and B. Guerin.** 1998. Quantitative analysis of some mechanisms affecting the yield of oxidative phosphorylation: dependence upon both fluxes and forces. Mol. Cell. Biochem. **184:**35–52.

336. **Rigoulet, M., R. Ouhabi, X. Leverve, F. Putod-Paramelle, and B. Guerin.** 1989. Almitrine, a new kind of energy-transduction inhibitor acting on mitochondrial ATP synthase. Biochim. Biophys. Acta **975:**325–329.
337. **Roise, D., S. J. Horvath, J. M. Tomich, J. H. Richards, and G. Schatz.** 1986. A chemically synthesized pre-sequence of an imported mitochondrial protein can form an amphiphilic helix and perturb natural and artificial phospholipid bilayers. EMBO J. **5:**1327–1334.
338. **Roise, D., F. Theiler, S. J. Horvath, J. M. Tomich, J. H. Richards, D. S. Allison, and G. Schatz.** 1988. Amphiphilicity is essential for mitochondrial presequence function. EMBO J. **7:**649–653.
339. **Rossi, C., L. Tuttobello, M. Ricci, C. G. Casinovi, and L. Radics.** 1987. Leucinostatin D, a novel peptide antibiotic from *Paecilomyces marquandii*. J. Antibiot. **40:**130–133.
340. **Rubin, E. J.** 2005. Toward a new therapy for tuberculosis. N. Engl. J. Med. **352:**933–934.
341. **Russell, J., S. J. Jeng, and R. J. Guillory.** 1976. Arylazido aminopropionyl ATP, and active site directed photoaffinity reagent for mitochondrial adenosine triphosphatase. Biochem. Biophys. Res. Commun. **70:**1225–1234.
342. **Saad, S. M., J. M. Halloin, and D. J. Hagedorn.** 1970. Production, purification, and bioassay of tentoxin. Phytopathology **60:**415–418.
343. **Saishu, T., Y. Kagawa, and R. Shimizu.** 1983. Resistance of thermophilic ATPase (TF_1) to specific F_1-atpase inhibitors including local anesthetics. Biochem. Biophys. Res. Commun. **112:**822–826.
344. **Sakai, Y., H. Kanazawa, M. Tsuda, and T. Tsuchiya.** 1990. Rapid purification and characterization of F_1-ATPase of *Vibrio parahaemolyticus*. Biochim. Biophys. Acta **1018:**18–22.
345. **Sakamoto, J.** 1984. Effect of dimethylsulfoxide on ATP synthesis by mitochondrial soluble F_1-ATPase. J. Biochem. (Tokyo) **96:**483–487.
346. **Sakamoto, J., and Y. Tonomura.** 1983. Synthesis of enzyme-bound ATP by mitochondrial soluble F_1-ATPase in the presence of dimethylsulfoxide. J. Biochem. (Tokyo) **93:**1601–1614.
347. **Salomon, A. R., D. W. Voehringer, L. A. Herzenberg, and C. Khosla.** 2001. Apoptolidin, a selective cytotoxic agent, is an inhibitor of F_0F_1-ATPase. Chem. Biol. **8:**71–80.
348. **Salomon, A. R., D. W. Voehringer, L. A. Herzenberg, and C. Khosla.** 2000. Understanding and exploiting the mechanistic basis for selectivity of polyketide inhibitors of F_0F_1-ATPase. Proc. Natl. Acad. Sci. USA **97:**14766–14771.
349. **Salomon, A. R., Y. Zhang, H. Seto, and C. Khosla.** 2001. Structure-activity relationships within a family of selectively cytotoxic macrolide natural products. Org. Lett. **3:**57–59.
350. **Santolini, J., F. Haraux, C. Sigalat, G. Moal, and F. Andre.** 1999. Kinetic analysis of tentoxin binding to chloroplast F_1-ATPase. A model for the overactivation process. J. Biol. Chem. **274:**849–858.
351. **Santolini, J., C. Minoletti, J. M. Gomis, C. Sigalat, F. Andre, and F. Haraux.** 2002. An insight into the mechanism of inhibition and reactivation of the F_1-ATPases by tentoxin. Biochemistry **41:**6008–6018.
352. **Satre, M.** 1981. The effect of asteltoxin and citreomontanine, two polyenic α-pyrone mycotoxins, on *Escherichia coli* adenosine triphosphate. Biochem. Biophys. Res. Commun. **100:**267–274.
353. **Satre, M., M. Bof, and P. V. Vignais.** 1980. Interaction of *Escherichia coli* adenosine triphosphatase with aurovertin and citreoviridin: inhibition and fluorescence studies. J. Bacteriol. **142:**768–776.
354. **Sayood, S. F., H. Suh, C. S. Wilcox, and S. M. Schuster.** 1989. Effect of citreoviridin and isocitreoviridin on beef heart mitochondrial ATPase. Arch. Biochem. Biophys. **270:**714–721.
355. **Schafer, G., and G. Onur.** 1979. 3′ Esters of ADP as energy-transfer inhibitors and probes of the catalytic site of oxidative phosphorylation. Eur. J. Biochem. **97:**415–424.
356. **Schafer, G., G. Onur, and M. Schlegel.** 1980. Use of modified adenine nucleotides in mechanistic studies on oxidative phosphorylation: structure and space at the catalytic site. J. Bioenerg. Biomembr. **12:**213–232.
357. **Schagger, H., and T. G. Ohm.** 1995. Human diseases with defects in oxidative phosphorylation. 2. F_1F_0 ATP-synthase defects in Alzheimer disease revealed by blue native polyacrylamide gel electrophoresis. Eur. J. Biochem. **227:**916–921.
358. **Schmitz, H., S. B. Deak, K. E. Crook, Jr., and I. R. Hooper.** 1963. Peliomycin, a new cytotoxic agent. I. Production, isolation, and characterization. Antimicrob. Agents Chemother. **161**:89–94.
359. **Schmitz, H., S. D. Jubinski, I. R. Hooper, K. E. Crook, Jr., K. E. Price, and J. Lein.** 1965. Ossamycin, a new cytotoxic agent. J. Antibiot. **18:**82–88.
360. **Scholes, P., P. Mitchell, and J. Moyle.** 1969. The polarity of proton translocation in some photosynthetic microorganisms. Eur. J. Biochem. **8:**450–454.
361. **Schuster, S. M., R. E. Ebel, and H. A. Lardy.** 1975. Kinetic studies on rat liver and beef heart mitochondrial ATPase. Evidence for nucleotide binding at separate regulatory and catalytic sites. J. Biol. Chem. **250:**7848–7853.
362. **Schuster, S. M., R. J. Gertschen, and H. A. Lardy.** 1976. Effect of inosine 5′-(β,γ-imido) triphosphate and other nucleotides on beef heart mitochondrial ATPase. J. Biol. Chem. **251:**6705–6710.
363. **Schuster, S. M., G. D. Reinhart, and H. A. Lardy.** 1977. Studies on the kinetic mechanism of oxidative phosphorylation. J. Biol. Chem. **252:**427–432.
364. **Sebald, W., W. Machleidt, and E. Wachter.** 1980. *N,N′*-dicyclohexylcarbodiimide binds specifically to a single glutamyl residue of the proteolipid subunit of the mitochondrial adenosinetriphosphatases from *Neurospora crassa* and *Saccharomyces cerevisiae*. Proc. Natl. Acad. Sci. USA **77:**785–789.
365. **Selwyn, M. J.** 1967. Preparation and general properties of a soluble adenosine triphosphatase from mitochondria. Biochem. J. **105:**279–288.
366. **Senior, A. E.** 1973. Relationship of cysteine and tyrosine residues to adenosine triphosphate hydrolysis by mitochondrial adenine triphosphatase. Biochemistry **12:**3622–3627.
367. **Sergeant, N., A. Wattez, M. Galvan-valencia, A. Ghestem, J. P. David, J. Lemoine, P. E. Sautiere, J. Dachary, J. P. Mazat, J. C. Michalski, J. Velours, R. Mena-Lopez, and A. Delacourte.** 2003. Association of ATP synthase α-chain with neurofibrillary degeneration in Alzheimer's disease. Neuroscience **117:**293–303.
368. **Shapiro, A. B., K. D. Gibson, H. A. Scheraga, and R. E. McCarty.** 1991. Fluorescence resonance energy transfer mapping of the fourth of six nucleotide-binding sites of chloroplast coupling factor 1. J. Biol. Chem. **266:**17276–17285.
369. **Sigalat, C., B. Pitard, and F. Haraux.** 1995. Proton coupling is preserved in membrane-bound chloroplast ATPase activated by high concentrations of tentoxin. FEBS Lett. **368:**253–256.
370. **Skidmore, R. A., J. D. Patterson, and R. S. Tomsick.** 1996. Local anesthetics. Dermatol. Surg. **22:**511–524.
371. **Sloothaak, J. B., J. A. Berden, M. A. Herweijer, and A. Kemp.** 1985. The use of 8-azido-ATP and 8-azido-ADP as photoaffinity labels of the ATP synthase in submitochondrial particles: evidence for a mechanism of ATP hydrolysis involving two independent catalytic sites? Biochim. Biophys. Acta **809:**27–38.
372. **Smith, J. B., and P. C. Sternweis.** 1977. Purification of membrane attachment and inhibitory subunits of the proton translocating adenosine triphosphatase from *Escherichia coli*. Biochemistry **16:**306–311.
373. **Solaini, G., A. Baracca, E. Gabellieri, and G. Lenaz.** 1997. Modification of the mitochondrial F_1-ATPase ε subunit, enhancement of the ATPase activity of the IF_1-F_1 complex and IF_1-binding dependence of the conformation of the ε subunit. Biochem. J. **327:**443–448.
374. **Solaini, G., and B. Tadolini.** 1984. Spermine binding to submitochondrial particles and activation of adenosine triphosphatase. Biochem. J. **218:**495–499.
375. **Sone, N., K. Ikeba, and Y. Kagawa.** 1979. Inhibition of proton conduction by chemical modification of the membrane moiety of proton translocating ATPase. FEBS Lett. **97:**61–64.
376. **Sone, N., M. Yoshida, H. Hirata, and Y. Kagawa.** 1975. Purification and properties of a dicyclohexylcarbodiimide-sensitive adenosine triphosphatase from a thermophilic bacterium. J. Biol. Chem. **250:**7917–7923.
377. **Souza, M. O., T. B. Creczynski-Pasa, H. M. Scofano, P. Graber, and J. A. Mignaco.** 2004. High hydrostatic pressure perturbs the interactions between CF_0F_1 subunits and induces a dual effect on activity. Int. J. Biochem. Cell. Biol. **36:**920–930.
378. **Steele, J. A., R. D. Durbin, T. F. Uchytil, and D. H. Rich.** 1978. Tentoxin. An uncompetitive inhibitor of lettuce chloroplast coupling factor 1. Biochim. Biophys. Acta **501:**72–82.
379. **Steele, J. A., T. F. Uchytil, and R. D. Durbin.** 1978. The stimulation of coupling factor 1 ATPase by tentoxin. Biochim. Biophys. Acta **504:**136–141.
380. **Steele, J. A., T. F. Uchytil, R. D. Durbin, P. Bhatnagar, and D. H. Rich.** 1976. Chloroplast coupling factor 1: a species-specific receptor for tentoxin. Proc. Natl. Acad. Sci. USA **73:**2245–2248.
381. **Steffens, K., E. Schneider, B. Herkenhoff, R. Schmid, and K. Altendorf.** 1984. Chemical modification of the F_0 part of the ATP synthase (F_1F_0) from *Escherichia coli*. Effects on proton conduction and F_1 binding. Eur. J. Biochem. **138:**617–622.
382. **Steinback, K. E., L. McIntosh, L. Bogorad, and C. J. Arntzen.** 1981. Identification of the triazine receptor protein as a chloroplast gene product. Proc. Natl. Acad. Sci. USA **78:**7463–7467.
383. **Steinke, L., R. Bacon, and S. M. Schuster.** 1987. The effects of exchange-inert metal-nucleotide complexes on the kinetics of beef heart mitochondrial F_1-ATPase. Arch. Biochem. Biophys. **258:**482–490.
384. **Steinke, L., and S. M. Schuster.** 1985. The effect of $Co(III)(NH_3)_4ATP$ on the kinetics of beef heart mitochondrial ATPase. Arch. Biochem. Biophys. **238:**629–635.
385. **Steinmeier, R. C., and J. H. Wang.** 1979. Reconstitution of oxidative phosphorylation by chemically modified coupling factor F_1: differential inhibition of reactions catalyzed by F_1 labeled with 7-chloro-4-nitrobenzo-2-oxa-1,3-diazole or 2,3-butanedione. Biochemistry **18:**11–18.
386. **Sternweis, P. C., and J. B. Smith.** 1980. Characterization of the inhibitory (ε) subunit of the proton-translocating adenosine triphosphatase from *Escherichia coli*. Biochemistry **19:**526–531.
387. **Stock, D., C. Gibbons, I. Arechaga, A. G. Leslie, and J. E. Walker.** 2000. The rotary mechanism of ATP synthase. Curr. Opin. Struct. Biol. **10:**672–679.
388. **Sutton, R., and S. J. Ferguson.** 1985. Tyrosine-311 of a β chain is the

essential residue specifically modified by 4-chloro-7-nitrobenzofurazan in bovine heart mitochondrial ATPase. Eur. J. Biochem. **148:**551–554.

389. **Suzuki, T., T. Murakami, R. Iino, J. Suzuki, S. Ono, Y. Shirakihara, and M. Yoshida.** 2003. F_oF_1-ATPase/synthase is geared to the synthesis mode by conformational rearrangement of ε subunit in response to proton motive force and ADP/ATP balance. J. Biol. Chem. **278:**46840–46846.
390. **Tagaya, M., T. Noumi, K. Nakano, M. Futai, and T. Fukui.** 1988. Identification of α-subunit Lys201 and β-subunit Lys155 at the ATP-binding sites in *Escherichia coli* F_1-ATPase. FEBS Lett. **233:**347–351.
391. **Takeda, K., J. Miki, H. Kanazawa, T. Tsuchiya, and M. Futai.** 1985. Change of inhibitor sensitivities of *Escherichia coli* F_1-ATPase due to a mutational substitution of Phe for Ser at residue 174 of the β subunit. J. Biochem. (Tokyo) **97:**1401–1407.
392. **Tamura, J. K., and J. H. Wang.** 1983. Changes in chemical properties of mitochondrial adenosinetriphosphatase upon removal of tightly bound nucleotides. Biochemistry **22:**1947–1954.
393. **Terwilliger, T. C., and D. Eisenberg.** 1982. The structure of melittin. I. Structure determination and partial refinement. J. Biol. Chem. **257:**6010–6015.
394. **Thomassen, J., and L. Klungsoyr.** 1983. ATPase of bovine heart mitochondria. Modulation of ITPase activity by ATP, ADP, acetyl ATP and acetyl AMP. Biochim. Biophys. Acta **723:**114–122.
395. **Thomasset, S. C., D. P. Berry, G. Garcea, T. Marczylo, W. P. Steward, and A. J. Gescher.** 2007. Dietary polyphenolic phytochemicals—promising cancer chemopreventive agents in humans? A review of their clinical properties. Int. J. Cancer. **120:**451–458.
396. **Thyagarajan, D., S. Shanske, M. Vazquez-Memije, D. De Vivo, and S. DiMauro.** 1995. A novel mitochondrial ATPase 6 point mutation in familial bilateral striatal necrosis. Ann. Neurol. **38:**468–472.
397. **Tiedge, H., U. Lucken, J. Weber, and G. Schafer.** 1982. High-affinity binding of ADP and of ADP analogues to mitochondrial F_1-ATPase. Eur. J. Biochem. **127:**291–299.
398. **Ting, L. P., and J. H. Wang.** 1980. Effect of phosphate and adenine nucleotides on the rate of labeling of functional groups at the catalytic sites of F_1-ATPase. J. Bioenerg. Biomembr. **12:**79–93.
399. **Ting, L. P., and J. H. Wang.** 1980. Functional groups at the catalytic site of F_1 adenosine triphosphatase. Biochemistry **19:**5665–5670.
400. **Tommasino, M., and R. A. Capaldi.** 1985. Effect of dicyclohexylcarbodiimide on unisite and multisite catalytic activities of the adenosinetriphosphatase of *Escherichia coli*. Biochemistry **24:**3972–3976.
401. **Tsunashima, K., M. Ide, H. Kadoi, A. Hirayama, and M. Nakata.** 2001. Synthesis of the C15–C27 portion of venturicidins: a formal total synthesis of venturicidin X. Tetrahedron Lett. **42:**3607–3611.
402. **Tsunoda, S. P., A. J. Rodgers, R. Aggeler, M. C. Wilce, M. Yoshida, and R. A. Capaldi.** 2001. Large conformational changes of the ε subunit in the bacterial F_1F_0 ATP synthase provide a ratchet action to regulate this rotary motor enzyme. Proc. Natl. Acad. Sci. USA **98:**6560–6564.
403. **Ueno, H., T. Suzuki, K. Kinosita, Jr., and M. Yoshida.** 2005. ATP-driven stepwise rotation of F_oF_1-ATP synthase. Proc. Natl. Acad. Sci. USA **102**: 1333–1338.
404. **Unitt, M. D., and D. Lloyd.** 1981. Effects of inhibitors on mitochondrial adenosine triphosphatase of *Tetrahymena pyriformis* ST. J. Gen. Microbiol. **126:**261–266.
405. **Usta, J., and D. E. Griffiths.** 1992. Organotin-flavone complexes: a new class of fluorescent probes for F_1F_0ATPase. Biochem. Biophys. Res. Commun. **188:**365–371.
406. **Vanderkooi, G., J. Shaw, C. Storms, R. Vennerstrom, and D. Chignell.** 1981. On the mechanism of action of anesthetics. Direct inhibition of mitochondrial F_1-ATPase by *n*-butanol and tetracaine. Biochim. Biophys. Acta **635:**200–203.
407. **van der Zwet-de Graaff, I., A. F. Hartog, and J. A. Berden.** 1997. Modification of membrane-bound F_1 by *p*-fluorosulfonylbenzoyl-5′-adenosine: sites of binding and effect on activity. Biochim. Biophys. Acta **1318:**123–132.
408. **van Dongen, M. B., J. P. de Geus, T. Korver, A. F. Hartog, and J. A. Berden.** 1986. Binding and hydrolysis of 2-azido-ATP and 8-azido-ATP by isolated mitochondrial F_1: characterisation of high-affinity binding sites. Biochim. Biophys. Acta **850:**359–368.
409. **Van Heeke, G., L. Deforce, R. A. Schnizer, R. Shaw, J. M. Couton, G. Shaw, P. S. Song, and S. M. Schuster.** 1993. Recombinant bovine heart mitochondrial F_1-ATPase inhibitor protein: overproduction in *Escherichia coli*, purification, and structural studies. Biochemistry **32:**10140–10149.
410. **van Raaij, M. J., J. P. Abrahams, A. G. Leslie, and J. E. Walker.** 1996. The structure of bovine F_1-ATPase complexed with the antibiotic inhibitor aurovertin B. Proc. Natl. Acad. Sci. USA **93:**6913–6917.
411. **van Raaij, M. J., G. L. Orriss, M. G. Montgomery, M. J. Runswick, I. M. Fearnley, J. M. Skehel, and J. E. Walker.** 1996. The ATPase inhibitor protein from bovine heart mitochondria: the minimal inhibitory sequence. Biochemistry **35:**15618–15625.
412. **Vasilyeva, E. A., I. B. Minkov, A. F. Fitin, and A. D. Vinogradov.** 1982. Kinetic mechanism of mitochondrial adenosine triphosphatase. Inhibition by azide and activation by sulphite. Biochem. J. **202:**15–23.
413. **Velours, J., and G. Arselin.** 2000. The *Saccharomyces cerevisiae* ATP synthase. J. Bioenerg. Biomembr. **32:**383–390.
414. **Verburg, J. G., and W. S. Allison.** 1990. Tyrosine α244 is derivatized when the bovine heart mitochondrial F_1-ATPase is inactivated with 5′-*p*-fluorosulfonylbenzoylethenoadenosine. J. Biol. Chem. **265:**8065–8074.
415. **Verburg, J. G., M. Yoshida, and W. S. Allison.** 1986. The use of dithionite reduction to identify the essential tyrosine residue in the F_1-ATPase from the thermophilic bacterium, PS3, that reacts with 7-chloro-4-nitrobenzofurazan. Arch. Biochem. Biophys. **245:**8–13.
416. **Verschoor, G. J., P. R. van der Sluis, and E. C. Slater.** 1977. The binding of aurovertin to isolated β subunit of F_1 (mitochondrial ATPase). Stoicheiometry of β subunit in F_1. Biochim. Biophys. Acta **462:**438–449.
417. **Vogel, P. D., and R. L. Cross.** 1991. Adenine nucleotide-binding sites on mitochondrial F_1-ATPase. Evidence for an adenylate kinase-like orientation of catalytic and noncatalytic sites. J. Biol. Chem. **266:**6101–6105.
418. **von Ballmoos, C., J. Brunner, and P. Dimroth.** 2004. The ion channel of F-ATP synthase is the target of toxic organotin compounds. Proc. Natl. Acad. Sci. USA **101:**11239–11244.
419. **Wagenvoord, R. J., I. van der Kraan, and A. Kemp.** 1979. Localisation of adenine nucleotide-binding sites on beef-heart mitochondrial ATPase by photolabelling with 8-azido-ADP and 8-azido-ATP. Biochim. Biophys. Acta **548:**85–95.
420. **Wagenvoord, R. J., I. Van der Kraan, and A. Kemp.** 1977. Specific photolabelling of beef-heart mitochondrial ATPase by 8-azido-ATP. Biochim. Biophys. Acta **460:**17–24.
421. **Wagenvoord, R. J., G. J. Verschoor, and A. Kemp.** 1981. Photolabelling with 8-azido-adenine nucleotides of adenine nucleotide-binding sites in isolated spinach chloroplast ATPase (CF_1). Biochim. Biophys. Acta **634:**229–236.
422. **Wahl, M. L., D. J. Kenan, M. Gonzalez-Gronow, and S. V. Pizzo.** 2005. Angiostatin's molecular mechanism: aspects of specificity and regulation elucidated. J. Cell. Biochem. **96:**242–261.
423. **Walter, P., H. A. Lardy, and D. Johnson.** 1967. Antibiotics as tools for metabolic studies. X. Inhibition of phosphoryl transfer reactions in mitochondria by peliomycin, ossamycin, and venturicidin. J. Biol. Chem. **242:** 5014–5018.
424. **Weber, J., R. S. Lee, E. Grell, and A. E. Senior.** 1992. Investigation of the aurovertin binding site of *Escherichia coli* F_1-ATPase by fluorescence spectroscopy and site-directed mutagenesis. Biochemistry **31:**5112–5116.
425. **Weber, J., R. S. Lee, S. Wilke-Mounts, E. Grell, and A. E. Senior.** 1993. Combined application of site-directed mutagenesis, 2-azido-ATP labeling, and lin-benzo-ATP binding to study the noncatalytic sites of *Escherichia coli* F_1-ATPase. J. Biol. Chem. **268:**6241–6247.
426. **Weber, J., U. Lucken, and G. Schafer.** 1985. Total number and differentiation of nucleotide binding sites on mitochondrial F_1-ATPase. An approach by photolabeling and equilibrium binding studies. Eur. J. Biochem. **148:**41–47.
427. **Weber, J., M. Rogner, and G. Schafer.** 1987. Novel approaches towards characterization of the high-affinity nucleotide binding sites on mitochondrial F_1-ATPase by the fluorescence probes 3′-*O*-(1-naphthoyl)adenosine di- and triphosphate. Biochim. Biophys. Acta **892:**30–41.
428. **Weber, J., S. Schmitt, E. Grell, and G. Schafer.** 1990. Differentiation of the nucleotide-binding sites on nucleotide-depleted mitochondrial F_1-ATPase by means of a fluorescent ADP analogue. J. Biol. Chem. **265:** 10884–10892.
429. **Weber, J., and A. E. Senior.** 1997. Binding of TNP-ATP and TNP-ADP to the non-catalytic sites of *Escherichia coli* F_1-ATPase. FEBS Lett. **412:**169–172.
430. **Weber, J., and A. E. Senior.** 1998. Effects of the inhibitors azide, dicyclohexylcarbodiimide, and aurovertin on nucleotide binding to the three F_1-ATPase catalytic sites measured using specific tryptophan probes. J. Biol. Chem. **273:**33210–33215.
431. **West, K. R., and J. T. Wiskich.** 1969. The action of Dio-9 on photophosphorylation. FEBS Lett. **3:**247–249.
432. **Wieker, H. J., and B. Hess.** 1985. α,β-Bidentate CrADP abolishes the negative cooperativity of yeast mitochondrial F_1-ATPase. Biochim. Biophys. Acta **806:**35–41.
433. **Wieker, H. J., D. Kuschmitz, and B. Hess.** 1987. Inhibition of yeast mitochondrial F_1-ATPase, F_0F_1-ATPase and submitochondrial particles by rhodamines and ethidium bromide. Biochim. Biophys. Acta **892:**108–117.
434. **Wiley, P. F., J. M. Koert, and L. J. Hanka.** 1982. Two new polypeptide antibiotics, CC-1014 and CC-1014B. J. Antibiot. **35:**1231–1233.
435. **Williams, N., and P. S. Coleman.** 1982. Exploring the adenine nucleotide binding sites on mitochondrial F_1-ATPase with a new photoaffinity probe, 3′-*O*-(4-benzoyl)benzoyl adenosine 5′-triphosphate. J. Biol. Chem. **257:** 2834–2841.
436. **Wise, J. G., T. M. Duncan, L. R. Latchney, D. N. Cox, and A. E. Senior.** 1983. Properties of F_1-ATPase from the uncD412 mutant of *Escherichia coli*. Biochem. J. **215:**343–350.
437. **Yagi, T., and Y. Hatefi.** 1984. Thiols in oxidative phosphorylation: inhibition and energy-potentiated uncoupling by monothiol and dithiol modifiers. Biochemistry **23:**2449–2455.
438. **Yagi, T., and Y. Hatefi.** 1987. Thiols in oxidative phosphorylation: thiols in

the F_0 of ATP synthase essential for ATPase activity. Arch. Biochem. Biophys. **254:**102–109.
439. **Yarlett, N., and D. Lloyd.** 1981. Effects of inhibitors on mitochondrial adenosine triphosphatase of *Crithidia fasciculata*: an unusual pattern of specificities. Mol. Biochem. Parasitol. **3:**13–17.
440. **Yoshida, M.** 1983. The synthesis of enzyme-bound ATP by the F_1-ATPase from the thermophilic bacterium PS3 in 50% dimethylsulfoxide. Biochem. Biophys. Res. Commun. **114:**907–912.
441. **Yoshida, M., W. S. Allison, F. S. Esch, and M. Futai.** 1982. The specificity of carboxyl group modification during the inactivation of the *Escherichia coli* F_1-ATPase with dicyclohexyl[^{14}C]carbodiimide. J. Biol. Chem. **257:** 10033–10037.
442. **Younis, H. M., M. M. Abo-El-Saad, R. K. Abdel-Razik, and S. A. Abo-Seda.** 2002. Resolving the DDT target protein in insects as a subunit of the ATP synthase. Biotechnol. Appl. Biochem. **35:**9–17.
443. **Younis, H. M., J. N. Telford, and R. B. Koch.** 1978. Adenosine triphosphatase from cockroach coxal muscle mitochondria. Isolation, properties, and response to DDT. Pestic. Biochem. Physiol. **8:**271–277.
444. **Yount, R. G., D. Babcock, W. Ballantyne, and D. Ojala.** 1971. Adenylyl imidodiphosphate, an adenosine triphosphate analog containing a P-N-P linkage. Biochemistry **10:**2484–2489.
445. **Zanotti, F., F. Guerrieri, Y. W. Che, R. Scarfo, and S. Papa.** 1987. Proton translocation by the H^+-ATPase of mitochondria. Effect of modification by monofunctional reagents of thiol residues in F_0 polypeptides. Eur. J. Biochem. **164:**517–523.
446. **Zanotti, F., G. Raho, A. Gaballo, and S. Papa.** 2004. Inhibitory and anchoring domains in the ATPase inhibitor protein IF_1 of bovine heart mitochondrial ATP synthase. J. Bioenerg. Biomembr. **36:**447–457.
447. **Zhang, S., D. D. Letham, and A. T. Jagendorf.** 1993. Inhibition of thylakoid ATPase by venturicidin as an indicator of CF_1-CF_0 interaction. Plant Physiol. **101:**127–133.
448. **Zheng, J., and V. D. Ramirez.** 2000. Inhibition of mitochondrial proton F_0F_1-ATPase/ATP synthase by polyphenolic phytochemicals. Br. J. Pharmacol. **130:**1115–1123.
449. **Zheng, J., and V. D. Ramirez.** 1999. Piceatannol, a stilbene phytochemical, inhibits mitochondrial F_0F_1-ATPase activity by targeting the F_1 complex. Biochem. Biophys. Res. Commun. **261:**499–503.
450. **Zheng, J., and V. D. Ramirez.** 1999. Purification and identification of an estrogen binding protein from rat brain: oligomycin sensitivity-conferring protein (OSCP), a subunit of mitochondrial F_0F_1-ATP synthase/ATPase. J. Steroid. Biochem. Mol. Biol. **68:**65–75.
451. **Zheng, J., and V. D. Ramirez.** 1999. Rapid inhibition of rat brain mitochondrial proton F_0F_1-ATPase activity by estrogens: comparison with Na^+, K^+-ATPase of porcine cortex. Eur. J. Pharmacol. **368:**95–102.
452. **Zhuo, S., and W. S. Allison.** 1988. Inhibition and photoinactivation of the bovine heart mitochondrial F_1-ATPase by the cytotoxic agent, dequalinium. Biochem. Biophys. Res. Commun. **152:**968–972.
453. **Zhuo, S., S. Garrod, P. Miller, and W. S. Allison.** 1992. Irradiation of the bovine mitochondrial F_1-ATPase previously inactivated with 5′-*p*-fluorosulfonylbenzoyl-8-azido-[^{3}H]adenosine cross-links His-β427 to Tyr-β345 within the same β subunit. J. Biol. Chem. **267:**12916–12927.
454. **Zhuo, S., S. R. Paik, J. A. Register, and W. S. Allison.** 1993. Photoinactivation of the bovine heart mitochondrial F_1-ATPase by [^{14}C]dequalinium cross-links phenylalanine-403 or phenylalanine-406 of an α subunit to a site or sites contained within residues 440–459 of a β subunit. Biochemistry **32:**2219–2227.